University of Alberta

Feasibility Study of Air Carbon Capture and Sequestration System

By

Mohamed Ashraf Ismail

A thesis submitted to the Faculty of Graduate Studies and Research
in partial fulfillment of the requirements for the degree of

Master of Science

Mechanical Engineering Department

Fall 2011
Edmonton, Alberta

To My Mother and the Spirit of My Father

Abstract

The atmospheric capture of CO_2 was proposed to offset past and future emissions from small distributed sources or past emissions from all sources. The objective of this study is to develop a feasible process to capture 300 Mton of CO_2 from the atmosphere, annually, and to integrate the proposed process into an integrated Carbon Capture and Storage system (CCS). Thermal Swing Adsorption (TSA) was proposed as a separation technology to strip CO_2 from the atmosphere by using Zeolite 13X as an adsorbent. A technically feasible design of the overall plant was presented for two locations, Vostok and Atacama, with an estimate of the capital and operating costs for each location. The total cost of the proposed system in 2010 US dollars was 50 \$/tonCO_2 for Vostok and 200 \$/tonCO_2 for Atacama. The proposed atmospheric CCS is considered technically and economically feasible if certain conditions are met.

Acknowledgement

First and Foremost I would like to express my deep gratitude to my supervisors, Dr. Michael Lipsett and Dr. Peter Flynn for their continuous, constructive, and supportive advice and guidance over the duration of this study. I really appreciate all their contributions of time, ideas, and funding to make my M.Sc. experience productive and stimulating.

During this study, I had the honor to work with Dr. Steve Kuznicki who proposed the idea of using CO_2 wheels in the adsorption process. In addition, he introduced me to Dr. Adolfo Avila who helped me to estimate the adsorption capacity according to different models.

I would like also to thank Dr. Amit Kumar and Dr. Mohamed Al-Hussein for reviewing my thesis and participating in my thesis defence as committee members. Their valuable comments were highly useful and beneficial in developing this thesis. Moreover, I greatly acknowledge Dr. Sherif Hassanien and Christine Baghdady, who helped me in the editing of my thesis.

At last, I'm totally indebt to my family, especially my wife Rania Gomaa for providing the support, love, and the appropriate environment to complete my thesis and studies successfully.

Table of Contents

List of Tables

List of Figures

Nomenclature

q	amount of moles of the adsorbate per the amount of the adsorbent
p	pressure
a, d, k	adsorption constant parameters that vary with temperature
t_{sat}	time needed for saturation
t_{cycle}	cycle time
$A_p\%$	percentage of process surface area to the total wheel area
$\dot{m}$	mass flow rate
V	volume
M_w	molecular weight
ρ	density
n	number of moles
T	temperature
T_{Ads}	adsorption temperature
T_{Des}	desorption temperature
$\dot{Q}$	thermal energy rate
c_p	heat capacity
dt	temperature difference
F	volumetric flow rate
v	velocity
A	area
p_i	saturation partial pressure over ice
x	water content in the atmosphere
p_a	atmospheric pressure
U	overall heat transfer coefficient
$LMTD$	log mean temperature difference
D_i	initial diameter
Re	reynold's number

μ	dynamic viscosity
ν	kinematic viscosity
f_F	fanning friction factor
ϵ	roughness of the pipeline
D	pipeline diameter
Z_{ave}	average compressibility
R	universal gas constant
L	length of pipeline segment
h	height or elevation at certain point
δ_t	pipeline thickness
σ	minimum yield stress for the pipeline material
E	longitudinal joint factor
S_F	design safety factor
D_o	pipeline outer diameter
α	location factor
β	terrain cost multiplier factor
ϑ, γ	pipeline cost estimate constants
i	discount rate
n	plant service life

Abbreviations and Acronyms

GHG	Greenhouse Gas
GDP	Gross Domestic Product
ASU	Air Separation Unit
IPCC	Intergovernmental Panel on Climate Change
EIA	US Energy Information Administration
CCS	Carbon Capture and Sequestration
IGCC	Integrated Gasification Combined Cycle
PSA	Pressure Swing Adsorption
TSA	Temperature Swing Adsorption
VSA	Vacuum Swing Adsorption
PVSA	Pressure Vacuum Swing Adsorption
TPSA	Temperature Pressure Swing Adsorption
ESA	Electrical Swing Adsorption
LNG	Liquid Natural Gas
MTS	Meteorological Services of Canada
NPS	Nominal Pipe Size
CFR	US Code of Federal Regulation
CMU	Carnegie Mellon University
NASA	US National Aeronautics and Space Administration
O&M	Operation and Maintenance
API	American Petroleum Institute
P&ID	Piping and Instrumentation Diagram
NETC	National Energy Technology Center
IEA	International Energy Agency
Ads	Adsorption
Des	Desorption
Ave	Average

Chapter 1 : Introduction

1.1 Greenhouse Gas (GHG) Emissions and Climate Change

The quality of life and the level of industrialization are directly related to Greenhouse Gas (GHG) emissions, due to human dependence on fossil fuels as a source of energy and deforestation activities. Most researchers expect that this relationship will be maintained for at least the next few decades. The increasing concentration of GHGs in the atmosphere has the potential to create a significant effect on the world climate [1]. Figure 1-1 shows that GHG emissions have increased dramatically from 1970 to 2004 [1]. Carbon dioxide ($CO_{2)}$ is the main contributor to GHG as it represents almost 80% of GHG components as shown in Figure 1-2 [1]. It also shows that the main source of atmospheric CO_2 is fossil fuel combustion, as it represents about 57% of total anthropogenic CO_2 emitted to the atmosphere, followed by deforestation and decay of biomass as the second main reason for anthropogenic CO_2 emissions. Figure 1-3 shows the contribution of different sectors to the total anthropogenic GHG. It is clear that large sources classified as Energy Supply and Industries are responsible for 45.3% of total GHG emissions, while Transportation, Residential and Commercial Buildings, Forestry and Agriculture are responsible for 51.9% of the total GHG emissions [1].

Options to reduce GHG emissions, especially CO_2 in the atmosphere, have been studied lately to mitigate its effects on the climate. Scientists and policy makers have been working on alternatives and possible solutions, which can be categorized as follows [2]:

1) Sustainable renewable energy sources.
2) Low carbon emission energy sources.
3) Improvement of Energy efficiency.
4) Enhancement of natural sinks.
5) Carbon dioxide capture and storage systems.

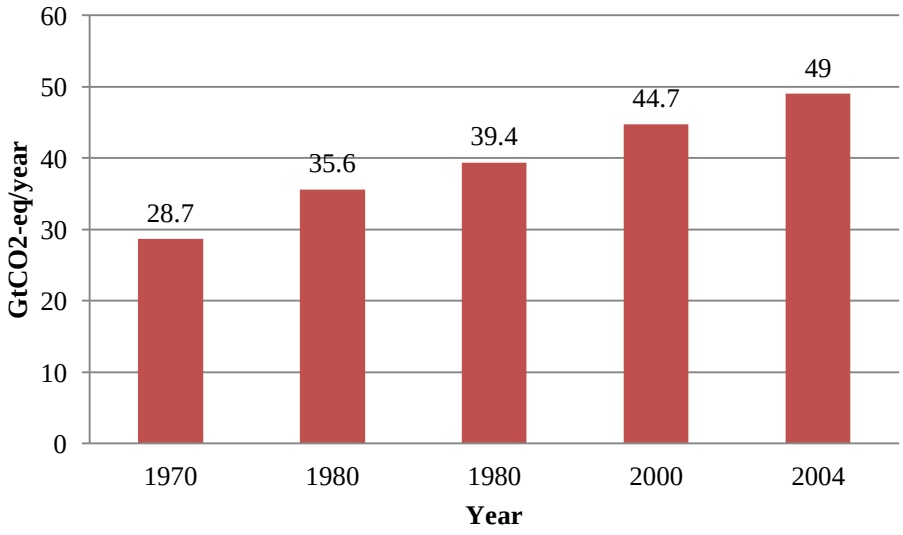

Figure 1-1 : Global annual emissions of anthropogenic GHGs [1]

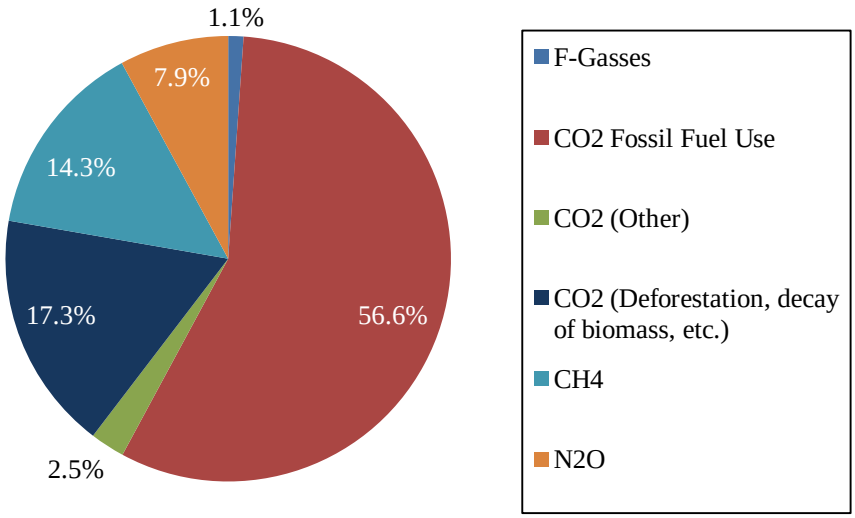

Figure 1-2 : Share of different anthropogenic GHGs in total emissions in 2004 in terms of CO_2-eq [1]

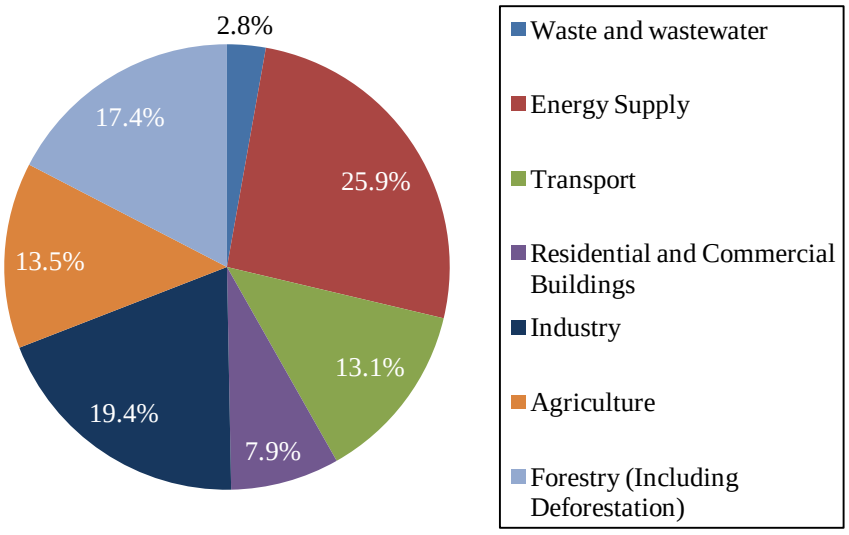

Figure 1-3 : Share of different sectors in total anthropogenic GHG emissions in 2004 in terms of CO_2-eq [1]

Renewable energy sources such as hydro, wind, solar, etc. are one of class solutions; however, the pace of implementation of renewable energy has been slow in developed countries, and even slower in developing countries where the cost penalty for renewable energy is a high fraction of the country's Gross Domestic Product (GDP), taking into consideration the massive increase in energy demands due to the development and economic growth [3]. Figure 1-4 shows the contribution of renewable energy sources in addition to nuclear energy sources to the total world energy sources as of 2006. It is clear that the total percentage of non-carbon-based energy sources is only 13% of the total world energy sources [4].

Lower carbon emission fossil fuel energy sources such as replacing coal with natural gas or natural gas combined cycle for power production (because of its lower carbon content per unit energy produced compared to that in coal and the higher energy efficiency of power obtained) are considered to be a mitigation solution for the problem of GHG emissions. This solution will mitigate or reduce

future emissions only. The amount of expected reduction does not fulfill or satisfy the required ultimate values of mitigation, which will maintain CO_2 concentrations in the atmosphere below the hazardous level of 450 ppm [5]. It also will not solve the problem of past emissions that already have been released into the atmosphere.

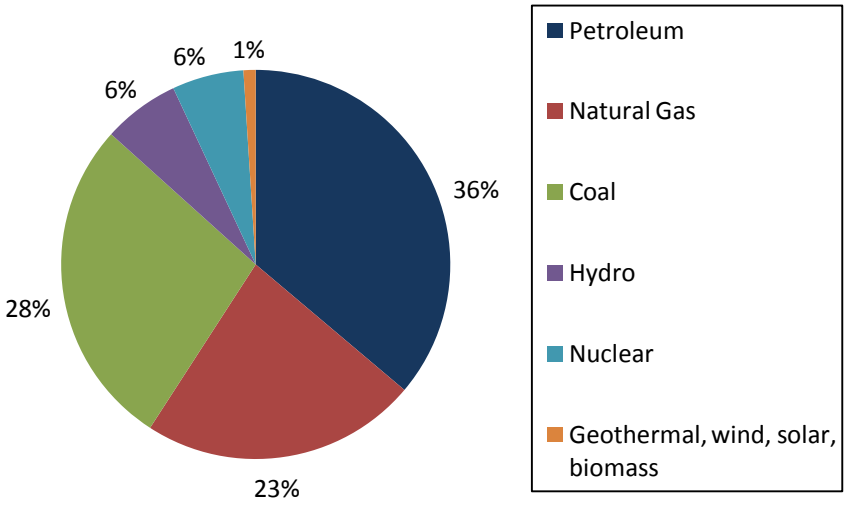

Figure 1-4 : World energy sources in 2006 [4]

Enhancement of natural sinks is one of the methods that help in extracting CO_2 from the atmosphere, either via the biosphere (the aggregate of living biomass on the planet) or the hydrosphere (which consists primarily of the ocean). According to the Intergovernmental Panel for Climate Change (IPCC), hydrosphere and biosphere uptake of CO_2 is 2.2 GtC per year and 0.9 GtC per year, respectively, for a total of 3.1 GtC per year for the period between 2000 and 2005 [6]. The total anthropogenic global emission of CO_2 is 8 GtC annually and projected to reach 12 GtC by 2030 according to the Energy Information Administration 2007 [6].

Last but not least, Carbon Capture and Storage (CCS) systems can be defined as those systems designed to reduce the CO_2 concentration in the atmosphere by

capturing CO_2 from different sources, usually large point sources, by utilizing different technologies and storing it either in the ocean or in deep geological formations.

1.2 Motivation for this research

The current global energy demand is fulfilled mainly with fossil fuels, even though some renewable alternatives are increasing, as shown in **Figure 1-5**. Therefore, the world will rely on the continued use and likely the growth of fossil fuels as a source of energy for at least the next few decades. As a result, more GHG emissions will be released into the atmosphere, causing a predicted increase in global temperature of between 1.4ºC to 5.8ºC by 2100 if no action is taken [7]. This increase is predicted to lead to many catastrophic environmental impacts, such as an increase in floods and the extermination of a significant number of species. Other possible environmental impacts include more acidic rain and hence ocean acidification. These predicted consequences have focused attention on the solutions discussed above. This thesis focuses on the fourth category of solutions, carbon capture and storage.

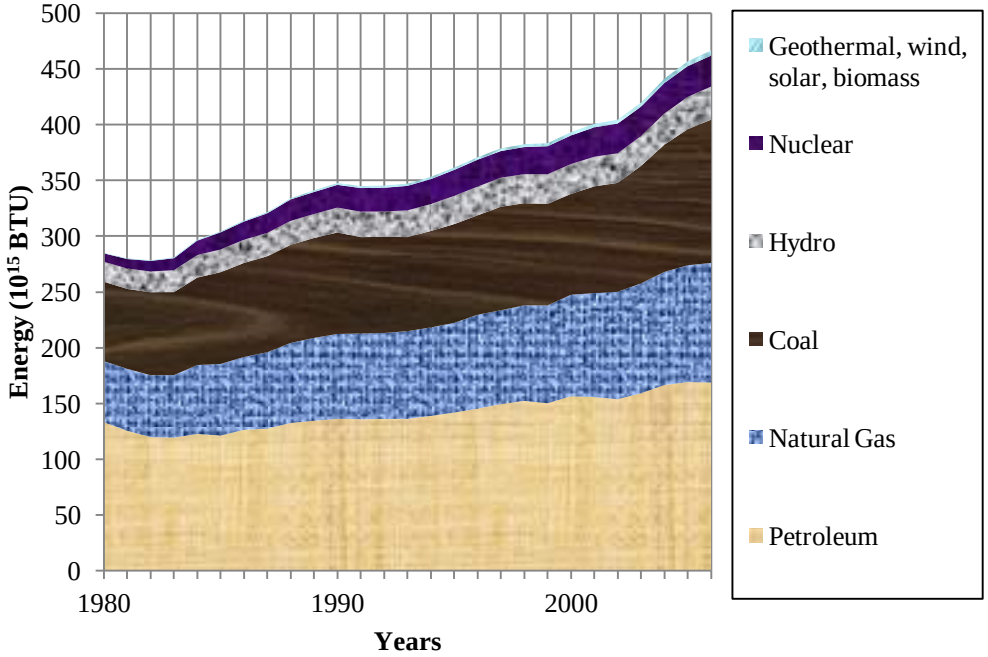

Figure 1-5 : World energy sources from 1980 to 2006 [4]

A CCS system has various subsystems and components, which are at different phases and stages of development. These phases range from the research and demonstration phase to the mature phase. There is also some experience in combining these different components into a fully integrated system [2]. Furthermore, there are still more applications for CCS systems beyond those proposed to date that have not yet been investigated, such as the integration of CCS into an atmospheric capture system.

1.3 Proposed Conceptual Framework and Organization of the Thesis

This work evaluates one specific CCS scheme. Atmospheric carbon capture, which strips CO_2 directly from the atmosphere, is investigated as a complete CCS system. The CCS system is considered to be made up of three major subsystems: a power plant, a carbon capturing plant, and a transportation and storage system. A set of key specifications is developed, and then concepts are designed for each subsystem. The focus of the present work is on the development of a process that is feasible for capturing CO_2 from the atmosphere. Ancillary systems are assumed to be existing available technology and therefore have no technology development issues. These systems are simply sized to match the carbon capture plant capacity. A technically feasible overall plant design is presented, with an estimate of the capital and operating costs. A key consideration in the development of capital and operating costs is the logistics involved in locating such a plant. The cost of the process is then calculated in terms of dollars per ton of captured CO_2 (i.e. \$/tonCO_2). Given that there is some uncertainty in some of the estimated parameters, a sensitivity analysis is conducted on a few key parameters to assess the range of costs that may be incurred to remove and store carbon using the proposed set of technologies.

In Chapter 2, individual components of the CCS system and separation technologies are reviewed in detail to select the best components and a separation technology which can be used in the air capture CCS system proposed. The suitable sites for the plant and its components are then selected in Chapter 3. In Chapter 4, a conceptual design for the process of capturing CO_2 from the atmosphere is conducted and integrated in a complete CCS system. Afterwards, the cost of such system is calculated to evaluate the feasibility of the whole plant in Chapter 5. In Chapter 6, conclusions from this work and further research recommendations are developed.

Chapter 2 : Review of Carbon Capture and Storage Technologies

2.1 Overview

Carbon capture and storage is defined as stripping CO_2 from some gas stream containing CO_2, so that it can be transported and sequestered in a location suitable for long-term storage, such as the deep ocean or a geological formation. The concept of capturing CO_2 is not a new technology; it has been used in different industries such as natural gas processing for over 80 years. However, the capture process involved capturing CO_2 and then venting it into the atmosphere [2]. The concept of developing a process to capture CO_2 for the purpose of long-term sequestration is relatively new. Thus, CCS systems involve three subsystems: capture, transportation and sequestration.

In this chapter, the concept of a CCS system is introduced. Different types of capture, transportation and sequestration are investigated to select the best option for each subsystem that can be used in the proposed air CCS plant. Several gas separation technologies are then investigated to choose the technologies that can be used in such a plant. Previous studies on the air capture system and proper CO_2 separation technologies are introduced and analysed. Based on these studies, the separation technology is selected and the utility requirements are determined.

2.2 CO_2 Capture from Process Streams

2.2.1 Overview

The capturing process can be divided according to the stage at which it takes place. There are three basic options: post-combustion, either in a flue gas (more

concentrated) or from the atmosphere (less concentrated); oxy-fuel, in order to concentrate CO_2 in the flue gas by removing nitrogen and trace gases from combustion air; and pre-combustion, where fossil fuel is partially oxidized before being combusted. Later in this chapter, the capturing process will be categorized according to the technology used in the separation of CO_2 from a gas mixture: by chemical/physical absorption, cryogenic separation, membrane separation or adsorption [8].

2.2.2 Post Combustion

The most typical post-combustion capture of CO_2 is from flue gas streams, such as at power plants or large point sources. In these plants, fossil fuel is combusted in a slight excess amount of air with respect to the stoichiometric ratio, producing a flue gas with a relatively low concentration of CO_2 due to the large amount of nitrogen that enters the combustion chamber along with the oxygen that is needed for combustion. For instance, the flue gas concentration in coal power plants ranges from 12% to 15% by volume, while it ranges from 4% to 8% by volume for natural gas power plants [8]. It is also possible to capture CO_2 after combustion flue gases have mixed in the atmosphere. In this case, the concentration of CO_2 is far lower; it is about 400 ppm today as discussed below.

2.2.3 Oxy-fuel Combustion

In oxy-fuel combustion, fuel is burnt in oxygen instead of air. Flue gas volume decreases by one-fifth to one-third due to the absence of nitrogen. Flue gas, which contains mainly water vapour and a highly concentrated stream of CO_2 (i.e. more than 80% v/v), can be concentrated through cryogenic separation, resulting in a pure CO_2 stream. Whether cryogenically purified or not, this stream can be compressed and transported for storage. A portion of the CO_2 stream is cooled and re-circulated to provide temperature control in the combustion chamber [2].

2.2.4 Pre-combustion

Pre-combustion techniques in fact remove CO_2 after partial oxidation. Fossil fuel is partially oxidized and produces syngas (containing carbon monoxide and hydrogen), which through the water-gas shift reaction is shifted into CO_2 and more hydrogen. The CO_2 is then captured prior to combustion. This technology is applied in the fertilizer, chemical, gaseous fuel and power production industries [2].

2.3 Transportation

After CO_2 is captured, it must be transported to suitable storage sites. This transport can be accomplished by pipeline, by ship or by land (trains or trucks) based on the amount of CO_2 to be transported, the distance to the storage site, and the type of terrain. With existing technology, utilizing pipelines for transportation is believed to be the simplest and most cost-effective form of large-scale CO_2 transportation because pipelines can transport large quantities over long distances and various types of terrains. Transportation of CO_2 by ship or by land is typically utilized when the pipeline option is not available or not economically efficient due to the small size of a shipment or long offshore distance (>500 km). The choice of transportation mode depends on the source and storage locations as well as the available infrastructure [2].

Generally, the pipeline that is used for CO_2 transportation is similar to that used for natural gas transportation; therefore, all known technologies and experience can be applied in the construction and operation of the pipeline. Transportation of CO_2 by pipeline is the least complicated element in the CCS chain. However, there is little experience with transporting large volumes of CO_2 through long pipelines, and so various operability and reliability issues may arise [9].

Carbon dioxide is transported through pipelines in its supercritical or liquid phase to avoid two-phase flows, which may lead to operational and material problems such as cavitation and slugging in pipeline components. The behaviour of CO_2 also varies under different pressures and temperatures. For instance, at atmospheric pressure, CO_2 will change directly from the gaseous state to the solid state, causing a huge decrease in temperature and forming dry ice which may clog the pipeline. Also, this phase transition may cause a rupture in the pipeline and lead to the leakage of CO_2 into the atmosphere [10]. Refer to Appendix I for further information. These problems are also explained in greater detail in Chapters 4 and 6.

2.4 Sequestration

2.4.1 Overview

The Captured CO_2 gas should be compressed and transported to a suitable location for permanent storage. There are different types of sites that can be used for CO_2 storage: geological, oceanic and terrestrial.

2.4.2 Geological Storage

2.4.2.1 Overview

The compressed CO_2 is injected into the underground geological formations at depths below 800 m by using the same technologies which are employed in the oil and gas industries, such as well drilling, compression and injection, simulation of storage reservoirs, and monitoring techniques. At that depth or below, several physical and geochemical properties of CO_2 prevent it from leaking back to the surface. Generally, CO_2 is collected and pumped to the injection wells through a distribution manifold. At the injection wells, a compression facility is used to inject the CO_2 into the well, and a control and monitoring facility is used to measure and control the injected CO_2 flow rate, pressure and temperature. If there is a difference between CO_2 supplies and demands, a buffer storage tank is needed at the storage site. Several successful existing enhanced oil and gas recovery

projects, such as Sleipner in Norway, Weybern in Canada and In-Salah in Algeria, may provide useful data in order to design programs for long-term storage of CO_2. Suitable formations are considered to have the ability to sequester CO_2 and keep it contained for thousands or millions of years. These formations comprise three categories: oil and gas reservoirs, deep saline formations, and deep coal seams.

2.4.2.2 Oil and Gas Reservoirs

An oil and gas reservoir is a porous layer that holds oil and gas covered by an impervious cap rock that acts as a seal. This layer holds oil and natural gas for millions of years; thus, these reservoirs have proven storage integrity. However, there are considerable concerns regarding leakage from wells that exist in certain types of formations, especially if refracturing has occurred [11]. Oil and gas reservoir storage capacities of CO_2 range from 675 to 900 Gton CO_2 [2].

2.4.2.3 Deep Saline Formation

A deep saline formation contains salty water in porous rock that is also covered by non-porous rock, similar to an oil and gas reservoir. Such a formation has the potential to hold large amounts of CO_2 [11]. Regardless of the uncertainties, deep saline formations are expected to have the capacity of storing at least 1,000 Gton CO_2 or much higher than this according to some studies [2].

2.4.2.4 Deep Coal Seams

Carbon dioxide can be injected into the coal beds containing methane (CH_4) that are deep, thin and uneconomical to be mined. Methane is recovered after adsorption of CO_2 by the coal because CO_2 is preferentially adsorbed over CH_4. A better understanding of CO_2 injectivity and adsorption on coal at supercritical conditions is needed. Therefore, this technology is not yet mature, and it requires more research and development to be viable [11]. The storage capacity of CO_2 in deep coal seams is estimated to range from 3 to 200 Gton CO_2.

2.4.3 Ocean Storage

2.4.3.1 Overview

The properties of CO_2 in sea water determine how it acts upon its release into the ocean. Carbon dioxide can be in the form of a liquid, gas, solid or CO_2 hydrate based on the temperature, pressure and depth at which it is released. These forms dissolve in sea water at different rates. Gaseous CO_2 exists at depths of less than 500 m, while liquid CO_2 is formed at depths below 500 m. The buoyancy of pure gaseous and liquid CO_2 is less than sea water at depths above 2,700 m, while solid and liquid CO_2 are heavier than sea water at depths of 3,000 m or below as illustrated in Figure 2-1.

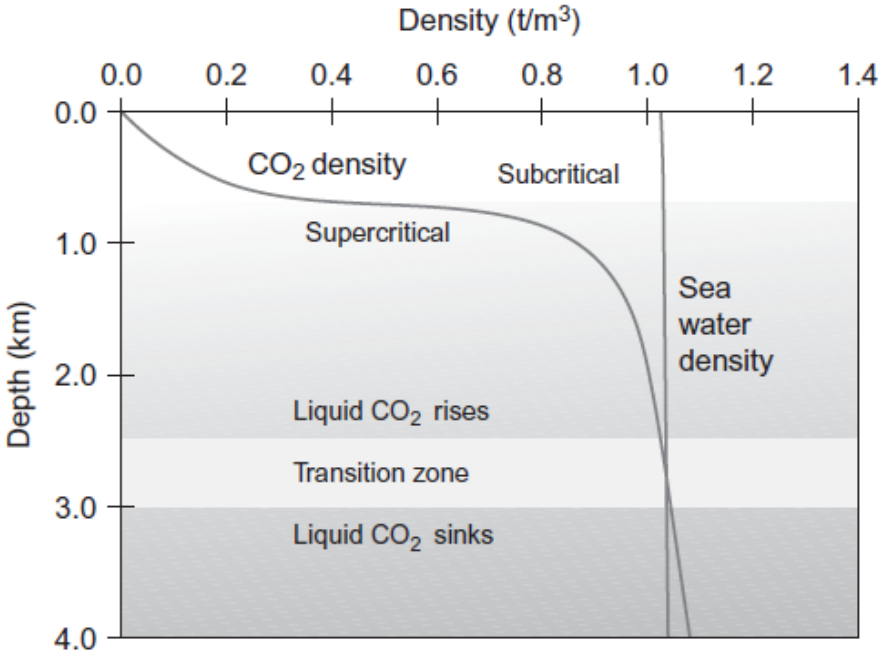

Figure 2-1 : Sea water and carbon dioxide densities versus depth [12]

The CO_2 hydrate is a solid form in which water molecules surround a CO_2 molecule. At a depth of 500 m or below, CO_2 hydrate is formed at approximately

9°C or lower, while the temperature of the deep ocean is about 4°C. A fully hydrated CO_2 hydrate crystal is denser than sea water.

Based on the characteristics mentioned above, three methods have been investigated to store CO_2 in the ocean based on the depth at which CO_2 will be released: droplet plume, CO_2 lake and dry ice.

2.4.3.2 Droplet Plume

Carbon dioxide is injected through a deep pipeline into the ocean in the form of small droplets that dissolve into the water below 1,000 m. These droplets will rise towards the surface; however, the formation of hydrate at the surface of the plume will decrease the size of the plume until it dissolves completely before reaching the surface. In other words, the plume will rise up while the edges of the plume sink down due to the formation of CO_2 hydrates on the plume boundaries. Pipes that are towed by moving ships, fixed offshore pipelines or floating platforms can be used to deposit CO_2 plumes into the ocean. At a depth of 2,700 m or below, the plume will sink due to its density. The possibility of leakage from rising plumes is the main disadvantage of this method [13].

2.4.3.3 CO_2 Lake

Injection is carried out by a vertical pipeline connected to an offshore platform or by a pipeline which has been laid onto the sea floor at depths below 3,000 m, where it forms permanent lakes of CO_2 because it has higher density than sea water at that depth. Figure 2-1 shows CO_2 density compared to sea water density at different depths [12]. At that depth or below, CO_2 can be sequestered effectively for several hundreds of years [14].

2.4.3.4 Dry Ice

At atmospheric pressure and a low temperature of -78°C, CO_2 solidifies into a white solid material called dry ice. In this form, it is dropped into the ocean at the surface by a moving ship. Solid dry ice is denser than sea water and so the blocks

will sink into the deep ocean. While dry ice sinks, the heat transfer causes CO_2 to peel off the dry ice and dissolves into the sea water. This method is simple compared to the previously discussed methods; however, it is not cost-effective due to the production and handling costs of dry ice and the high energy demands required for the freezing process [13].

2.4.4 Terrestrial Ecosystem Storage

Terrestrial ecosystem storage refers to the storage in organisms and their environments that exist on the landmasses of continents or islands. It also can be defined as the enhancement of CO_2 uptake by plants (either natural or cultivated) and soils (agricultural), including all reforestation and forest preservation activities [15].

2.5 Technologies for Carbon Dioxide Capture

2.5.1 Overview

Carbon dioxide capture and separation technologies were developed and used in industry since 1930 [2]. For instance, chemical solvents were developed to strip CO_2 from natural gas. These technologies are now used in power plants, chemical industries, and food processing plants to capture CO_2 from flue gases and process streams. Technology selection always depends on several parameters, such as CO_2 concentration in the stream, temperature, type of impurities, required purity of the product, and operating costs of the process [8]. These technologies can be classified into four categories: Chemical/physical absorption, membrane separation, cryogenic separation, and adsorption.

2.5.2 Chemical/Physical Absorption

Separation of CO_2 by chemical absorption is applied in several gas processing industries. Amine-based processes are used to purify process gas streams from acid gas impurities such as CO_2 and H_2S. In this process, the amine solution and gas stream are in contact with each other in an absorption tower. The gas stream

enters the tower from the bottom, while the solution enters the tower from the top. The gas stream then flows upwards and leaves from the top, while the solution flows downwards and leaves from the bottom. During this process, the amine solution scrubs impurities from the gas stream. The amine is then passed through a regeneration unit where it is heated and the absorbed acid gas impurities are released. This stage can be done in relatively low pressures to enhance desorbing CO_2 from the liquid. Any vaporized amine solution is recovered by using a condenser. Hot lean amine solution is returned to the contacting tower through a heat exchanger where it heats the rich amine solution coming from the contacting tower. This process is shown in
Figure **2-2**. There are three groups of amines used for CO_2 removal from gas streams: primary amines (MEA); secondary amines (DEA); tertiary amines (TEA or MDEA) [16].

For alkaline-salt-based processes, alkali salts of various weak acids are utilized for removing CO_2. Many salts such as sodium and potassium carbonate salts have been used. The advantage of this process is that it can be used to strip very small concentrations of CO_2 at ambient temperature, while the disadvantage is the enormous thermal energy requirement associated with such a process [16]. This process is explained in detail further in this chapter.

In physical absorption, CO_2 is absorbed physically into a solvent according to Henry's Law. This process usually occurs at high partial pressures and low temperatures. Solvents are then regenerated by either pressure reduction or heating. The advantage of this method is that it requires lower energy than chemical absorption, but it requires that CO_2 partial pressure to be relatively high. This process is suitable for stripping CO_2 from Integrated Gasification Combined Cycle (IGCC) systems as the exhaust CO_2 leaves the gasifier at high partial pressures. Selexol and Rectisol are two processes that are commonly used for physical absorption [16].

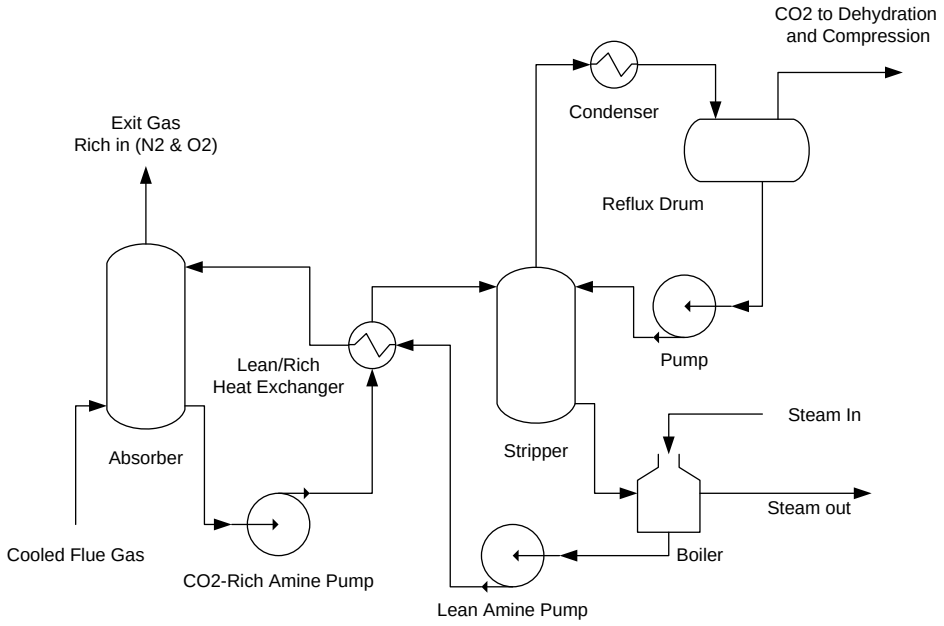

Figure 2-2 : Amine absorption unit for CO_2 recovery from flue gas [16]

2.5.3 Membrane Separation

Separation membranes are thin barriers that allow selective permeation of certain gases due to different diffusivity of gases in a polymer. They are predominately based on polymeric materials. Membranes for gas separation are usually formed as hollow fibers arranged in a tube-and-shell configuration, or as flat sheets, which are typically packaged as spiral-wound modules. The membrane process has been widely used on the commercial scale for hydrogen recovery from purge gases in ammonia synthesis, refinery and natural gas dehydration, sour gas removal from natural gas, and nitrogen production from air [2, 8].

A number of solid polymer membranes are commercially available for the separation of CO_2 from gas streams. These membranes selectively transmit CO_2 versus CH_4. The driving force for the separation is the pressure differential across the membrane as shown in Figure 2-3. As such, unless the gas stream is already at high pressure, compression is required for the feed gas to provide the driving force for permeation; and the separated CO_2 is at low pressure and requires

additional compression to meet pipeline pressure requirements. The energy required for gas compression is significant.

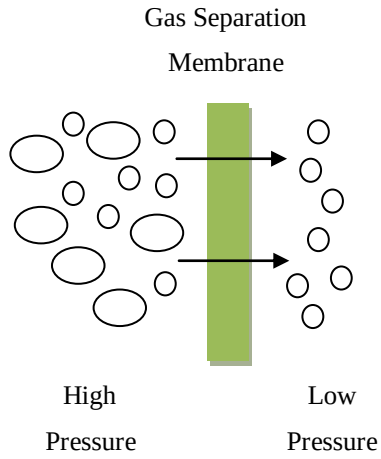

Figure 2-3 : The principle of gas separation by membranes

2.5.4 Cryogenic Separation

Low temperature distillation (cryogenic separation) is a commercial process commonly used to liquefy and purify CO_2 from relatively high purity (> 90%) sources. It involves cooling the gases to a very low temperature so that the CO_2 can be liquefied and separated.

Distillation generally has good economies of scale. This method is worth considering where there is a high concentration of CO_2 in the waste gas and a significant volume of gas. The advantage is that it produces liquid CO_2 that is ready for transportation by pipeline. The major disadvantages of this process are the amount of energy required to provide the refrigeration and the necessary removal of components (such as water) that have freezing points above normal operating temperatures to avoid freezing and eventual blockage of process equipment.

2.5.5 Adsorption

Adsorption is defined as the separation of gases such as CO_2 due to the intermolecular forces between these gases and the surfaces of certain solid materials. Adsorption capacity depends on the partial pressure of these gases which would be separated, temperature, surface forces, and pore size of the solid material. Desorption occurs when the gas leaves that solid material.

There are two major steps in an adsorption process: adsorption and desorption. These steps are repeated in cycles. The technical feasibility of an adsorption process is ruled by the adsorption step, while the desorption step controls the economic viability of the process. An effective adsorption process uses a strong affinity adsorbent to remove undesired gas from a gas mixture stream; however, the stronger the affinity, the more difficult it is to desorb the undesired gas and the higher the amount of energy requirement to regenerate the adsorbent for the next cycle. Therefore, adsorption and desorption steps should be carefully balanced to achieve a successful process.

Solid adsorbents such as activated carbon or zeolites are packed into beds. A gas mixture stream passes through these beds where undesired components are adsorbed, after which the desorption cycle is initiated to desorb the undesired gases. When the bed is fully saturated with inlet impurities, the gas mixture stream is diverted to another bed with fresh regenerated adsorbent to start a new adsorption cycle. At the same time, the other bed (which is saturated) will be regenerated.

Several adsorption processes can be used in capturing carbon dioxide such as pressure swing adsorption (PSA), temperature swing adsorption (TSA), vacuum swing adsorption (VSA), and electric swing adsorption (ESA). It is also possible to capture carbon dioxide by combining two methods such as (PVSA) and (TPSA). These processes are used commercially to regenerate adsorbents. In PSA

and VSA process temperatures of the feed and regeneration streams are kept constant, while in TSA and ESA processes pressures are kept constant. Generally, the above-mentioned processes depend on the preferential adsorption of one or more components of the mixed stream of gases at a given operating temperature and pressure (P_H, T_L). The adsorbed species are then released either by reducing pressure, in the case of PSA and VSA, or increasing temperature, in the case of TSA or ESA (P_L, T_H). The adsorption process can be represented graphically by isotherms, which are the amounts adsorbed at equilibrium versus different partial pressures at fixed temperatures. The difference between adsorption capacities at certain temperatures or at certain pressures represents the working capacity or the adsorption capacity (q) for this process, which can be expressed in terms of moles adsorbate per unit mass of adsorbent as shown in Figure 2-4 [12].

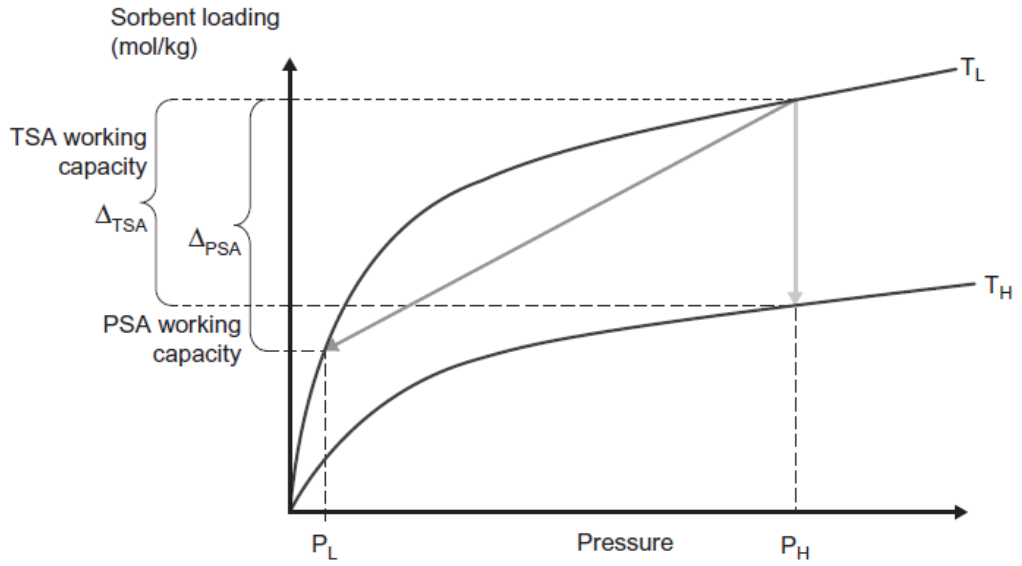

Figure 2-4 : Adsorbate (sorbent) working capacities for temperature and pressure swing adsorption [12]

Zeolite is currently one of the primary materials for CO_2 separation by adsorption under consideration. Other materials such as silica gel, activated alumina and activated carbon are also used as adsorbents in adsorption technology. The main advantage of adsorption amongst chemical/physical absorption and other

separation methods is that adsorption is a simple and relatively energy efficient process.

2.5.6 Design Factors in Separation Technology Selection

Based on the above review of the separation technologies, it is clear that several technologies can be used to strip CO_2 from a gas stream. Some technologies are preferred among the others based on CO_2 concentration and temperature in the gas stream. Cryogenic separation can be used for high concentration streams of CO_2 (more than 90%). Membrane separation requires a high pressure feed to drive the molecules through the membrane and therefore it will not be cost-effective for low concentrations of CO_2 in a low pressure gas stream, especially if it is integrated within CCS systems where the CO_2 must be compressed again to meet transportation and sequestration pressure requirements. Although physical absorption requires a lower energy demand than chemical absorption, however it occurs at high partial pressures of CO_2 (40% to 60%). Therefore, adsorption or chemical absorption technologies are preferred for capturing low concentrations of CO_2.

PSA adsorption is not preferred in the first stage of adsorption for a low pressure gas stream because of the huge energy demand required to compress the gas. The concentration of CO_2 currently in the atmosphere is approaching 400 ppm, which means that high amounts of energy would be required in a PSA process to compress a very large volume of gas in order to capture a small amount of CO_2 in air. Therefore, the PSA process is not recommended to be used in CO_2 atmospheric capture processes. Conversely, the TSA process requires only heat to drive off the small amount of adsorbed CO_2, and hence it is the recommended process for capturing extremely low concentrations of CO_2 from a low pressure gas stream.

2.6 Carbon Dioxide Capture from the Atmosphere

2.6.1 Overview

According to an IPCC report, more than 50% of GHG emissions are from many small dispersed sources such as residential and commercial buildings, forestry, transportation, and agriculture [2]. Therefore, even if a CCS system was completely applied for large point sources such as power plants and industrial facilities, there would still be a very significant amount of dispersed emissions as long as fossil fuels are being used for heating and transportation. As well, air capture is the only way to capture past emissions.

2.6.2 Historical Background

2.6.2.1 Capturing CO_2 from the Atmosphere by Chemical Absorption

Capturing CO_2 from air for the purpose of GHG mitigation was proposed in 1999 by Lakner et al. [17]. They reported that the cost of carbon capture from air would be \$100/ton CO_2 using existing technology [17, 18]. Aqueous calcium hydroxide ($Ca(OH)_2$) was proposed as a sorbent to react with CO_2 from the atmosphere and produce calcium carbonate ($CaCO_3$), which would be heated in order to produce CO_2 and calcium oxide (CaO). The CaO would be returned in order to react with water (H_2O) to produce aqueous calcium hydroxide and heat. The process and chemical reactions equations are shown in Figure 2-5.

Keith et al. discussed the challenges of CO_2 capture from the atmosphere, such as thermodynamic limitations, energy requirements, and the cost of the proposed process [20]. They concluded that the cost of the process would range from \$55/ton CO_2 to \$136/ton CO_2. In addition, if air capture is used to offset emissions from fossil fuels, the amount of power produced per unit area of capturing facility will be 50 W/m^2 for a coal-power plant and 100 W/m^2 for a natural gas power plant. Furthermore, the concept that is used for wind power

plants to avoid wind shadowing (i.e. the effect of one unit on another) was recommended to be utilized. In large wind farms, 5 to 10 times the rotor diameter is the space difference between stems of wind turbines; and so the recommended spacing between contactors of CO_2 air capture system would be 5 to 10 times the diameter of the contactor to allow for circulation and diffusion of CO_2 [20].

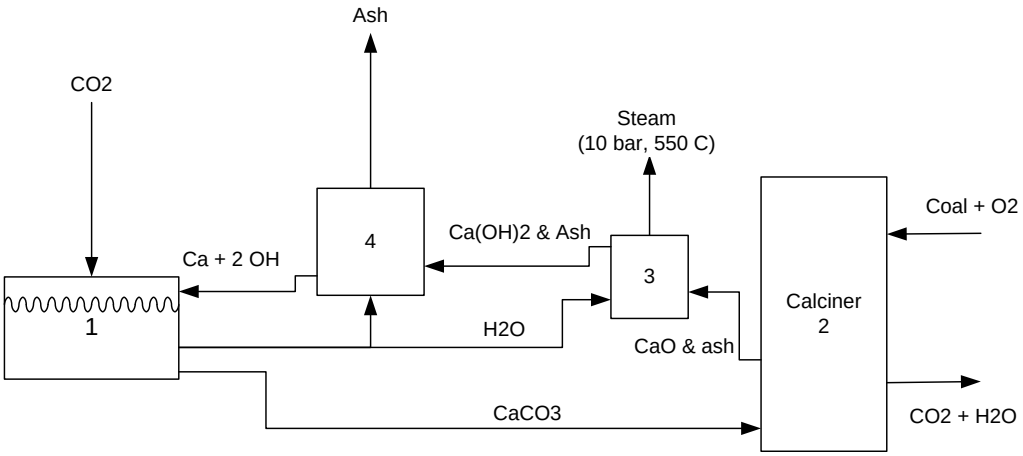

Figure 2-5 : Air capture with calcium hydroxide [19]

Herzog, however, has challenged the conclusions of Lackner et al. and Keith et al. [18]. He cost doubt on some parameters used in their analyses, such as kiln thermal efficiency, and oxygen (O_2) and natural gas prices. Moreover, the cost associated with compression and recycling flue gas from the calciner was not included.

A modification in the process of capturing carbon dioxide has been studied by Keith et al. [20]. A sodium hydroxide (NaOH) solution was used instead of $Ca(OH)_2$. The solution is sprayed in a tower similar to conventional cooling towers. Carbon dioxide is absorbed from air forming sodium carbonate (Na_2CO_3), which is reacted with lime CaO in a vessel called a causticizer to produce NaOH again and solid $CaCO_3$. As in the original process, $CaCO_3$ is heated to strip off

CO_2 and produce CaO. This process usually takes place in a kiln. Carbon dioxide is then collected and compressed for sequestration as shown in Figure 2-6 [20].

Chemistry of Na/Ca capture system

	Reaction	Enthalpy of reaction[a], ΔH° kJ/mol-C	GJ/tC
(1)	$CO_2(g) + 2Na^+ + 2OH^- \rightarrow CO_3^{2-} + Na^+ + H_2O$	−110	−9
(2)	$CO_3^{2-} + Ca^{2+} \rightarrow CaCO_3(s)$	12	1
(3)	$CaO(s) + H_2O(l) \rightarrow Ca^{2+} + 2\,OH^-$	−82	−7
(4)	$CaCO_3(s) \rightarrow CaO(s) + CO_2(g)$	179	15

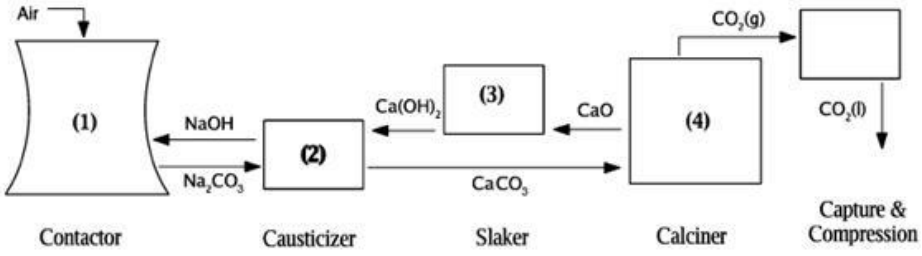

Figure 2-6 : Sodium hydroxide air capture system [20]

Stolaroff et al. constructed the first prototype contactor for capturing CO_2 from the atmosphere [21]. Sodium hydroxide was used as an absorbent to strip off CO_2 from the atmosphere. The prototype showed that such a process is technically feasible. Material and energy requirements were calculated so that the cost can be determined more precisely. Figure 2-7 shows a diagram of the contactor column used for this process.

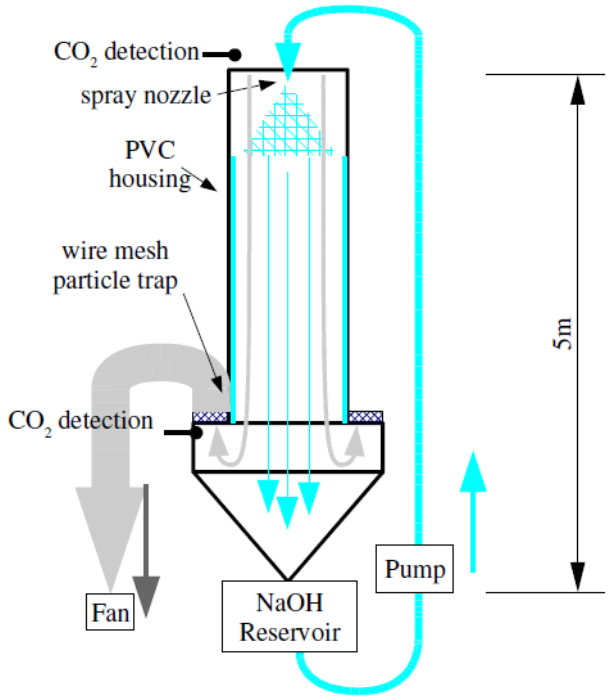

Figure 2-7 : Prototype for CO_2 contactor [21]

Baciocchi et al. studied the process design and calculated energy requirements for two process options [22]. Both options used an NaOH solution as an absorbent but with different implementations and configurations. The study and calculation were based on an atmospheric CO_2 concentration of 500 ppm, which is the concentration expected to be reached by the end of this century. The energy requirements for the two proposed process options are 10.6 GJ/ton CO_2 (of which 8.8 GJ is thermal energy and 1.8 GJ is mechanical energy) and 7.6 GJ/ton CO_2 (6 GJ thermal and 1.6 GJ mechanical), respectively. By applying 35% efficiency for electricity generation and 75% for direct utilization of thermal energy, the required energy will be 17 GJ/ton CO_2 and 12 GJ/ton CO_2 for both options proposed. The study concluded that in order to make the process feasible, the avoidance of fossil fuels as a source of energy is essential. Mechanical energy can be provided by electric machines powered by hydroelectric, wind, or photovoltaic

solar power sources. Thermal energy can be produced from solar, nuclear, and in some locations geothermal plant.

Zeman also conducted an energy and material balance for the process of capturing carbon dioxide from atmosphere by using sodium hydroxide [23]. Kiln efficiency was improved when high purity oxygen was used for combustion instead of air to create a rich CO_2 combustion environment. Energy requirements of the process were compared with those that were calculated by Baciocchi et al. and Keith et al. [20, 22]. The research concluded that the total energy requirement for the process, after improving kiln efficiency, is approximately 10 GJ/ton CO_2 versus 15 and 12 GJ/ton CO_2 for Keith and Baciocchi, respectively [23].

Stolaroff et al. reported the cost of capturing CO_2 in a full-scale contactor system [24]. The contactor prototype mentioned previously was used in this study. A numerical model of drop collision and coalescence was developed to predict the full-scale system operating parameters, allowing the scale-up cost to be calculated precisely for that system. It was reported that the cost would be 96 \$/ton CO_2, neglecting sequestration costs and solution recovery. The calculation of energy requirements done by Zeman was also confirmed [24].

2.6.2.2 Carbon Dioxide Capture by Adsorption

Rege et al. studied the PSA process to remove air impurities such as H_2O and CO_2 for the purpose of nitrogen (N_2) and O_2 production from air by an Air Separation Unit (ASU) [25]. They studied this process by using different adsorbents such as Zeolite 13X and activated alumina. The process performance when using one bed for each adsorbent was compared against using one bed containing two adsorbents (13X and γAl_2O_3) in contact with each other. It was concluded that the overall performance of the latter is much better than the former. They also concluded that the best adsorbent for capturing CO_2 is Zeolite 13X, especially at low concentrations of CO_2. In addition, Zeolite 13X was found to have the highest

adsorption capacity for H_2O at concentrations above 100 ppm, while below that concentration γAl_2O_3 and K^+ clinoptilolite were the best adsorbent candidates.

Shimomura proposed using CO_2 wheels for CO_2 capture by adsorption [26]. Lithium silicate was used as an adsorbent in a TSA process and was loaded on a Ljungstrom rotary heat exchanger to capture CO_2 by swinging the temperature from 450°C to 750°C or above. He used a liquid natural gas (LNG) fired furnace for heat generation in order to regenerate the adsorbent. The proposed CO_2 wheel had a compact and simple design as well as a continuous steady operation. In addition, there was no need to increase or decrease flue gas pressure. For a 250-MW coal-fired power plant, he proposed a wheel 20 m in diameter and 1.5 m in depth that would capture 63% of the total CO_2 output of the plant with an expected purity of 99%. The CO_2 capture rate would be 169 ton/hr.

Merel et al. studied the use of a TSA process as a technology for CO_2 capture from a mixture of N_2 and 10% CO_2 by using Zeolite 13X [27]. Indirect thermal swing adsorption was used to separate CO_2 from N_2 by implementing indirect heating in the desorption phase. An internal coaxial heat exchanger was used to transmit heat to the adsorbent by steam, which condensed and transmitted its heat to the heat exchanger walls. In their study, a purge gas was not used, and so a stream of almost 100% concentration of CO_2 was collected after desorption. In this process, specific heat consumption was 7.9 GJ/ton CO_2, with the potential to achieve 5.9 GJ/ton CO_2 after optimization and scaling up the system.

The removal of CO_2 from flue gas by TSA was also studied by Konduru et al. [28]. Zeolite 13X was used as an adsorbent in this process. Carbon dioxide concentration was 1.5% at standard condition and the regeneration temperature was 135°C. Helium was used as a purge gas. The capturing capacity decreased from 78 g/kg to 60 g/kg after five cycles, and further decreased to 40 g/kg after eleven cycles.

Previous studies did not consider humidity and other impurities that exist in the flue gas streams; therefore, Li et al. studied the capture of CO_2 from flue gas streams with relative humidity of 95% [29]. The concentration of CO_2 was 12% at 30°C. Zeolite 13X also was used as an adsorbent. The recovery of CO_2 from the system dropped from 78.5% for a dry mixture to 60% for a humid mixture.

Zeolites are defined as inorganic polymer crystalline structures of alumino-silicates that link with cation elements (Na, K, Li, Mg, Cu, etc.) in extensive tetrahedra frameworks by sharing oxygen ions between AlO_4 and SiO_4. These structures form cavities and pores of different sizes, which can be occupied by different molecules such as CO_2, H_2O, and some hydrocarbons [30, 31]. Zeolites are potential candidates for capturing CO_2 emissions by adsorption. The adsorption capacity of different types of zeolites depends on several factors such as size, polarization power, Si/Al ratio, the polarity and size of the adsorbate molecule, and the presence of water or other gases. It also depends on adsorption conditions such as partial pressure and temperature [31]. Most of the work on zeolites for carbon capture has focused on large point sources such as power plants.

Bonenfant et al. discussed different factors affecting CO_2 adsorption on zeolites, particularly the presence of water [31]. The amount adsorbed at different feed pressures and temperatures was determined for different types of zeolites. The results of their study revealed that zeolites have a great potential for CO_2 adsorption. Moreover, the study concluded that Zeolite 13X is an attractive candidate for such a process.

There is extensive literature that discusses the CO_2 capture from large point sources by physical adsorption [32-37]. As previously noted, emissions from small dispersed sources, such as transportation, building, heating, and

deforestation activities contribute in almost 50% of the total CO_2 emissions. In addressing these distributed emissions, Lackner and Keith each proposed the idea of capturing carbon dioxide from the atmosphere by using chemical absorption and discussed its technical and economical feasibility [17, 19, 21, 23]; but these studies did not consider transportation and sequestration costs. Moreover, capturing CO_2 from air by adsorption was not investigated in detail, although adsorption was studied as a technology for capturing CO_2 from flue gases of power plants that have a relatively high concentration of CO_2 compared to that in air [32-37].

This study investigates the feasibility of adsorption as the separation technology in an integrated atmospheric carbon capture and sequestration system (CCS). The CCS system is considered to be made up of three major subsystems: a power plant, a carbon capture plant, and a transportation and storage system. The CO_2 wheel that was proposed by Shimomura for mass transfer in adsorption and desorption is used as the base case for the core process in the capture facility [26, 38].

A theoretical assessment is done to confirm that Zeolite 13X is a good candidate for capturing CO_2 from the atmosphere. This requires that its adsorption capacity is estimated in extremely low concentrations of CO_2 and at different temperatures.

Humidity is a major problem when capturing CO_2 by zeolite because of the preferential adsorption of water. Therefore, to avoid the impact of water content in the atmosphere, two techniques are considered in order to improve CO_2 separation performance and efficacy. These techniques include choosing a capturing plant location in an extremely arid environment and using a desiccant material prior to stripping CO_2 from the atmosphere.

2.6.3 Utility Requirements

The utility power plant for a CCS facility has to be chosen carefully to provide the needed thermal energy. A low carbon emission heat source is required to achieve maximum capture efficiency without offsetting emissions.

As noted above, in an atmospheric capture plant, the use of energy sources other than fossil fuels was recommended [31]. A nuclear power plant produces an extremely high amount of electrical and thermal energy per unit area, especially if compared with other zero emission sources such as wind and solar power. Unlike these zero emission sources, the output from a nuclear power plant can be adjusted to provide a large amount of thermal energy relative to electrical power. Its technology is considered to be mature and does not require any large-scale modifications to be applied. In addition, it produces almost zero emissions of CO_2. Therefore, Sherman proposed utilizing nuclear energy instead of fossil fuels powered utility plant to increase the net capturing efficiency of CO_2 in an air capture plant [39]. Following this reasoning, a nuclear utility power plant is the source of energy for the atmospheric CCS system proposed in this thesis. It is worth noting that implementing nuclear energy for this application has certain drawbacks. A nuclear power plant should operate at almost full capacity all the time. A high initial capital investment is needed for the development of such a plant, and decommissioning of a nuclear power plant incurs a significant expense. There are also public concerns with respect to safe operation, and storage and disposal of radioactive wastes. Regulatory issues involved in authorizing and licensing a new nuclear power plant generally take years to be approved in most jurisdictions [5]. Despite these drawbacks, nuclear energy remains the best choice for near-zero emission electrical and thermal energy compared to available alternatives.

Chapter 3 : Air Capture Plant Location

3.1 Overview

The location of the capturing plant has to be chosen carefully to have an efficient capturing process. The plant has to be built in an area of low humidity, ideally the driest spot on earth, because of Zeolite 13X's aggressive attraction to water vapour. Climate conditions for three locations are studied regarding temperature, absolute humidity, and wind speed & direction. The water content in the air at saturation increases exponentially with temperature increase. Refer to appendix II for further details. The three locations evaluated are: Alert in the Arctic, the Atacama Desert in Chile, and the Vostok region of Antarctica. Water content in air for each location will be estimated.

Ocean profiles around these locations will be assessed for the suitability as a location for deep ocean storage of CO_2. A depth of 3000 m or more will be the criteria for choosing those locations. For a 30 years plant, an air CCS plant requires a storage site of capacity of at least 9000 Mm^3. In this thesis, Google Earth software is used to estimate distances, elevations, and ocean depths.

3.2 Alert, Canada

Alert is situated in the northern part of Ellesmere Island, which is part of the Queen Elizabeth Islands. It is in the climate zone known as the polar desert, with a cold dry climate. Figure 3-1 shows the location of Alert in detail, which is considered the most northern establishment for humans on the earth, with installations for Canadian Forces as well as The Meteorological Service of Canada (MSC) [40]. The data collected from the MSC station is used in this analysis. The annual daily average temperature is -18°C with daily averages ranging from -33.4°C in the winter to 3.3°C in the summer. Wind speed ranges from 6.2 km/hr to 13 km/hr, with the predominant direction being west or northwest, except in June and July when it blows from the northeast [41]. The

saturated water content of air at -18°C is about 1100 ppm. The nearest suitable location is the Fram Basin in the Arctic Ocean which is located 670 km to the northwest of Alert. The capacity of CO_2 storage in the Fram Basin is limited because it is surrounded with water of 2000 m depth or less.

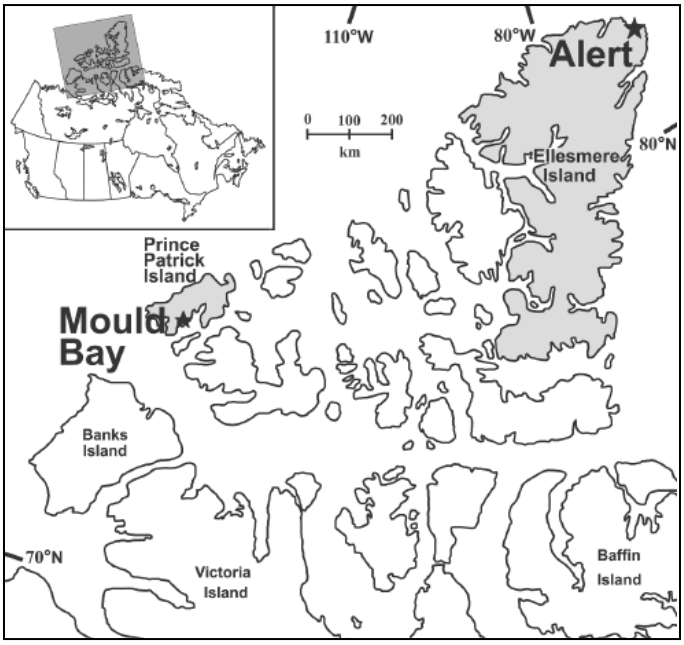

Figure 3-1: Location map of Alert in the Canadian Arctic [40]

3.3 Atacama, Chile

The Atacama Desert in Chile is one of the driest spots on the planet [43, 44]. It extends over 1000 km from 20° S to 30° S, bordered on the west by the Andes Mountains and on the east by the Pacific Ocean in South America. The driest spot in this plateau is from 22° S to 26° S [44]. Figure 3-2 shows the area.

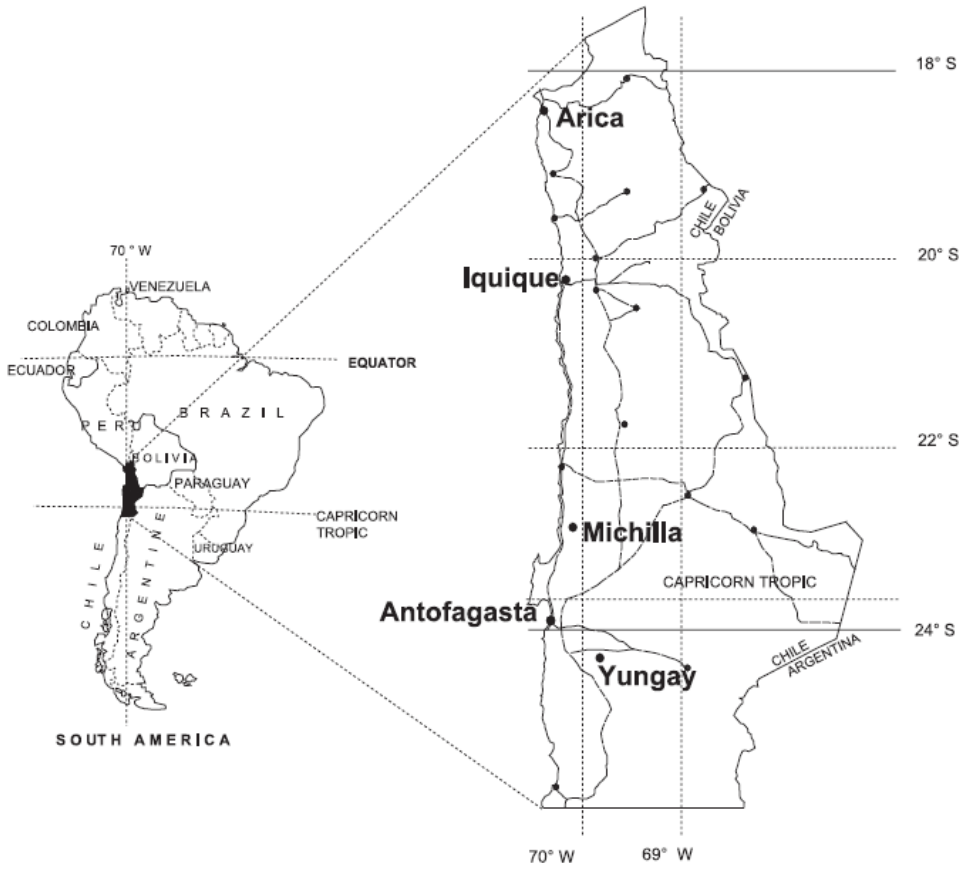

Figure 3-2 : Atacama desert in Chile [45]

The Atacama Desert has a wide range in altitude, from a few hundred meters above sea level (ASL) to over 5000 m; and temperature, humidity and wind speed vary significantly with altitude [46, 47]. The reported driest part of the desert is in the Yungay area, with a mean annual temperature of 16.6°C, and a relative humidity that can reach 70% [48, 49]. This region has an average annual wind speed of 10 km/hr with a predominant direction of west or northwest. The saturated water content of the air at 16.6°C is about 17700 ppm. The arid Yungay region is about 65 km from the Pacific coast, and a further 60 km from a suitable deep ocean disposal area. The capacity of CO_2 storage is huge because it is open to the Pacific Ocean.

3.4 Vostok, Antarctica

Vostok is located at the geomagnetic South Pole, approximately 1265 km from the geographical South Pole. It is in the East Antarctica region, the largest, coldest and driest region in Antarctica [50]. The coldest recorded temperature of -89.9^{o}C occurred at Vostok in July 1983. The area elevation ranges from 3400 m to 3700 m above sea level [51]. The average annual temperature is about -55.2°C, and ranges from an average of -31.9°C during summer to an average of -68.1°C in the winter. Average wind speed is reported to be 5 m/s [50]. Mean annual relative humidity is reported to be 67.8%. The saturated water content of the air at -55.2°C is only about 38 ppm. The cold and arid Vostok region is about 1350 km from the Southern Ocean coast at McMurdo Station, and a further 650 km from a suitable deep ocean disposal area. In the east there is another location which is suitable for deep ocean sequestration; however, due to the difficult terrain of this location and the fact that Antarctica's only permanent port is at McMurdo, the eastern location was not considered for deep ocean sequestration although it is 300 km shorter. The capacity of CO_2 storage is enormous because it is open to the Southern Ocean. Figure 3-3 shows the Antarctic contour map including McMurdo and Vostok research stations. Figure 3-4 shows the annual snow accumulation rate all over the Antarctica. Vostok has a very low snow accumulation rate of 20 kg/m^2 annually compared to the rest of the continent [51].

Of the three locations, Vostok, Antarctica was chosen as the preferred TSA capturing site location, because it is the driest spot in the driest continent on the planet. At mean annual temperatures and saturation conditions its atmosphere will hold only 38 ppm of water vapour compared to 1100 ppm and 17700 ppm for Alert and Atacama respectively. This low value of water content that ambient air can hold is due to the extreme cold weather in Vostok. The low moisture and water vapour content in the ambient air will maximize the CO_2 capturing efficiency of Zeolite.

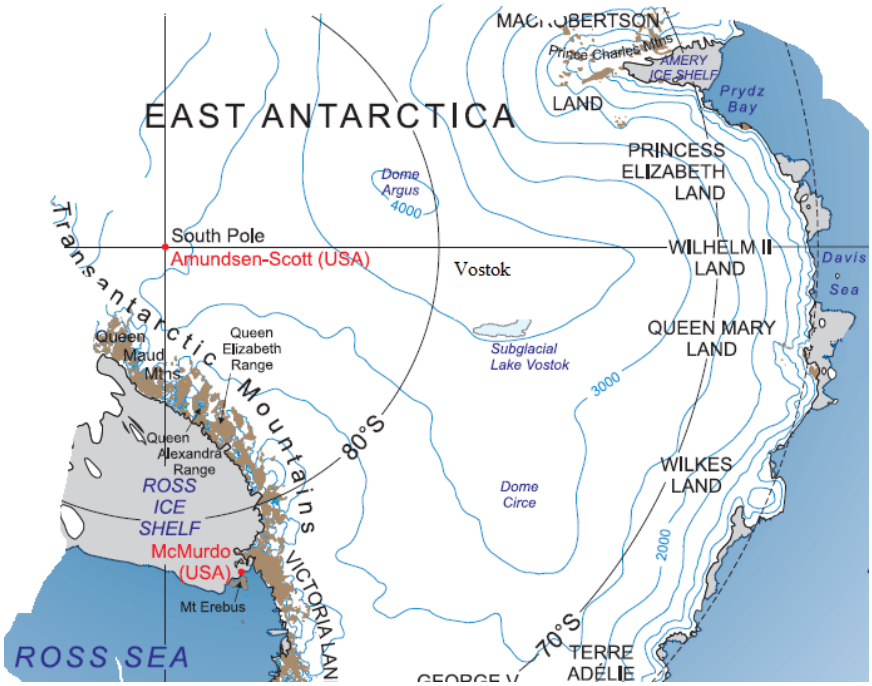

Figure 3-3 : Antarctica contour map showing Vostok and McMurdo [52]

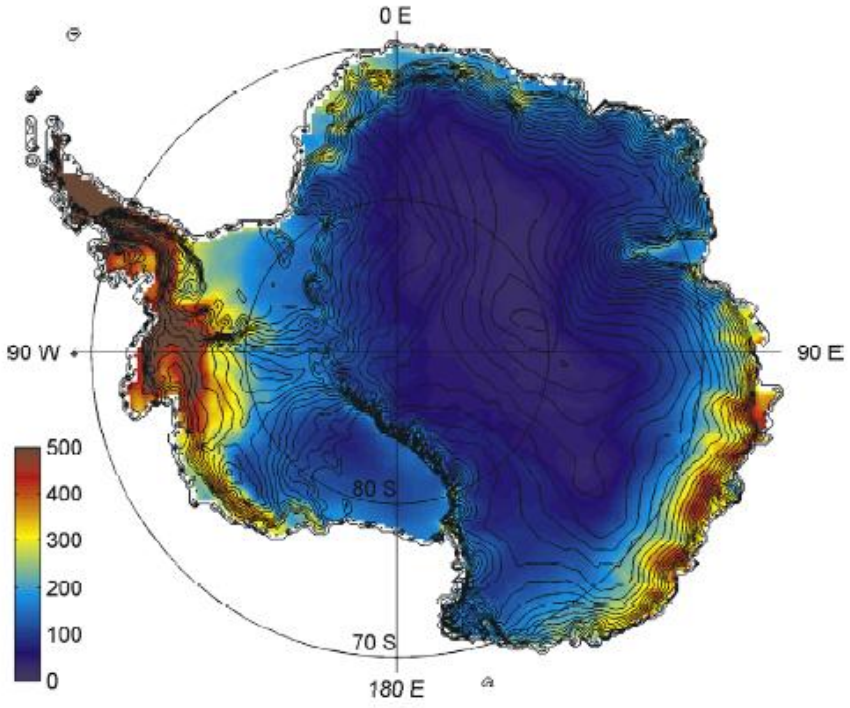

Figure 3-4 : Annual snow accumulation rate in Antarctica kg/m^2 [49]

In contrast, if a capturing site is built in the Atacama Desert where the minimum average relative humidity is 20%, then the atmosphere will hold about 3500 ppm of water vapour. This value is 9 times the carbon dioxide concentration in the atmosphere will lead to a decrease in adsorption efficiency by 90% compared to the dry condition adsorption as explained previously. To address the effect of ambient temperature and water content in the atmosphere on the process economics, two locations are chosen for the capturing plant: Vostok and Atacama. Vostok is located in an extremely remote area which makes construction of such project prone to uncertainties. In addition Vostok ocean sequestration disposal location is very far from the capturing plant compared to an Atacama site. Therefore, the total cost for both cases is determined then compared to stand on the effect of each parameter on the cost associated for each case. Other factors, such as regulatory frameworks for each jurisdiction, are not considered. Technical feasibility of a process flow sheet will be considered, followed by economic assessment.

Chapter 4 : Conceptual Design of an Air CCS System

4.1 Overview

As noted in Chapter 1, the total anthropogenic carbon emissions are about 8 GtC annually. Natural sinks absorb about 3.1 GtC of these emissions, while 4.9 GtC, equivalent to about 18 Gton of CO_2, are considered to be accumulated annually in the atmosphere [6]. In this study, the complete chain of carbon dioxide capture from air is studied to determine the feasibility of air capture as a complete CCS system. The nominal capacity of the proposed capture plant is 0.3 Gton of CO_2 annually. The selection of this plant capacity is arbitrary, but it is meant to be large enough to ensure that economies of scale are realized. The proposed CCS system can be broken down into three subsystems: a power plant, a capture plant, and a transportation and sequestration system as shown in Figure 4-1. These subsystems are explained in details in sections 4.4 and 4.5 for the locations under study.

As noted in Chapter 3, three locations were screened, and two, Vostok and Atacama, were selected for further evaluation. The initial design of the process is developed for Vostok, taking into consideration environmental and location parameter variations such as temperature, humidity, wind speed, and distance to the deposit site, and then the design is adapted to Atacama. Based on the process design, equipment, systems, and units needed for an air capture plant in Vostok are selected then sized in order to study the feasibility of the entire system. Consequently, key design parameters of the following items are investigated:

- Adsorption material selection
- Adsorption/desorption process
- Air CCS plant in Vostok
- Air CCS plant in Atacama

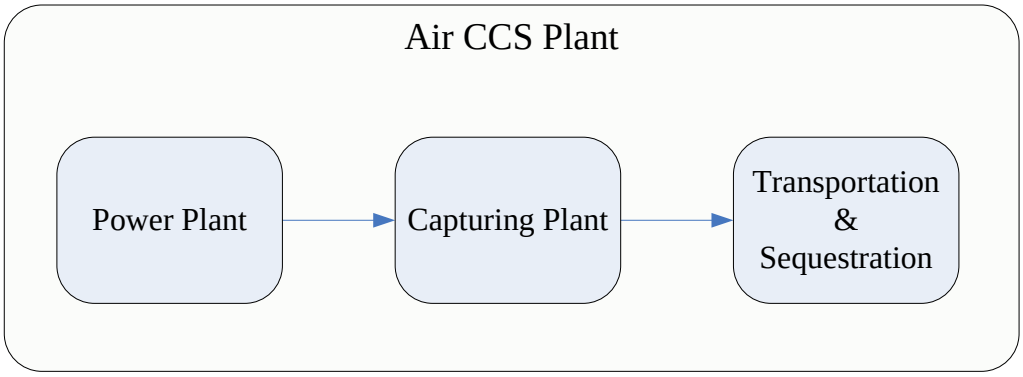

Figure 4-1 : Air carbon capture and sequestration plant

4.2 Adsorption Material Selection

One of the most important factors in designing an adsorption process is choosing the right adsorbent. The adsorbing material (adsorbent) should be selected carefully according to certain parameters. These parameters can be summarized as follows [12]:

- Preferential adsorbate adsorption: the adsorbent is highly selective for the adsorbate material (carbon dioxide in this case) relative to other components in the gas mixture (air).
- Low heat of adsorption: the energy needed for desorption, initiated either by a decrease in pressure or an increase in temperature, is not high.
- High working capacity of adsorbent: the higher the working capacity, the lower the quantity or volume of adsorbent needed for a given throughput of gas mixture; a high working capacity of an adsorbent leads to reductions in its bed size, energy requirement, related equipment size, and the associated capital costs.
- A steep adsorption isotherm: for a given working capacity, the low pressure or temperature differences are required for desorption, leading to a low energy penalty.

As discussed in Chapter 2 and based on the available literature, Zeolite 13X is considered a good candidate for CO_2 capture from the atmosphere [53]. The adsorption isotherms of Zeolite 13X with CO_2 and N_2 are compared with other adsorbents and types of Zeolites in Figure 4-2 and Figure 4-3. At very low concentrations of CO_2, Zeolite 13X has the highest working capacity compared to other adsorbents. Moreover, it has a good selectivity criterion for carbon dioxide adsorption versus other air components such as N_2. Zeolite 13X has also a very steep isotherm which makes it the best candidate for CO_2 capture process, especially at low concentrations of CO_2. However Figure 4-4 shows that Zeolite 13X has a high affinity to water vapour; therefore, in order to have an efficient separation of CO_2 from the atmosphere by adsorption, a dry environment is needed. Consequently, activated alumina (γAl_2O_3) is used as a pre-treatment desiccant material because it has a good selectivity for water vapor over the CO_2, as shown in Figure 4-3 and Figure 4-4.

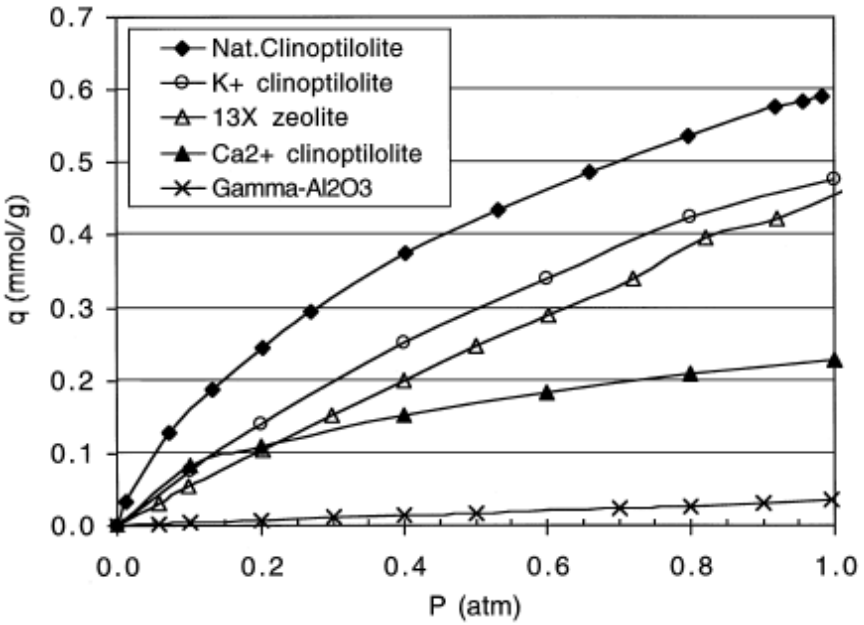

Figure 4-2 : Adsorption isotherms of N_2 at 22^{o}C for different adsorbents [53]

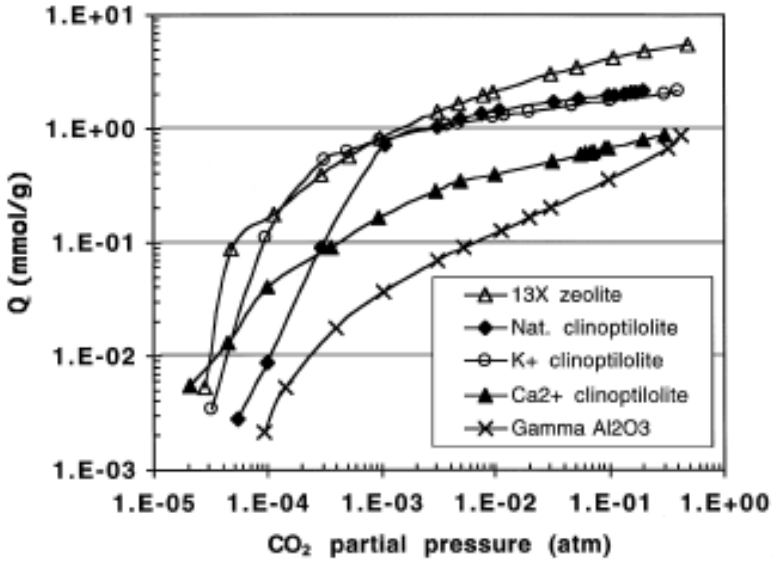

Figure 4-3 : Adsorption isotherms of CO_2 at 22°C for different adsorbents [53]

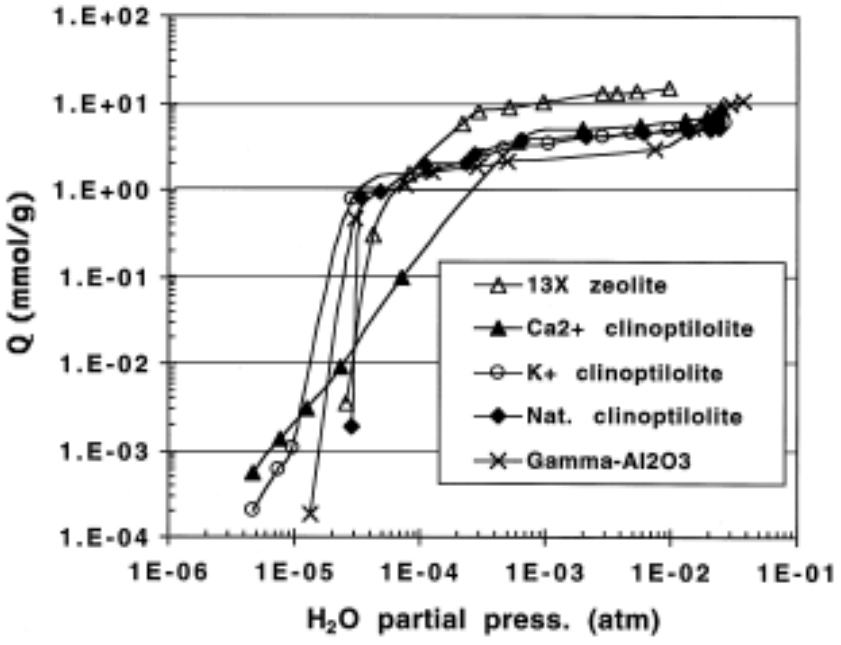

Figure 4-4 : Adsorption isotherms of H_2O at 22°C for different adsorbents [53]

4.3 Adsorption/Desorption Process

As discussed in Chapter 2, thermal swing adsorption (TSA) is used in the separation process to strip carbon dioxide from air. In order to design such a process, adsorption capacities of the different capture sites at ambient temperatures must be calculated. Generally, the adsorption process is presented graphically by isotherms that determine the working capacity of each adsorbent versus the concentration of a given component at a fixed temperature. Isotherms are represented mathematically by many models such as Langmuir and Toth adsorption models. Both models are used to represent adsorption and desorption values to calculate the adsorption capacity of a process. Adsorption and desorption values were calculated according to both models and compared with experimental results reported by Lee et al. [54]. The Toth equation models the reported experimental values more accurately than Langmiur's. In addition, Lee et al. recommended using the Toth model to represent the adsorption process of activated carbon and Zeolite due to its simplicity in addition to its correct representations at low and high concentrations of CO_2 [54]. Therefore the Toth model is used in this study to predict adsorption isotherms for temperatures and concentrations of CO_2 that have not been reported experimentally in the literature. The calculation procedure is explained in detail below.

The Toth model is represented mathematically by Equation 1.

$$q = \frac{ap}{(d + p^k)^{\frac{1}{k}}} \qquad [Eq\ 1]$$

where

q is the amount of moles of the adsorbate per the amount of the adsorbent (mol adsorbate/kg adsorbent)

p is the partial pressure of the adsorbate

a, d, k are adsorption constant parameters that vary with temperature.

Original experimental data used in the calculation are extracted from values reported in the literature [54]. The values of adsorption parameters a, d, and k at temperatures of 0^oC, 20^oC, 40^oC, 60^oC and 80^oC are also extracted from the reported values in literature [54]. Table 4-1 shows these values which are plotted graphically and then a trend line equation that best fit these values is developed. Figure 4-5 shows the plotted values of each parameter and the trend line equations which are developed according to these values. It also shows the regression values (R^2) of each equation which are 0.999, 0.992, and 0.998 for the parameters a, d, and k, respectively.

Table 4-1 : Adsorption parameters according to Toth model determined at different temperatures [54]

	Constants		
T (^oC)	a	d	k
0	9.01	0.311	0.168
20	8.28	0.436	0.19
40	7.51	0.591	0.213
60	6.94	0.936	0.25
80	6.44	1.19	0.265

The developed trend line equations predict the adsorption constant parameters (a, d, k) below 0^oC and higher than 80^oC. By calculating Toth model constants at each temperature, low and high temperature adsorption isotherm values are determined. Consequently, the adsorption capacity of the adsorbent is determined at different concentrations and temperatures of carbon dioxide. For further details see appendix III.

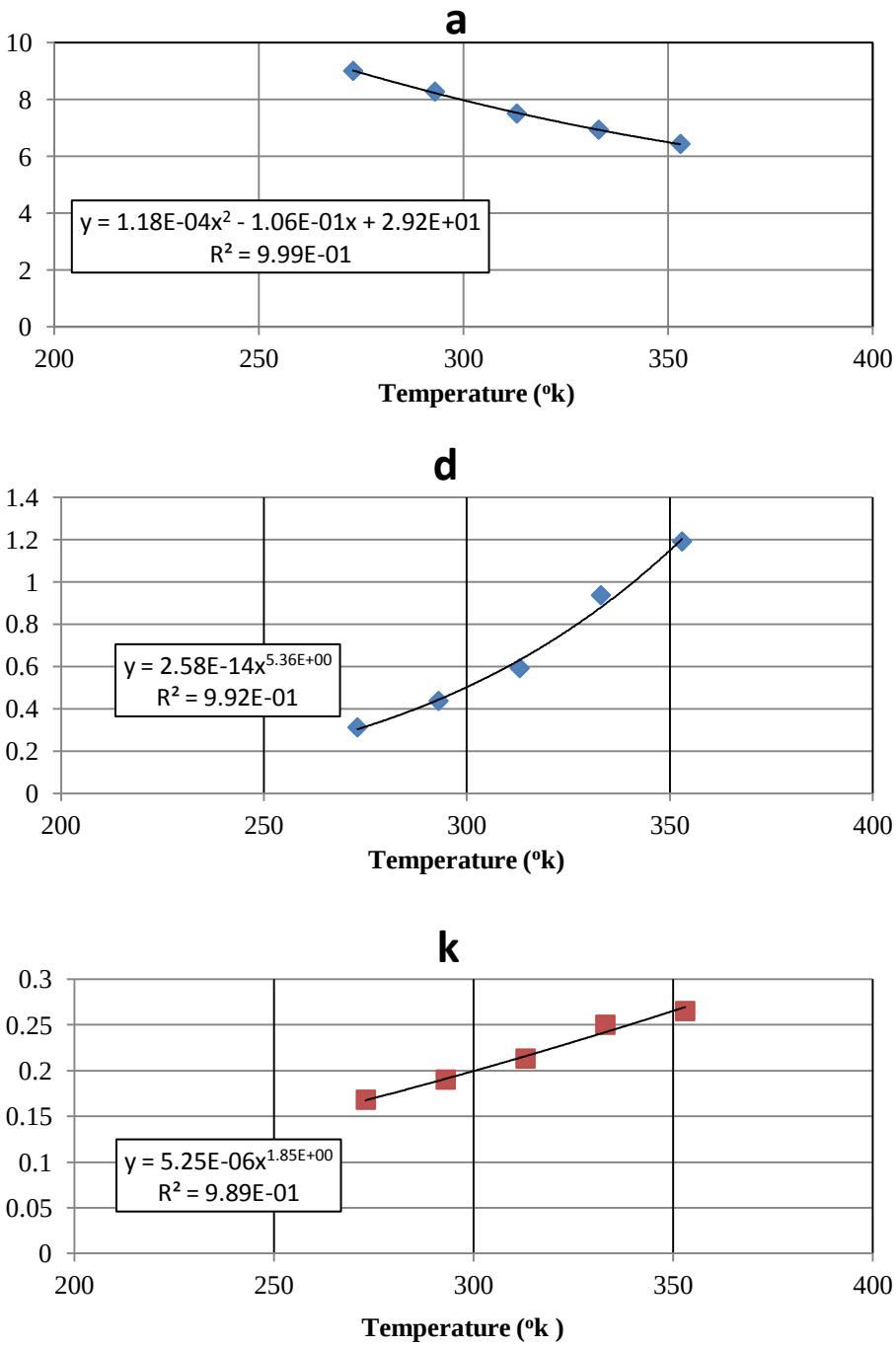

Figure 4-5 : Adsorption parameter constants at different temperatures [54]

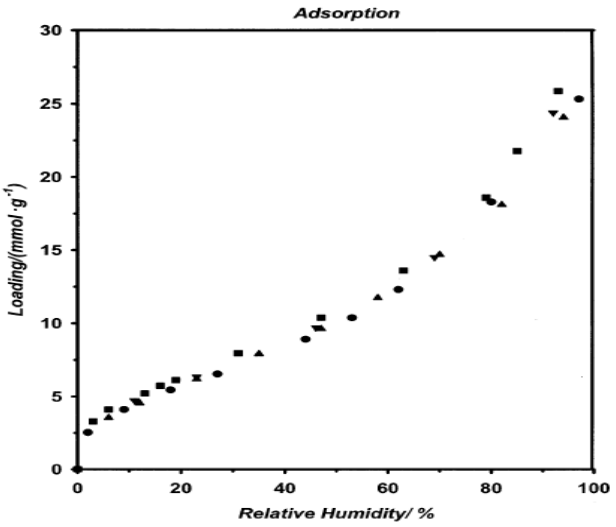

Figure 4-6 : Adsorption values for H_2O on F-200 at different temperatures: ▼, t=5°C; ▲, t=15°C; ■, t=25°C; ●, t=35°C [55]

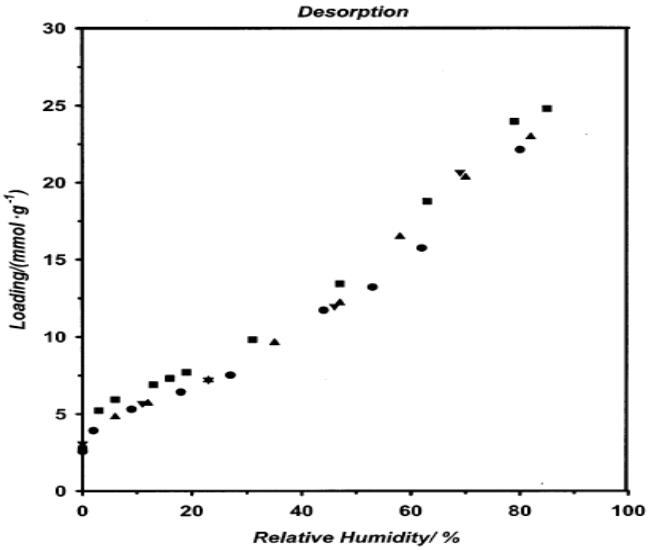

Figure 4-7 : Desorption values for H_2O on F-200 at different temperatures: ▼, t=5°C; ▲, t=15°C; ■, t=25°C; ●, t=35°C [55]

For removal of water content, according to reported literature F-200 activated alumina is selected because it is widely used in air drying processes in industry in a TSA process. Unlike CO_2 adsorption on Zeolite 13X, H_2O adsorption on activated alumina is independent of temperature at constant relative humidity

[55]. In other words, the adsorption and desorption values of H_2O with F-200 activated alumina is a function of relative humidity only. Figure 4-6 and Figure 4-7 are used to determine adsorption and desorption values for H_2O on F-200 activated alumina so that adsorption capacity can be determined and hence the desiccant wheel can be sized.

4.4 Air CCS Plant in Vostok

4.4.1 Overview

The proposed air CCS system is broken into three subsystems, power plant, capture plant, and transportation and sequestration system as shown in Figure 4-1. As noted in Chapter 2, a nuclear power plant is utilized to supply the needed electrical power and thermal energy for the separation process. It is also used to supply the power needed to compress and inject the purified and concentrated stream of CO_2 in the pipelines.

In the capture plant, thermal swing adsorption is used as a separation technology to strip carbon dioxide from air due to its effectiveness in purifying low pressure gas stream mixtures from low concentration gas impurities. A good example of such process is purifying air from carbon dioxide and water vapour in nitrogen and oxygen manufacturing processes. Currently, the carbon dioxide concentration in air is approaching 400 ppm which requires the use of consecutive TSA processes in the capture plant to achieve the necessary degree of concentration.

Transportation by pipelines is the most suitable method to transport massive amounts of CO_2, especially if there is a continuous production of it. On the other hand, tankers are better for offshore transportation if the distance to the disposal site is 500 km or more. In this work, the sequestration is in the deep ocean below

3000 m by forming a CO_2 lake, because CO_2 density is higher than water at that depth.

In conclusion, CO_2 is captured, concentrated, and purified in the capture plant. Nuclear power plant is used to provide the required energy for the process. Hence, CO_2 is pumped to the shipping port through pipelines where it is transported to a floating platform at the disposal site by giant CO_2 tankers. Afterwards, the CO_2 is injected through vertical pipelines into the deep ocean.

4.4.2 CO_2 Capture Plant

4.4.2.1 Main Equipment Selection

In an air capture system, a collecting element is needed to be in contact with the atmosphere to strip CO_2. The affinity of Zeolite 13X to adsorb water over CO_2 and the low concentration of CO_2 in the atmosphere (0.04%) necessitate three stages of TSA to effectively separate H_2O and CO_2 from air. The first stage is to strip water content from air to increase the adsorption efficiency of CO_2 on Zeolite 13X in the following stages. The second stage is to collect CO_2 from the atmosphere and increase its concentration to an intermediate concentration of 5%-10%. The final stage is to concentrate CO_2 to higher concentration of 80%-90%. Subsequently, cooling and compression is used to increase CO_2 concentration to more than 99%, removing other remaining impurities such as N_2 and O_2. Therefore the CO_2 capture plant involves two plants, a contacting towers plant which has many towers to collect CO_2 from the atmosphere and concentrate it by adsorption, and a single hub plant to collect the concentrated CO_2 stream and transfer it to the suitable form for transportation by compression and cooling. The scheme of capture plant is shown in Figure 4-8.

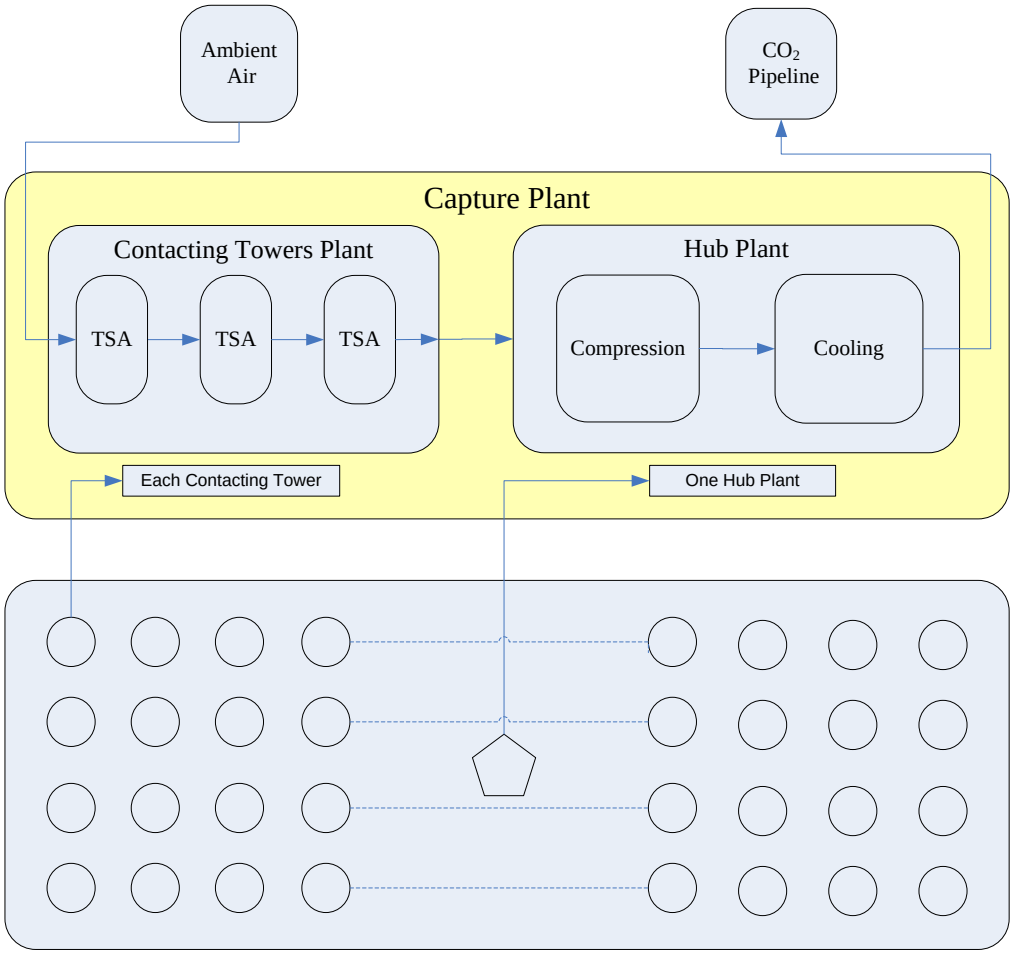

Figure 4-8 : Capture Plant Facilities and the Processes in each Facility

The main equipment required for the TSA adsorption process is adsorption beds, fans, and heating and cooling sources. Three wheels connected in series are used as adsorption beds for the three stages of TSA. These wheels are called contacting wheels: a desiccant wheel, CO_2 first stage wheel, and CO_2 second stage wheel. A fan is required to boost the pressure of CO_2 air stream mixture after the CO_2 first stage wheel. Heat exchangers are used either for heating or cooling processes where needed in order to provide the heating and cooling sources required for TSA process. The contacting wheels and heat exchangers are installed on the top of towers of 20 m height. These towers are built in four parallel rows perpendicular to the wind direction. The rows are separated by one kilometre

distance to avoid wind shadowing and to ensure that each row has the same concentration of carbon dioxide at the inlet ducts.

The main equipment required for the hub plant processes are compressors and heat exchangers. Figure 4-8 shows a schematic for the capture plant clarifying the process sequence in each facility. The contacting towers plant and hub plant are supplied with electrical power, high and low pressure steam, and refrigerant. The process steps are introduced below followed by a detailed sizing for the main equipment of the process.

4.4.2.2 Process Concept

Once the main equipment of the capture plant is selected, the process can be summarized as follows:

- Figure 4-9 shows the details of the process. Table 4-2 and Table 4-3 list the process stream parameters for the contacting towers plant and the hub plant such as pressure, temperature, and concentration.

- The wind speed is used as a natural mechanism for driving the ambient air through the desiccant wheel (E3) and CO_2 first stage wheel (E1). Water content and CO_2 are adsorbed by consequently. The clean air stream is then vented back to the atmosphere (Streams No. 2 & 3). The operation and structure of the wheels are clarified in section 4.4.2.3.1.

- The hot air direct heating and the steam indirect heating are used to increase the temperature of CO_2 first stage wheels (E1) in order to desorb the CO_2 (Stream No. 15). The hot air is also used as a carrier of the desorbed CO_2 to the next stages of the process (Streams No. 16).

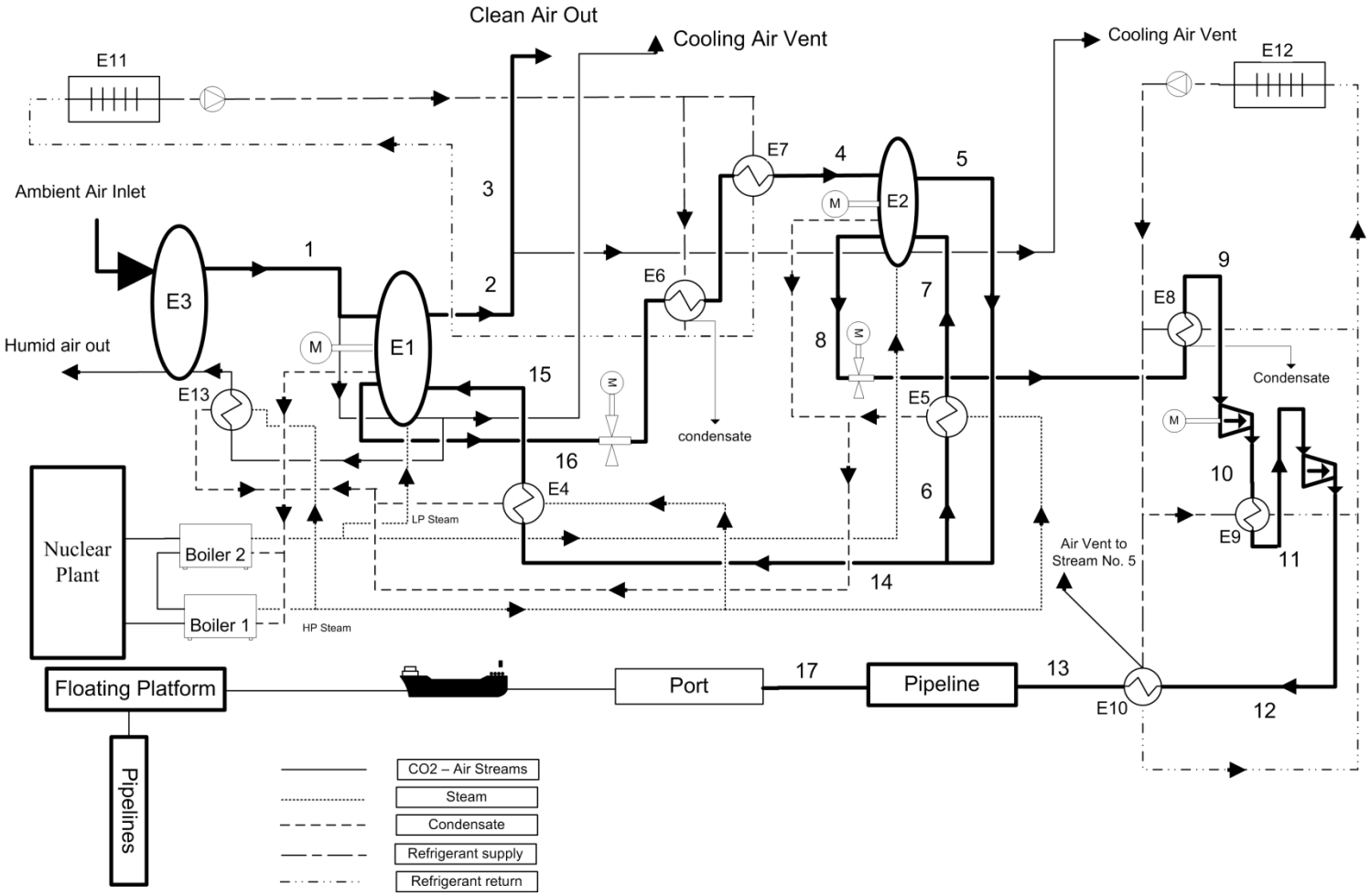

Figure 4-9 : Nuclear CO_2 air capture process in Vostok

Table 4-2 : Stream lines parameters of the main components in the contacting towers plant

	One Tower Process										
Stream No.	1	2	3	4	5	6	7	8	14	15	16
Mass flow rate (kg/s)	12,356	11,862	11,411	33.62	33.62	3.95	3.95	3.95	33.62	33.62	33.62
Concentration (v/v)	0.04%	0.004%	0.004%	10%	1%	1%	1%	90%	1%	1%	10%
Pressure (MPa)	0.067	0.067	0.067	0.1	0.1	0.1	0.1	0.1	0.1	0.1	0.1
Temperature (°C)	-40	-40	-40	-20	-20	-20	90	90	-20	100	100

Table 4-3 : Stream lines parameters of the main components in the hub plant and CO_2 pipeline

	Hub Plant / Compressor				Pipeline Upstream	Pipeline Downstream
Stream No.	9	10	11	12	13	17
Mass flow rate (CO_2) (kg/s)	1,157.41	1,157.41	1,157.41	1,157.41	10,416.0	10,416.0
Concentration (v/v)	90%	Not calculated	Not calculated	Not calculated	99%	99%
Pressure (MPa)	0.1	7.5	7.5	15	15	10
Temperature (°C)	5	260	5	260	40	-5

- The lower the temperature the higher the uptake of carbon dioxide on the CO_2 wheel. Therefore a cold air stream, which is branched off the main ambient dry inlet air (Stream No. 1), is used to cool CO_2 wheels before starting a new cycle. This air stream is vented back to the atmosphere (Stream No. 2). Moreover, the desorbed CO_2 which is diluted in hot air (Stream No. 16) is cooled by refrigerant in two heat exchangers (E6 & E7) connected in series before passing through the CO_2 second stage wheel (Stream No. 4). Condensed water is removed as a liquid between the two stages.

- In the third stage of TSA separation, axial fans are used to drive the desorbed CO_2 air stream mixture (Stream No. 16) through the CO_2 second stage wheel (E2). The operation and structure of the wheel are clarified in detail in section 4.4.2.3.1.

- The air stream is then re-circulated to both CO_2 wheels (Stream No. 5) for use as a purge gas for the CO_2 first stage wheel (Stream No. 14) and the CO_2 second stage wheel (Stream No. 6). This air stream is used as a purge gas because of its negligible humidity after passing through the desiccant wheel.

- Similar to the CO_2 first stage wheel, the hot air direct heating and steam indirect heating are used to heat the CO_2 second stage wheel (E2) in order to desorb the CO_2 (Streams No. 7). Axial fans are used to drive CO_2 hot concentrated stream through next stages of the process (Stream No. 8).

- All the desorbed CO_2 is then collected from different contacting towers. The concentrated CO_2 stream is then transferred to the hub plant where it is cooled in the pre-cooler heat exchanger (E8).

- Two stage compressors are used to increase the pressure of the CO_2 stream to 15 MPa. Between the two stages the CO_2 stream is cooled again in the inter-cooler heat exchanger (E9). After CO_2 is compressed, post-coolers (E10) are used in order to increase its concentration to more than 99%; non-condensable gas would be returned to the circulating dry air stream (Stream No. 5) where it is re-circulated to both CO_2 wheels.

- Cooling is provided by a circulating liquid refrigerant. This refrigerant is cooled in a separate finned cooler in each tower of the contacting towers plant and in centralized finned coolers in the hub plant. These heat exchangers are open to the atmosphere. Whether remote cooling of refrigerant in multiple units is more economical would be resolved in a future design analysis.

- The circulated air which is used to increase the contacting wheels temperature for regeneration purpose, is heated by air steam heat exchangers (E4 & E5 & E13).

- A pair of boilers through which hot liquid from the nuclear power plant flows in series is assigned for every ten contacting towers to generate high and low pressure steam for desorption purposes. The high pressure steam is used in the air steam heat exchangers, while the low pressure steam is used in CO_2 capture wheels. Using a hot circulating liquid from the nuclear power plant to carry heat out to distributed boilers reduces the risk of steam condensing and the resulting water freezing in the long pipe run from the power plant to the capturing towers.

4.4.2.3 Main Equipment Sizing

The sizing of key process equipment is crucial in order to determine the cost and economic feasibility of the whole project. These equipment and subsystems are

sized based on the nominal production capacity of the capture plant of 300 Mton CO_2/year. The number of the contacting towers are then determined based on the desorbed amount of CO_2 from the CO_2 second stage wheel taking into consideration the total operating hours in the year. Based on that, the key equipment such as contacting wheels, compressors and heat exchangers are sized. The process design and sizing of the main equipment for the previous process is based on the following assumptions:

1) The amount of CO_2 that exists in $1m^3$ of the atmosphere is 0.62 gm. This value is based on a concentration of 400 ppm by volume at an elevation of 3400 m.
2) In Vostok the average monthly temp from February to November is -40^oC or lower, while in January and December it reaches -30^oC. Since the adsorption capacity of CO_2 with Zeolite 13X is inversely proportional to the temperature, the capture plant is designed to be completely shut down during December for an annual maintenance turnaround. The turnaround would include all maintenance operations, the replacements of the adsorbents and the regeneration of the desiccant wheel. In addition, the low adsorption capacity of CO_2 in January is compensated by increasing the CO_2 wheels rotational speed in June, July, and August. The total operating hours of the plant per year is assumed to be 8000 hours.
3) The time needed to increase or decrease the temperatures in the main equipment is assumed to be negligible.

4.4.2.3.1 Contacting Wheels

The contacting wheels structure and operation is crucial in sizing those wheels. As noted in Chapter 2, the CO_2 capture wheel concept was proposed previously by Shimomura [26]. In this study, these wheels are loaded with Zeolite 13X as an adsorbent instead of lithium silicate which was the proposed adsorbent in the Shimomura study. The process of CO_2 capture by using CO_2 wheels is similar to the dehumidification process by using desiccant wheels where TSA adsorption process is used to strip water content from a stream of humid air. The contacting

wheels are the core equipment for the adsorption and desorption processes in the capture facility plant. Consequently, the desiccant wheels are loaded with activated alumina while CO_2 wheels are loaded with Zeolite 13X according to adsorption material selection analysis discussed in section 4.2.

Generally, the contacting wheels are regenerated continuously. Desiccant wheel diameter is selected to be of the same diameter of the first stage CO_2 wheel, while the thickness is determined based on the amount of water content in the atmosphere. The structure of desiccant wheels is similar to that of CO_2 wheels. The detailed design calculations are explained further in this section.

Both types of wheels are going through two processes, adsorption and desorption. These processes take place in the contacting wheels simultaneously but at different zones of the wheel. A third process is added for cooling the wheels before starting a new cycle; cooling increases the uptake of H_2O and CO_2 in the new cycle. Consequently, during the process each wheel is divided into three zones; adsorption, desorption and cooling as shown in Figure 4-10. The adsorption section represents 75% of the total facing area of the wheel, while the desorption and cooling sections represent 20% and 5%, respectively.

By rotating the CO_2 wheel, the saturated adsorption zone of the wheel moves to the hot zone which is the desorption zone as shown in Figure 4-11. Thermal energy is used to increase the temperature of the wheels and the adsorbent to the desorption temperature and provides the thermal energy needed for desorption (the enthalpy of the adsorption process) [53]. The direct heating is generated by a stream of hot air which is moved through the desorption zone of the wheel and the adsorbent. The indirect heating is generated by the condensation of the low pressure steam which is injected in distributed piping inside the wheel. (The detailed design of these wheels is out of the scope of this study.) In the CO_2 first stage wheel, direct heating produces only 10% of the total thermal energy needed while indirect heating produces 90% of that energy. In the CO_2 second stage, the

indirect heating percentage increases to 97% to increase the CO_2 concentration to 90% after the CO_2 second stage wheel. Similar to the CO_2 wheels, desiccant wheels are regenerated by providing thermal energy to the wheel and the adsorbent to increase their temperature to the desorption temperature, at which the relative humidity of the air is low enough to desorb the water. The thermal energy needed for H_2O desorption is provided by direct heating only.

The water mass flow rate determines the thickness of the desiccant wheels. The TSA process low temperature for the desiccant wheel, CO_2 first stage wheel, and second stage wheel are -40°C, -40°C, and -20°C, respectively, while the high temperatures are 160°C, 100°C, and 120°C, respectively. These temperatures are used to determine the adsorption capacity in each stage based on the concentration of the adsorbate as noted in section 4.3.

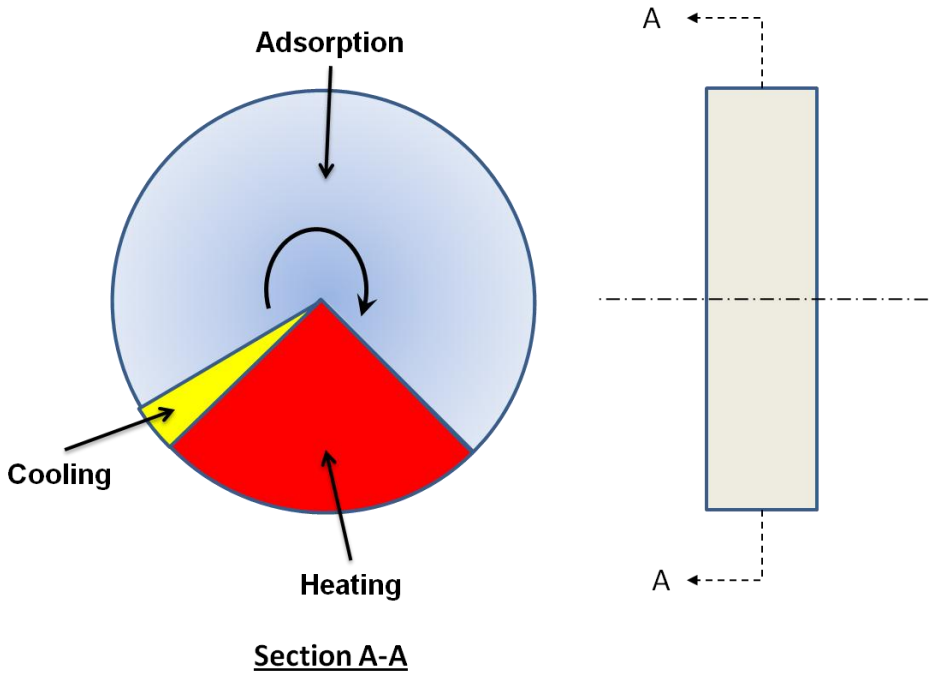

Figure 4-10 : Contacting wheels zones

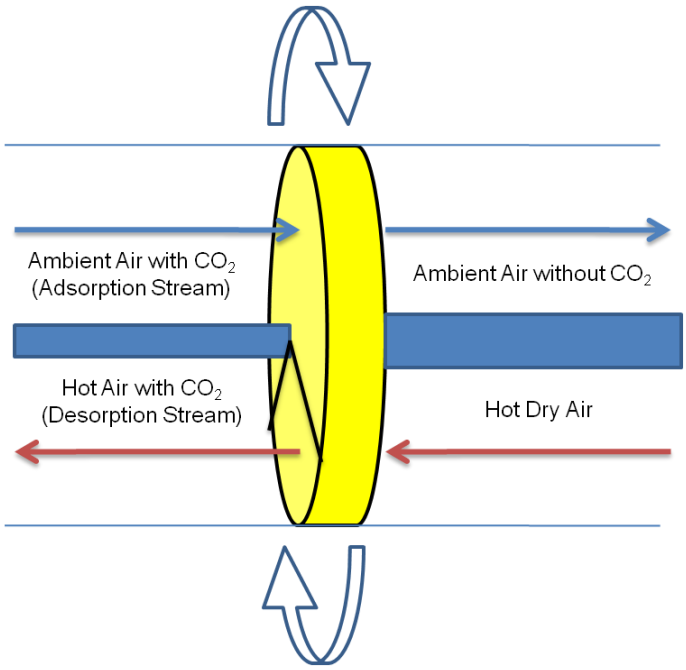

Figure 4-11 : CO_2 wheel process proposed by Shimomura in 2003 [26]

The following assumptions are developed to simplify the mass flow rates and the energy requirements of CO_2 wheels:

1) Thermal transfer efficiency is assumed to be 100%, i.e. all heat supplied by the heating medium is transferred to the material (i.e. the process is adiabatic).
2) Adsorption efficiency is assumed to be 90%.
3) The time needed to saturate the CO_2 first stage wheel is set to be 50 minutes, a value used in other experimental studies [28]. In the second stage wheel, the time is set to 20 minutes due to the increase of CO_2 concentration.
4) Zeolite bulk density is assumed to be 0.65 kg/L [27]. The bulk density is the weight of Zeolite 13X per unit volume of the bed (wheel in this case). The wheel steel structure is assumed to represent 20% of the total wheel weight while Zeolite 13X represents 80%. These values are used to calculate the heat required for regeneration.
5) The enthalpy of adsorption is a constant value of 780MJ/ton CO_2 [53].

6) Mechanical power which is needed to rotate the CO_2 wheels and fans is neglected.
7) The high pressure steam line temperature and pressure are 220^{o}C and 2.3 MPa, while the low pressure steam line temperature and pressure are 120^{o}C and 0.22 MPa.
8) Carbon dioxide concentration in the desorbed stream is calculated by dividing the rate of the CO_2 moles desorbed per hour by the sum of CO_2 moles desorbed per hour plus the hot air moles passing through the regeneration zone per hour.

The first stage CO_2 wheel is sized based on the largest currently available rotary heat exchanger which is of 20 m diameter and 1.5 m in thickness according to the reported literature [26]. Consequently, the amount of Zeolite 13X used in the wheel is calculated according to its bulk density. The adsorption capacity of CO_2 is determined according to the adsorbed and desorbed values which are calculated according to the Toth model. In addition, according to the time needed for saturation and the percentage of the processing area (adsorption area) to the total area, the time needed for the wheel to complete one cycle is calculated by using Equation 2.

$$t_{cycle} = \frac{t_{sat}}{A_p\%} \qquad [Eq\ 2]$$

where

t_{sat} is the time needed for saturation (min)

t_{cycle} is the cycle time (min)

$A_p\%$ is the percentage of process surface area to the total wheel area

Hence, the amount of CO_2 which is captured by the first wheel is calculated per revolution then per hour. Table 4-4 shows the first stage contacting wheel operational parameters and dimensions. It also shows the rate of desorbed carbon

dioxide per wheel. Equations 3 and 4 are used to calculate the mass flow rate of CO_2 for the CO_2 first stage wheel.

$$\dot{m}_{\,CO2\ Des\ per\ rev} = V_{wheel} \times M_w \times \rho_{bulk} \times n_{Des} \qquad [Eq\ 3]$$

$$\dot{m}_{\,CO2\ Des\ per\ hour} = m_{CO2\ Des\ per\ rev} \times \frac{60}{t_{cycle}} \qquad [Eq\ 4]$$

where:

V_{wheel} is wheel volume (m^3)

M_w is molecular weight (g/mol CO_2)

ρ_{bulk} is Zeolite 13X bulk density (kg 13X/L)

n_{Des} is the number of moles of CO_2 desorbed per unit weight of Zeolite 13X at certain pressure and temperature (mol CO_2/kg 13X)

Table 4-4 : CO_2 first Stage wheel parameters

Parameter	Value	Unit
Inlet CO_2 Concentration per unit volume air	0.62	gm/m^3
Molar Adsorption @ -40°C & 0.04% CO_2 v/v	2.76	molCO_2/kg13X
Efficiency of Adsorption Process	90.00%	
Molar Desorption @ 100°C & 10% CO_2 v/v	1.88	molCO_2/kg13X
Time needed for Saturation (t_{sat})	50	min
Cycle Time (t_{cycle})	66.67	min
Adsorption Temperature($T_{Ads\ first\ wheel}$)	-40	°C
Desorption Temperature($T_{Des\ first\ wheel}$)	100	°C
Wheel diameter	20	m
A_p%	75.00%	
Wheel total Surface Area	314	m^2
Wheel Processing Area	235.5	m^2
Wheel Thickness	1.5	m
V_{wheel}	471	m3
ρ_{bulk}	0.65	kg/L
$\dot{m}$ *Zeolite to be heated /rev*	306.2	ton/rev
$\dot{m}$ *Steel to be heated /rev*	61.2	ton/rev
$\dot{m}_{CO2\ Des\ per\ revolution\ 1st\ stage}$	22.8	ton/rev
Wheel Speed	0.90	r.p.hr.
$\dot{m}_{CO2\ Des\ per\ hour\ 1st\ stage}$	20.5	ton/hr

The thermal energy requirement for the wheel is the sum of the process enthalpy and the thermal energy needed to increase the wheel structure and the adsorbent to the desorption temperature. Based on the enthalpy of adsorption and the heat capacity of the steel and the Zeolite 13X, the thermal energy needed to increase the temperature of the wheel materials to the desorption temperature is calculated by using Equation 5. Table 4-5 shows the assumed heat capacities for the steel and the Zeolite 13X, the total thermal energy requirement for the wheel, and the specific thermal energy for the CO_2 first stage wheel.

$$\dot{Q} = \dot{m}\, c_p dt \qquad [Eq\ 5]$$

where:

$\dot{Q}$ is the thermal energy required per revolution (kJ/rev)

$\dot{m}$ is the mass to be heated per revolution (kg/rev)

c_p is heat capacity (kJ/kg^{o}K)

dt is temperature difference (^{o}K)

Table 4-5 : Heat requirements for CO_2 first stage wheel

Parameter	Value	Unit
Zeolite Heat Capacity ($C_{p\ Zeolite}$)	1.3	kJ/kg^{o}K
Steel Heat Capacity ($C_{p\ Steel}$)	0.49	kJ/kg^{o}K
$\dot{m}$ *Zeolite to be heated /rev*	306.2	ton/rev
$\dot{m}$ *Steel to be heated /rev*	61.2	ton/rev
$\dot{Q}$ *needed for Zeolite /rev*	55.7	GJ/rev
$\dot{Q}$ *needed for steel /rev*	4.2	GJ/rev
$\dot{Q}$ *needed for Desorption /rev*	17.8	GJ/rev
Total Thermal Energy / rev	77.7	GJ/rev
Total Specific Thermal Energy	3.4	MJ/kg CO_2

Based on the total thermal energy requirement for each wheel, the amount of thermal energy that should be provided by direct heating is calculated. The amount of hot air required for regeneration is calculated by using Equation 6.

$$\dot{m}_{hot\ air} = \frac{\dot{Q}_{hot\ air}}{C_p dt} \qquad [Eq\ 6]$$

where:

$\dot{m}_{hot\ air}$ is mass flow rate of air.

$\dot{Q}_{hot\ air}$ is thermal energy rate delivered by hot air.

C_p is air heat capacity at certain temperature.

dt is temperature difference.

The minimum amount of the ambient air that should be processed to produce such amount of CO_2 per revolution is calculated by using Equation 7.

$$F_{air\ needed} = \dot{m}_{CO_2\ Des} \times \frac{1000}{\rho_{CO_2}} \qquad [Eq\ 7]$$

where:

$F_{air\ needed}$ is the minimum air flow needed to be processed by natural draft (m^3/hr).

$\dot{m}_{CO_2\ Des}$ is the desorbed mass flow rate of CO_2 (kg/hr).

ρ_{CO_2} is the amount of CO_2 that exists in unit volume of air (g/m3).

Based on the average annual wind speed in Vostok of 5 m/s and the adsorption facing area, the maximum air flow that can flow through the adsorption zone is calculated by using Equation 8.

$$F_{air\ available} = v_{\ wind} \times A \qquad [Eq\ 8]$$

where:

$F_{air\ available}$ is the flow of air (m^3/hr)

$v_{\ wind}$ is the wind speed (m/s)

A is the cross section area (m^2).

Since the natural air draft is used as a mechanism to drive the air into the system, the increase in the cross section area of the wheel is calculated by dividing the needed flow by the maximum allowable flow. Since, the air amount which is

processed is not enough to produce the required amount of CO_2, the inlet cross sectional area is increased as shown in Table 4-6. A plenum is used to capture the required air flow.

Based on the mass flow rate of air and the mass flow rate of the desorbed CO_2, the CO_2 concentration in the desorption line is calculated as shown in Table 4-6.

Table 4-6 : Needed air flow for CO_2 first stage wheel and the concentration in the desorption stream

Parameter	Value	Unit
$F_{air\ needed}$	33.6	(10^6) m^3/hr
$\dot{m}_{Air}$	13.1	ton/s
v_{wind}	5.00	m/s
$F_{air\ available}$ *(natural Air draft)*	4.2	(10^6) m^3/hr
Air flow increasing ratio	6	
$A_{Inlet\ Duct}$	1,884	m^2
Concentration of CO_2 in Air	400	ppm
No. of CO_2 moles per hour	466	(10^3) moles/hr
Desorbed CO_2 volume rate per hour	14.5	(10^3) m^3/hr
No. of moles of Air in desorption per hour	4,332	(10^3) moles/hr
Air flow rate	134.4	(10^3) m^3/hr
Concentration of desorbed CO_2 (By Volume)	10%	

The desiccant wheel is sized based on the air flow required for the CO_2 wheel. Water content is determined based on the following assumptions:

1) Ambient air temperature is assumed to be -40°C.
2) Water content of air at saturation is calculated.
3) Adsorption capacity is then determined based on average relative humidity of 60% in adsorption.
4) Desiccant wheel diameter is assumed to be 20 m and the thickness is determined based on the amount of water content in the flow and the adsorption capacity with at least 0.25 m thickness.
5) The heat of adsorption is 46 kJ/mol H_2O [56].

6) The time needed to saturate the desiccant wheel is set to be one hour.

7) Activated alumina bulk density is 769 kg/m^3 [56].

Water vapour saturation pressure over ice is calculated by using the Goff Gratch formula [57]. The Gratch formula is mathematically represented by Equation 9. The water content in a given amount of air at certain temperature is then calculated by using Equation 10.

$$\log_{10} p_i = -9.09718\left(\frac{273.16}{T-1}\right) - 3.56654\log_{10}\left(\frac{273.16}{T}\right) + 0.876793\left(\frac{1-T}{273.16}\right) + \log_{10}(6.1071) \qquad [Eq\ 9]$$

where

p_i the saturation partial pressure over ice (hPa)

T the ambient temperature (^{o}K)

$$x = 0.62198 \times \frac{p_i}{p_a - p_i} \qquad [Eq10]$$

where

x the water content in the atmosphere (kg $_{water}$ / kg $_{dry\ air}$)

p_a the atmospheric pressure

Saturation partial pressure at -40^{o}C is approximately 0.125 mbar. The concentration of water vapor at saturation is about 125 ppm at the same temperature. The water content is 0.08 gm $_{water}$ / kg $_{dry\ air}$. Adsorption capacity is calculated according to adsorption and desorption charts of H_2O on F-200 activated alumina [55]. Accordingly, a desiccant wheel of 20 m diameter and 25 cm thickness holds a sufficient amount of activated alumina to adsorb all the water content from the inlet ambient air flow. The desiccant wheel (E3) has to be

regenerated continuously by a stream of hot dry air which is heated through air steam heat exchanger.

The size of the CO_2 second stage wheel is selected based on the amount of desorbed CO_2 from the previous stage (CO_2 first stage wheel). The same methodology is used to calculate the different parameters of this stage. These parameters are the mass flow rate of air needed to get 90% concentration of CO_2 at 120^{o}C, the second CO_2 wheel dimensions, operating temperatures and the amount of captured carbon dioxide.

Table 4-7 : CO_2 Second stage wheel parameters and outputs

Parameter	Value	Unit
$\dot{m}_{CO2\ Des\ per\ hour\ from\ 1st\ stage}$	20.5	ton/hr
Air flow rate	134.4	(10^3) m^3/hr
Inlet CO_2 Concentration per unit Volume	158.34	gm/m^3
$T_{Ads\ second\ wheel}$	-20	^{o}C
$T_{Des\ secondwheel}$	120	^{o}C
Molar Adsorption @ -20^{o}C & 10% CO_2 v/v	4.07	mol/kg
Efficiency of Adsorption Process	90%	
Molar Desorption @ 120^{o}C & 90% CO_2 v/v	2.26	mol/kg
A_p%	75.00%	
Time needed for Saturation (t_{sat})	20.00	min
Cycle Time (t_{cycle})	26.67	min
$\dot{m}_{CO2\ Ads\ per\ hour\ per\ kg\ Zeolite}$	0.22	kg/kg 13X hr
$m_{Zeolite\ needed\ for\ processing}$	91.7	ton
ρ_{bulk}	0.65	kg/L
V_{wheel}	141	m^3
Wheel thickness	1.50	m
Wheel diameter	11	m
Wheel Speed	2.25	rph
$\dot{m}_{CO2\ Des\ per\ rev\ 2nd\ stage}$	8.2	ton/rev
$\dot{m}_{CO2\ Des\ per\ hour\ 2nd\ stage}$	18.5	ton/hr
No. of CO_2 moles per hour	420	(10^3) moles/hr
Concentration of Desorbed CO_2	90.00%	
No. of moles of Air per hour	46.6	(10^3) moles/hr
$\dot{m}_{Air}$	0.38	kg/s
Temperature Difference (dt)	120	^{o}C
$T_{Air\ inlet\ (Desorption)}$	210.00	^{o}C
$T_{Air\ outlet\ (Desorption)}$	90	^{o}C

Table 4-7 shows the operating parameters of this stage. Therefore, the number of wheels needed to produce 300 Mton/year is determined based on total operation hours of 8000 hours. In addition, the thermal energy needed for this wheel is calculated by using the same methodology used in the CO_2 first stage wheel. Table 4-8 shows the heat requirement for the second stage wheel per unit weight of CO_2.

Table 4-8 : Heat Requirements for second Stage Wheel

Parameter	Value	Unit
$C_{p\ Zeolite}$	1.30	kJ/kg^{o}K
$C_{p\ Steel}$	0.49	kJ/kg^{o}K
$\dot{m}_{\ Zeolite\ to\ be\ heated\ /rev}$	91.7	ton
$\dot{m}_{\ Steel\ to\ be\ heated\ /rev}$	18.3	ton
$\dot{Q}_{needed\ for\ Zeolite\ /rev}$	16.7	GJ/rev
$\dot{Q}_{needed\ for\ Steel\ /rev}$	1.3	GJ/rev
$\dot{Q}_{needed\ for\ Desorption\ /rev}$	6.4	GJ/rev
Total Thermal Energy / rev	24.4	GJ/rev
Total Specific Thermal Energy	3	MJ/kg CO_2

4.4.2.3.2 Compressors

CO_2 has to be in the supercritical dense form to be transported through a pipeline in order to avoid material and operational problems of the two phase flow. Cavitation in the components or blockage of the pipeline due to the formation of solid ice is an example of such problems. Therefore, carbon dioxide pressure has to be more than 7.38 MPa and its temperature should not be less than -60^{o}C to avoid solid ice formation [10]. Therefore, all CO_2 concentrated stream lines that are captured by the contacting towers plant are collected in the hub plant to be cooled, compressed, and then cooled again to be in the dense form for pipeline transportation. Refer to appendix I for more details.

In the hub plant, Ramgen compressing technology is used instead of the conventional compressing technologies [58]. Ramgen is a novel technique for

compressing CO_2 by using supersonic shock waves. The novel technique enables the compressor to achieve a compression ratio of 1:100 by only two stages instead of 5 to 8 stages if the conventional technology is used [58]. The number of required compressors is calculated based on the manufacturer's technical specifications which give the maximum inlet flow of carbon dioxide per compressor of 1157 kg/s. Hence nine compressors are needed. For further details see appendix IV.

The pre-cooling, inter-cooling, and post-cooling heat exchangers are sized based on the mass flow rate and temperature difference of each heat exchanger. Table 4-9 shows the inlet and outlet temperatures of carbon dioxide stream in the pre-cooler, inter-cooler and post-cooler and the amount of heat needed to be extracted at each stage.

Table 4-9 : Heat needed to be extracted in the hub plant

Parameter	Value	Unit	Notes
Max. inlet for each compressor	21,400	cfm	
	36,400	m^3/min	
$\dot{m}_{CO2}$ (By weight)	37.5	(10^6) kg/hr	For the Whole Plant
Density at compressor Inlet	1.90	kg/m^3	
$\dot{m}_{CO2}$ (By volume)	19. 7	(10^6) m^3/hr	
	328	(10^3) m^3/min	
No. of Compressors	9		
$\dot{m}_{CO2}$ (By weight)	1157	kg/s	Per Compressor
$C_{P\ CO2\ at\ 120C}$	0.92	kJ/kg^{o}K	
$C_{P\ CO2\ at\ 260C}$	1.03	kJ/kg^{o}K	
$C_{p\ CO2\ at\ -25C}$	0.79	kJ/kg^{o}K	
$T_{in\ Pre\text{-}cooler}$	90	^{o}C	
$T_{out\ Pre\text{-}cooler}$	5	^{o}C	
$T_{in\ Inter\text{-}cooler}$	260	^{o}C	
$T_{out\ Inter\text{-}cooler}$	5	^{o}C	
$T_{in\ Post\text{-}cooler}$	260	^{o}C	
$T_{out\ Post\text{-}cooler}$	40	^{o}C	
$Q_{Pre\text{-}cooler}$	90.4	MW	Per Compressor
$Q_{Inter\text{-}cooler}$	304	MW	Per Compressor
$Q_{Post\text{-}cooler}$	201.4	MW	Per Compressor

4.4.2.3.3 Heat Exchangers

Heat exchangers are used in the proposed system in the contacting towers plant and in the hub plant for heating and cooling. Syltherm XLT is a synthetic heat transfer fluid made of silicon polymers. It is chosen to be used in the proposed system because of its low freezing temperature (-100^{o}C), high boiling temperature (260^{o}C) and good thermal stability [59]. Therefore, the fluid is used for cooling and heating. The heat exchangers and coolers are sized based on the thermal energy rate either added or extracted. The following assumptions are used to size the heat exchangers:

1) Thermal efficiency in the heat exchangers is assumed to be 100% (adiabatic operation).
2) The overall heat transfer coefficient is obtained from the available table in the Delta T Heat Exchangers website [60]. Table 4-10 shows these values for different types of heat exchangers used in the process. It also shows the different types of heat exchangers used in the proposed process.

The total surface area of the heat transfer medium which is needed to calculate the number of the heat exchangers required for transferring the thermal energy is calculated by Equations 11 and 12.

$$\dot{Q} = \dot{m}\, c_p dt \qquad [Eq\ 11]$$

where:

$\dot{Q}$ is thermal energy rate (MW).

c_p is heat capacity (kJ/kg^{o}K).

dt is temperature difference (^{o}K).

$$\dot{Q} = U\, A\, LMTD \qquad [Eq\ 12]$$

where:

$\dot{Q}$ is heat transfer rate (MW).

U is overall heat transfer coefficient (W/m^{2o}K).

A is the surface area of heat transfer medium (m^{2}).

$LMTD$ is the Log Mean Temperature Difference.

Table 4-10 : Overall Heat Transfer Coefficient

Exchanger No.	Exchanger Name	Type	Fluids inside the Exchanger		Service	Overall Heat Transfer Coefficient ($W/m^{2o}K$)
			Shell Side	Tube Side		
(E4&E5&E16)	Air steam Heat Exchanger (Wheels)	Shell-Finned tube	Air	Steam	Air Heater	700
(E6&E7)	Air cooler (Wheels)	Shell-Finned tube	Air	Coolant	Air Cooler	400
(E8)	Pre-cooler (Hub)	Shell-Finned tube	CO_2	Coolant	CO_2 Cooler	400
(E9)	Inter-cooler (Hub)	Shell – Bare tube	CO_2	Coolant	CO_2 Cooler	300
(E10)	Post-cooler (Hub)	Shell – Bare tube	CO_2	Coolant	CO_2 Cooler	300
(E11&E12)	Coolant cooler (Wheels & Hub)	Atmospheric finned tube	N/A (Atmospheric)	Coolant	Coolant Cooler	500

4.4.2.3.3.1 Air Steam Heat Exchangers

In air steam heat exchangers, the steam is passed through finned tubes, while the cold air is flown outside these tubes within the heat exchanger shell as shown in Figure 4-12. Consequently, the overall heat transfer coefficient (U) is assumed to be of the same value of air cooled heat exchanger for steam condensation which is 700 $W/m^{2o}K$. Table 4-11, Table 4-12, and Table 4-13 show the operating temperatures, thermal energy rates and the contact surface area of the air steam heat exchangers which are used in the contacting towers plant. The total heat transfer areas of the air steam heat exchangers of the desiccant wheel, CO_2 first stage wheel, and CO_2 second stage wheel are 2000, 2800, and 30 ft^2, respectively. These heat exchangers are of pressure rating of 3.1 MPa (450 psi).

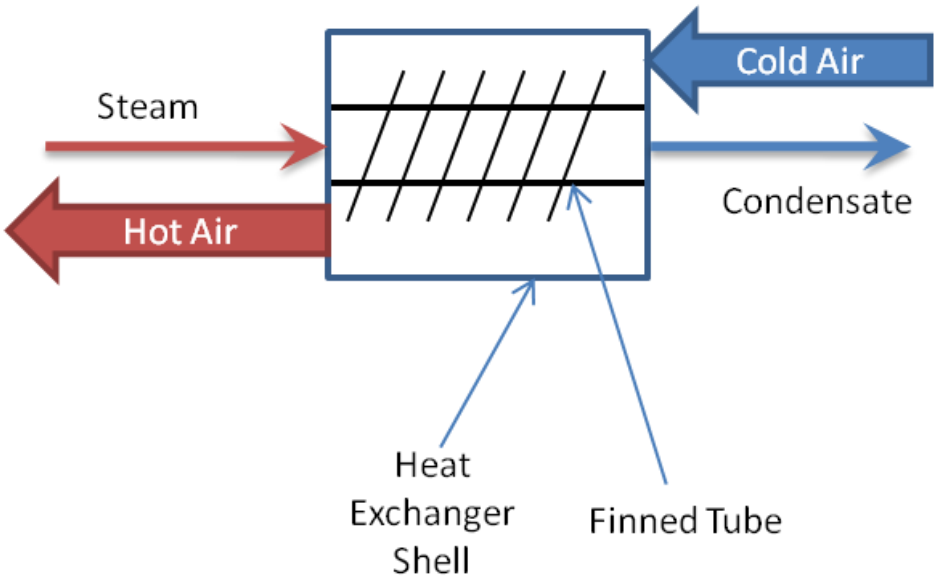

Figure 4-12 : Scheme for air steam heat exchangers clarifying the structure and inlet and outlet streams

Table 4-11 : Heat exchanger parameters for desiccant wheel

Parameter	Value	Unit
$T_{steam\ in}$	220	^oC
$T_{steam\ out}$	100	^oC
$T_{Air\ in}$	-40	^oC
$T_{Air\ out}$	210	^oC
U	700	$W/m^{2o}K$
$LMTD$	49.26	
$\dot{Q}$	6.3	MW
$Area$	183	m^2
$Area$	2000	ft^2
Number of heat Exchangers	1	Per Wheel

Table 4-12 : Heat exchanger parameters for CO_2 first stage

Parameter	Value	Unit
$T_{steam\ in}$	220	^oC
$T_{steam\ out}$	100	^oC
$T_{Air\ in}$	-20	^oC
$T_{Air\ out}$	210	^oC
U	700	$W/m^{2o}K$
$LMTD$	44.27	
$\dot{Q}$	8.1	MW
$Area$	260	m^2
$Area$	2800	ft^2
Number of heat Exchangers	1	Per Wheel

Table 4-13 : Heat exchanger parameters for CO_2 second stage

Parameter	Value	Unit
$T_{steam\ in}$	220	^oC
$T_{steam\ out}$	100	^oC
$T_{Air\ in}$	-20	^oC
$T_{Air\ out}$	210	^oC
U	700	$W/m^{2o}K$
$LMTD$	44.27	
$\dot{Q}$	0.09	MW
$Area$	2.8	m^2
$Area$	30	ft^2
Number of heat Exchangers	1	Per Wheel

4.4.2.3.3.2 Air Coolers Heat Exchangers

The cooling of the air CO_2 stream mixture before the CO_2 second stage wheel is performed in two stages by using two heat exchangers connected in series, cooler I and cooler II. The first is used for condensing any traces of water content by cooling the air stream to 5^{o}C, while the second is used to increase the adsorption capacity of the second stage by decreasing the stream temperature to -20 ^{o}C. Similar to air steam heat exchangers, the refrigerant is pumped through finned tubes, while the hot air is passed outside these tubes within the shell of the heat exchanger. Hence, the overall heat transfer coefficient (U) for these coolers is assumed to be of the same value of air-cooled heat exchanger for liquids which is 400 W/m^{2o}K. Table 4-14 and Table 4-15 show the operating temperatures, heat capacities, the mass flow rates of the coolant and the stream mixture for both coolers, and the total thermal energy rate needed to be extracted. The mass flow rate of the coolant and thermal energy rate are used to size the heat exchanger that is used to extract the heat from the coolant. The heat transfer area of the coolers is also determined by using Equations 11 and 12. The heat exchangers are of pressure rating of 1 MPa (150 psi).

Table 4-14 : Air cooler I between both CO_2 stages

Parameter	Value	Unit
$\dot{m}_{\text{Air}}$	34.9	kg/s
$T_{hot\ in}$	100	^{o}C
$T_{hot\ out}$	5	^{o}C
$C_{p\ Air}$	1.009	kJ/kg^{o}K
$\dot{Q}$	3.34	MW
$C_{p\ Syltherm}$	1.6	kJ/kg^{o}K
$T_{cold\ in}$	-35	^{o}C
$T_{cold\ out}$	0	^{o}C
$\dot{m}_{Syltherm}$	59.7	kg/s
U	400	W/m^{2o}K
LMTD	65.48	
Area	127.6	m^{2}
Area	1373	ft^{2}
Number of Coolers	1	

Table 4-15 : Air cooler II between both CO_2 stages

Parameter	Value	Unit
$\dot{m}_{Air}$	34.9	kg/s
$T_{hot\ in}$	5	^oC
$T_{hot\ out}$	-20	^oC
$C_{p\ Air}$	1.005	kJ/kg^oK
$\dot{Q}$	0.88	MW
$C_{p\ Syltherm}$	1.6	kJ/kg^oK
$T_{cold\ in}$	-35	^oC
$T_{cold\ out}$	-20	^oC
$\dot{m}_{Syltherm}$	36.5	kg/s
U	400	W/m^{2o}K
$LMTD$	19.58	
$Area$	112	m^2
$Area$	1204	ft^2
$Number\ of\ Coolers$	1	

4.4.2.3.3.3 CO_2 Coolers Heat Exchangers

In the hub plant, pre-coolers are used to cool the CO_2 concentrated stream before the compressors to 5^{o}C, while the inter-coolers and post-coolers are used to cool the concentrated stream between compression stages and after the compressors to 5^{o}C and 40^{o}C, respectively. These heat exchangers are of pressure rating of 1 MPa (150 psi), 8.3 MPa (1200 psi), and 15.1 MPa (2200 psi), respectively. Therefore, pre-coolers are similar in structure to the previous coolers, while inter-coolers and post-coolers are shell and tube heat exchangers due to the high pressure of CO_2. The overall heat transfer coefficient (U) for shell and tube heat exchanger is assumed to be of the same value which is 300 W/m^{2o}K for tubular cooling of high pressure gases by liquid. Accordingly, the overall heat transfer coefficients (U) for the pre-coolers, the inter-coolers, and the post-coolers are 400, 300, and 300 W/m^{2o}K, respectively. Table 4-16, Table 4-17, and Table 4-18 show the pre-cooler, inter-cooler, and post-cooler operating parameters. One pre-cooler, 16 inter-coolers and 8 post-coolers are used for each compressor. Table 4-19 shows the cooling loads, the operating temperatures and the total mass flow rate of the coolant needed for the pre-coolers, the inter-coolers and the post-coolers in the hub plant.

Table 4-16 : Pre-cooler operating parameters

Parameter	Value	Unit
$CO_2\ T_{in}$	90	^oC
$CO_2\ T_{out}$	5	^oC
$T_{cold\ in}$	-35	^oC
$T_{cold\ out}$	5	^oC
U	400	$W/m^{2o}K$
LMTD	59.64	
$\dot{Q}$	90.4	MW
Area	3787	m^2
Area	40,763	ft^2
Number of Heat Exchangers	1	Per Compressor

Table 4-17 : Inter-cooler operating parameters

Parameter	Value	Unit
$CO_2\ T_{in}$	260	^oC
$CO_2\ T_{out}$	5	^oC
$T_{cold\ in}$	-35	^oC
$T_{cold\ out}$	5	^oC
U	300	$W/m^{2o}K$
LMTD	116.07	
$\dot{Q}$	304	MW
Area	8,730	m^2
Area	94,000	ft^2
Number of Heat Exchangers	16	Per Compressor

Table 4-18 : Post-cooler operating parameters

Parameter	Value	Unit
$CO_2\ T_{in}$	260	^oC
$CO_2\ T_{out}$	40	^oC
$T_{cold\ in}$	-35	^oC
$T_{cold\ out}$	-25	^oC
U	300	$W/m^{2o}K$
LMTD	153.93	
$\dot{Q}$	201.4	MW
Area	4,362	m^2
Area	47,000	ft^2
Number of Heat Exchangers	8	Per Compressor

Table 4-19 : Cooling loads in the hub plant

	$C_{p\ Syltherm}$ (kJ/kg^{o}K)	T_{in} (^{o}C)	T_{out} (^{o}C)	$\dot{Q}$ (MW)	$\dot{m}_{Syltherm}$ (Ton/s)
Pre-cooler	1.6	-35	5	90.4	1.4
Inter-cooler	1.6	-35	5	304	4.7
Post-cooler	1.6	-35	-25	201.4	12.6
For the whole Hub plant / each compressor				595.8	18.7

4.4.2.3.3.4 Coolant Coolers Heat Exchangers

In the coolant coolers heat exchangers either for the contacting towers plant or in the hub plant, the overall heat transfer coefficient (U) is assumed to be 500 W/m^{2o}K. By using Equations 11 and 12, the total thermal energy rate is 4.62 MW for each pair of CO_2 wheels in series; hence the total area of the coolant cooler exchangers in each contacting tower is 7,124 ft^2. Table 4-20 shows the operating parameters for the wheels exchangers. It also shows that in the contacting towers plant, only one finned coolant cooler is used for each set of wheels (each tower). In further detailed design, grouping these exchangers into a central cooling plant similar to that of the hub plant can be evaluated. Table 4-21 shows the operating parameters for the coolant coolers in the hub plant. The total thermal energy rate in the coolant coolers of the hub plant is 5.4 GW; therefore 88 finned coolers are used in the hub plant each of total surface area of 150000 ft^2. All the coolers are made of carbon steel with a pressure rating of 1 MPa (150 psi).

Table 4-20 : Wheels coolant cooler heat exchanger

Parameter	Value	Unit
$\dot{m}_{Syltherm}$	96.17	kg/s
C_p	1.60	kJ/kg^{o}K
T_{in}	-5.00	^{o}C
T_{out}	-35.00	^{o}C
$\dot{Q}$	4.62	MW
LMTD	13.95	
U	500.00	W/m^{2o}K
Area	662	m^2
Area	7,124	ft^2
Number of Heat Exchangers	1	Per Wheel

Table 4-21 : Hub plant coolant cooler heat exchangers

Parameter	Value	Unit
$\dot{m}_{Syltherm}$	169.2	ton/s
C_p	1.60	kJ/kg^{o}K
T_{in}	-15.00	^{o}C
T_{out}	-35.00	^{o}C
$\dot{Q}$	5.4	GW
LMTD	10.80	
U	500.00	W/m^{2o}K
Area	1	(10^6) m^2
Area	10.8	(10^6) ft^2
Number of Heat Exchangers	72	

4.4.2.4 Design summary

In summary, the CO_2 capture plant is divided into two plants, a contacting towers plant and hub plant. The contacting towers plant has 2031 towers, each with a desiccant wheel and a pair of CO_2 wheels connected in series. Direct heating of the wheels for regeneration purposes is provided by hot air which is heated through one air steam heat exchanger for each contacting wheel. The CO_2 air stream mixture is cooled by a coolant between both CO_2 wheels which in turn is cooled in a finned cooler of 662 m^2 area. In the hub plant the CO_2 streams from the contacting towers are collected and passed to nine compressors. Each compressor has one pre-cooler to decrease the stream temperature before being compressed by a two stage compressor. In each compressor 16 inter-coolers are used between the two stages of compression to cool the CO_2 stream down. After the compression, each stream is passed through 8 post-coolers to cool the stream and increase the CO_2 concentration to (99% v/v). All the cooling processes in the hub plant are provided by the coolant which is cooled in 88 coolers each of 14000 m^2.

4.4.3 Nuclear power plant for thermal and electrical energy

A nuclear power plant is utilized to produce the required thermal and electrical power. The thermal power is in the form of steam and is used to regenerate the adsorbent by heating of the wheels as well as the heating of purge air. Electrical power is used for all other power requirements and its generation efficiency in the nuclear power plant is assumed to be 30%.

The total thermal power needed for the contacting towers plant is the sum of the thermal power needed for regeneration of the desiccant wheel in addition to the two stages of CO_2 capture and concentration. The electrical power is determined based on the power required for operating CO_2 compressors in the hub plant, while and the power needed to rotate the wheels and operate the fans in the contacting towers plant is neglected. The compressors power requirement of 7.3 MW is determined based on the manufacturer's technical data sheet [58]. Table 4-22 shows the specific thermal energy for each stage of CO_2 capture and concentration, in addition to the power requirements of the compressors. It also shows the total thermal power requirement for the regeneration of desiccant wheels and CO_2 wheels. It is clear that the amount of the thermal energy needed for the regeneration process is much higher than the electrical energy needed for the whole plant. In other words, the nuclear plant is used mainly to produce heat instead of producing electricity.

Table 4-22 : Total power requirement for the capture plant

Parameter	Value	Unit
Specific Thermal Energy for CO_2 first stage Wheel	3.40	MJ/kgCO2
Specific Thermal Energy for CO_2 second stage Wheel	3.00	MJ/kgCO2
Total Specific Thermal Energy	6.40	MJ/kgCO2
Total Thermal Power for CO_2 Wheels	66.43	GWth
Total Thermal Power for Desiccant Wheels	5.77	GWth
Compressor Power	0.22	GWth
Total Power Needed from Nuclear Plant	72.42	GWth

4.4.4 Transportation & Sequestration

4.4.4.1 Overview

Due to the location of the disposal site, the transportation & sequestration system utilizes two subsystems, onshore and offshore. The onshore subsystem involves CO_2 pipelines to transport the carbon dioxide from the capture plant at Vostok to the shipping port at McMurdo station. The offshore subsystem consists of tankers, a floating platform, and vertical pipelines to transport CO_2 to the deep ocean. The CO_2 is transported by tankers to the offshore floating platform in order to be injected in the vertical pipelines. The CO_2 is then disposed at a depth of more than 3000 m. Transportation is already a mature and developed technology and its cost is not significant compared to the cost of capture [61].

4.4.4.2 The Onshore System

The onshore system utilizes two pipelines to transport the CO_2 from the capture plant in Vostok to the port at McMurdo station. As noted in Chapter 2, pipelines are the most cost efficient method to transport CO_2 in large amounts over long distances. Carbon dioxide physical properties play a major role in determining the proper operating parameters of CO_2 pipelines. For instance, at pressures lower than 0.52 MPa and temperature less than -56.5^{o}C, CO_2 transfers from the gaseous state to the solid state without going through the liquid phase as shown in Figure 4-13 [2]. Moreover, transportation of CO_2 at low pressures results in high pressure drop per unit length compared to high pressure transportation. Therefore, CO_2 is transported either in the supercritical phase or in the liquid phase. In this study, CO_2 is assumed to be transported in the supercritical phase. In Vostok, the ambient temperature drops to -70^{o}C and less during the winter; therefore CO_2 pipeline should be insulated and heat traced to avoid solid ice formation as shown in Figure 4-13 [2].

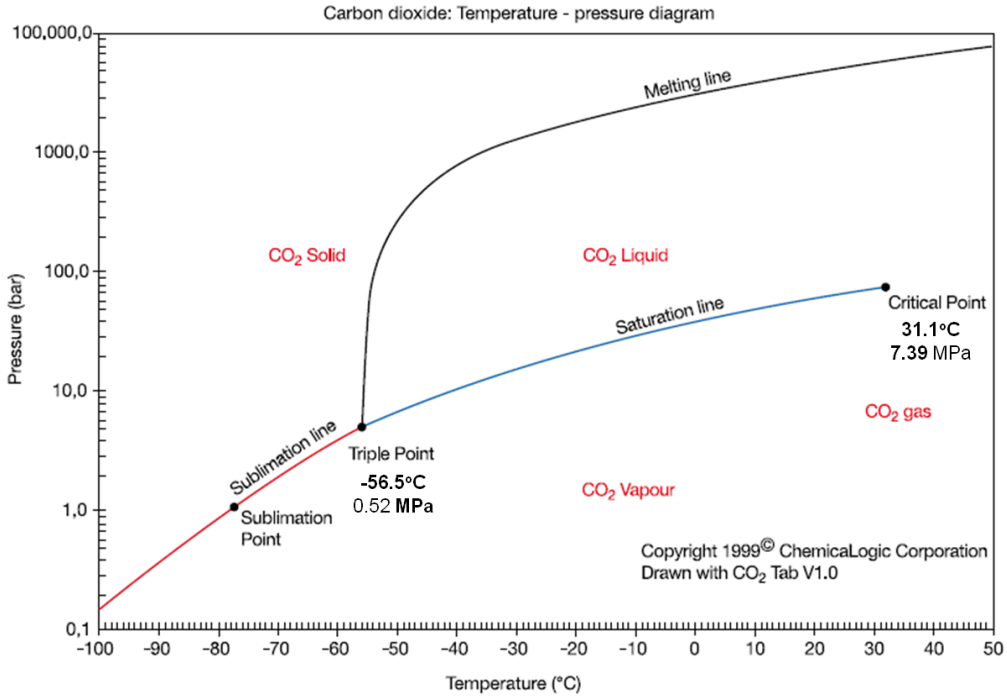

Figure 4-13 : CO_2 phase diagram [2]

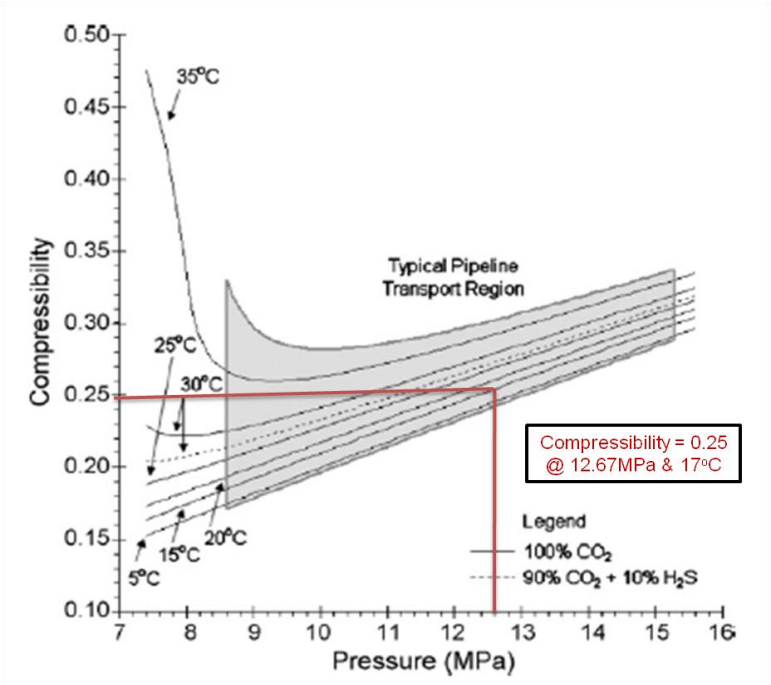

Figure 4-14 : CO_2 compressibility at pipeline operating range of pressure and temperature [62]

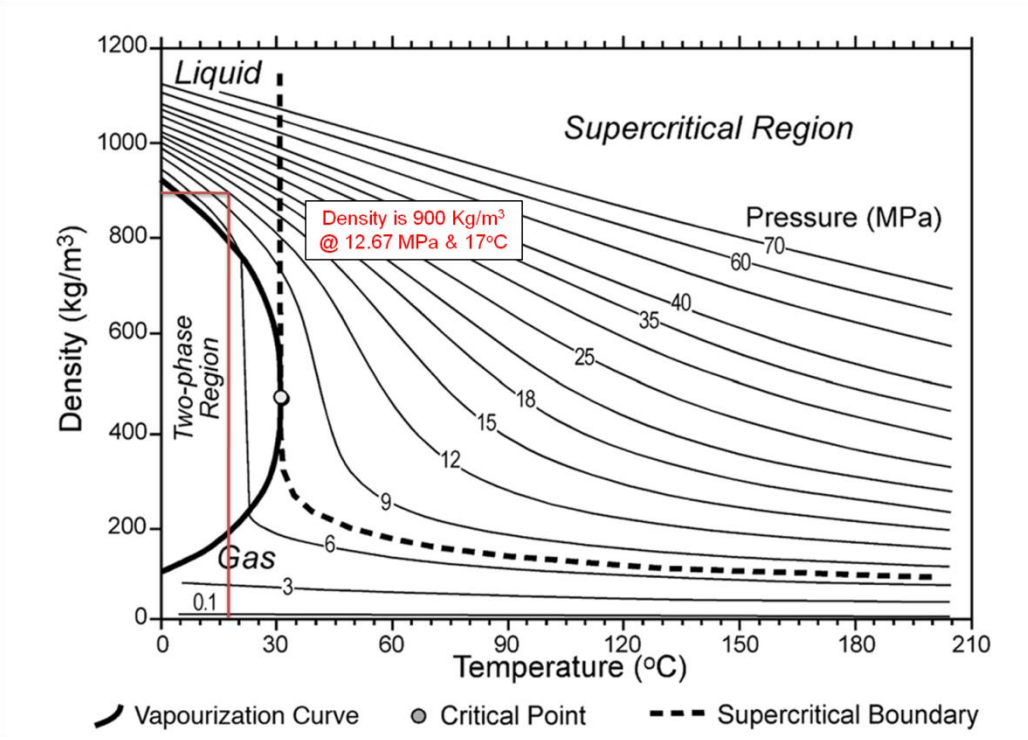

Figure 4-15 : CO_2 density at different pressures and temperatures [2]

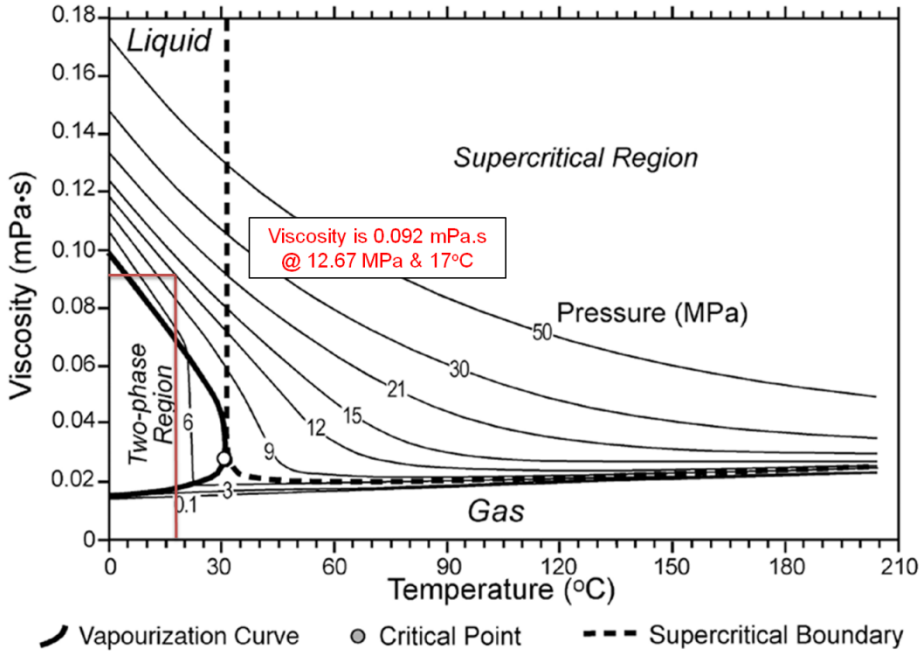

Figure 4-16 : CO_2 viscosity at different pressures and temperatures [2]

The pipeline dimensional properties have to be calculated to determine its cost. Since the distance between Vostok and McMurdo is approximately known, then the diameter must be calculated. Several assumptions are developed to calculate the pipeline diameter. These assumptions are as follows:

1) Vostok altitude is about 3400 m.
2) McMurdo station is on the sea level.
3) The distance from Vostok to McMurdo is approximately about 1200 km.
4) The upstream pressure is assumed to be 15 MPa, while the downstream pressure is assumed to be 10 MPa.
5) Upstream temperature is 40^{o}C, while downstream temperature is adjusted to be -5^{o}C by heat tracing the pipeline to control the CO_2 temperature.
6) Average compressibility factor, density, and viscosity are obtained and calculated based on the average operating pressure and temperature over the whole pipeline. A chart reported by McCoy is used to determine the compressibility, while two other charts were reported in IPCC report are used to determine the density and viscosity [2, 62, 62]. These charts are shown in
7) Figure 4-14, Figure 4-15, and Figure 4-16. The average compressibility, density, and viscosity are, respectively, 0.25, 900 kg/m^3, 8.6×10^{-5} Pa.s.
8) Pipeline internal diameter calculation is done by considering the pipeline as one segment.

An iterative method, which was reported by McCoy, is used to calculate CO_2 pipeline diameter [62]. The method is shown in Figure 4-17. The steps of the method are as follows:

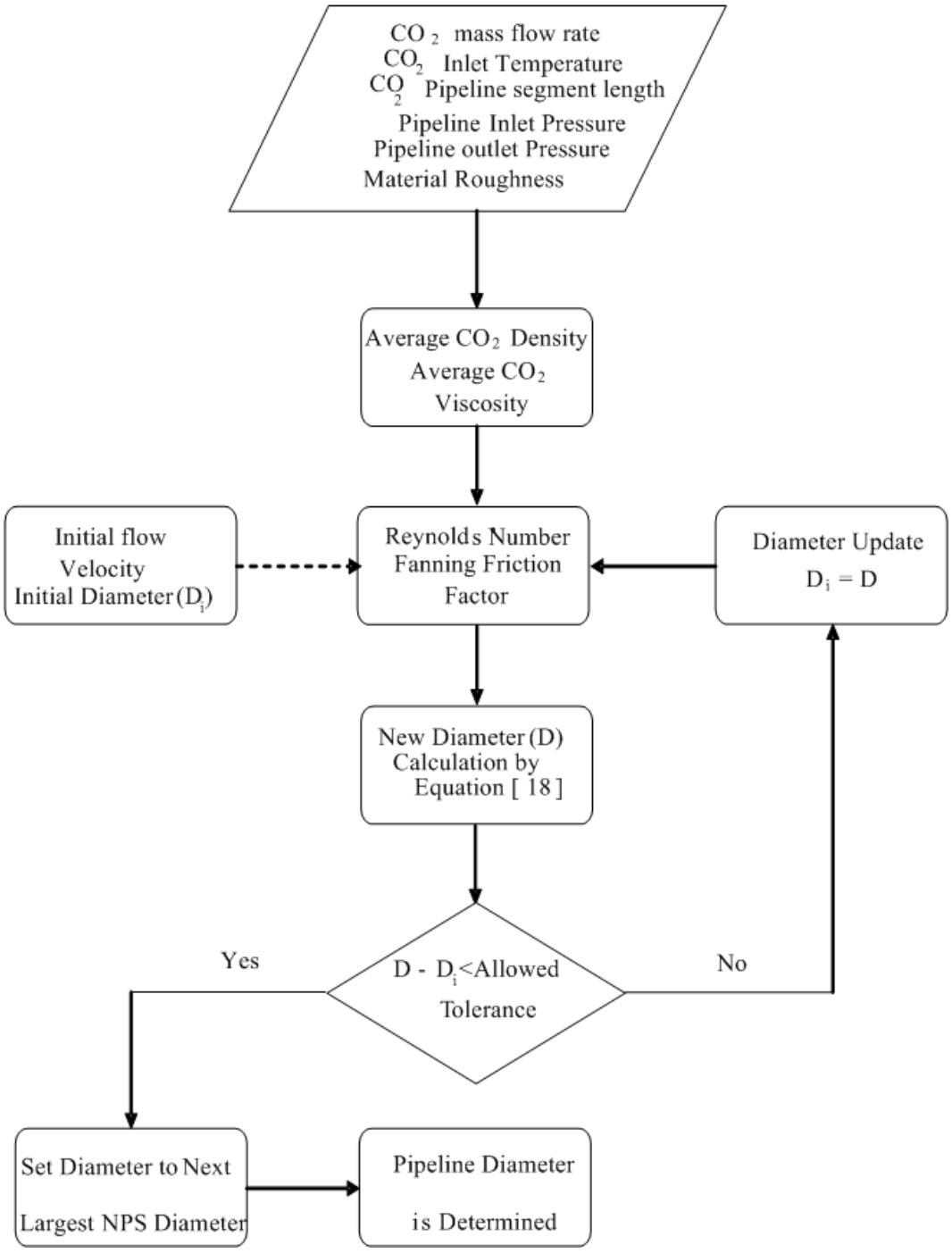

Figure 4-17 : CO_2 pipeline diameter calculation method [62]

1) Starting with initial velocity of 1.36 m/s, an initial internal diameter is calculated according to Equations 13 and 14.

$$F = v\ X\ A \qquad [Eq\ 13]$$

$$D_i = \sqrt{\frac{4A}{\pi}} \qquad [Eq\ 14]$$

where:

Q is the Volumetric flow rate (m^3/s)

V is the flow velocity (m/s)

A is the cross sectional area of the pipeline (m^2)

D_i is the initial internal diameter (m)

2) Reynolds number is calculated by using Equations 15 and 16.

$$Re = \frac{4\dot{m}}{\mu\pi D_i} \qquad [Eq\ 15]$$

$$\mu = v\ X\ \rho \qquad [Eq\ 16]$$

where :

Re is Reynolds number

$\dot{m}$ is the mass flow rate (kg/s)

μ is the dynamic viscosity (Pa s)

v is the kinematic viscosity (m^2/s)

ρ is the density at certain temperature (kg/m^3)

3) Fanning friction factor is calculated by using Equation 17.

$$\frac{1}{2\sqrt{f_F}} = -2\log\left\{\frac{\frac{\epsilon}{D_i}}{3.7} - \frac{5.02}{Re}log\left[\frac{\frac{\epsilon}{D_i}}{3.7} - \frac{5.02}{Re}log\left(\frac{\frac{\epsilon}{D_i}}{3.7} + \frac{13}{Re}\right)\right]\right\} \qquad [Eq\ 17]$$

where:

f_F is the fanning friction factor

D_i is equal to the initial inlet diameter used to calculate Reynolds number (m)

ϵ is the roughness of the pipe (m). In case of using commercial steel pipe this value will be 0.0457 mm [62].

4) A new internal diameter (D) is calculated and compared with the proposed initial diameter. If the new diameter is not within the allowable tolerance range then steps 2, 3 and 4 have to be repeated applying the new diameter value instead of the proposed one. Equations 18 and 19 are used to determine the new diameter and average pressure values.

$$D = \left\{\frac{-64 Z_{ave}^2 R^2 T_{ave}^2 f_F \dot{m}^2 L}{\pi^2 [M_w Z_{ave} R T_{ave} (P_2^2 - P_1^2) + 2 g P_{ave}^2 M^2 (h_2 - h_1)]}\right\}^{1/5} \quad [Eq\ 18]$$

$$P_{ave} = \frac{2}{3}\left(P_2 + P_1 - \frac{P_2 P_1}{P_2 + P_1}\right) \quad [Eq\ 19]$$

where

D is the new internal diameter (m)

Z_{ave} is the average fluid compressibility all over the pipeline

R is the universal gas constant (Pa m^3/mol^{o}K)

T_{ave} is the average fluid temperature (^{o}K)

L is the length of pipeline segment (m)

M_w is the molecular weight of the stream (kg/kgmol)

P is the pressure at certain point or location (Pa)

h is the height or elevation at certain point (m)

1 & 2 are the upstream and down stream locations or points.

After 3 iterations and based on two pipelines, the internal diameter of each pipeline is about 55 inch. However, the diameter should be selected according to the available Nominal Pipe Size (NPS) which matches the outer diameter. The method specified in US Code of Federal Regulation (CFR), which was reported by McCoy is used to calculate the thickness of the pipe (Schedule) according to NPS diameter [62]. According to the American Petroleum Institute (API) carbon

dioxide pipelines are generally constructed from steel (API 5L X-70) of minimum yield stress (S) of 483 MPa. The thickness of the pipeline is calculated by using Equation 20 which was reported by McCoy [62].

$$\delta_t = \frac{P_{mop} D_o}{2\sigma E S_F} \qquad [Eq\ 20]$$

where:

δ_t is the pipeline thickness (m)

P_{mop} is maximum operating pressure (Pa)

D_o is the pipeline outer diameter (m)

σ is the minimum yield stress for the pipeline material (Pa)

E is the longitudinal joint factor (reflecting different types of longitudinal pipeline welds which is equal to 1 according to CFR)

S_F is the design safety factor (assumed as 0.72 according to CFR)

Therefore two parallel pipelines of diameter of 64 inch and thickness of 1.4 inches are used to transform carbon dioxide from Vostok to McMurdo station. The flow velocity of CO_2 in the pipeline is 2.64 m/s.

4.4.4.3 The Offshore System

Tankers, a floating platform, and vertical pipelines are the offshore items. The size of these items is determined according to "Large Scale CO2 Transportation & Ocean Sequestration" report [61].

Tankers of capacity 135000 m^3 are used for offshore CO_2 transportation because the distance to the disposal site is more than 500 km. Tankers speed is expected to be 18 knots [61]. Assuming that the time of filling and discharging is 12 hours, then each tanker travels 200 trips a year based on 8000 hours of operation. Consequently, 12 tankers are needed to transport the required capacity of CO_2 annually.

The floating platform is to be equipped with a mooring system, pumping stations, carbon dioxide storage tanks and some safety instrumentation. These systems are used to guarantee the safe transportation of carbon dioxide from the tankers to the storage vessels in the platform and from the storage vessels to the pumping station where it is pumped into the vertical pipelines. Platform design would consider sloshing which may result from the platform motion [63].

In the previous study, a vertical pipeline of 64 inches diameter or six vertical pipelines each of 30 inches diameter are proposed to deposit 200 Mton of CO_2 per year into the deep ocean [61]. The flow velocity of CO_2 inside the pipelines is assumed to be 3 m/s. Based on 300 Mtons of CO_2 per year in this study, two vertical pipelines are proposed each of 64 inches diameter with CO_2 flow velocity of 2.25 m/s. The design of these pipelines should take into consideration the axial stresses and the hydrodynamic forces of surface waves of ocean as well as the internal pressure to keep the carbon dioxide in its liquid form. However, all these parameters are out of scope of this study.

4.5 Air CCS Plant in Atacama

4.5.1 Overview

The Yungay region of the Atacama Desert is an alternative location to Vostok: warmer and more humid, but with a far less severe climate and location for construction and operation. The difference in temperature and relative humidity compared to Vostok affects the mass flow rates and energy requirements of the developed process. Moreover, this region is very close to the Pacific Ocean, and hence the onshore and offshore distances to the disposal site are very short compared to those of Vostok. As a result of these differences, the process is modified to be adapted with the new location. These modifications are mainly in the capture plant, the power plant size, and the transportation & sequestration system.

4.5.2 CO_2 Capture Plant

In Atacama the fundamental design of the capture plant is the same, i.e. water removal followed by CO2 adsorption. However the higher ambient temperature and humidity impacts the adsorption capacity, the amount of water to be removed, and the energy requirements in the capture plant. In contrast to this, the hub plant modifications are only in sizing of the cooling equipment and the cooling methodology used in the plant because the hub plant is used only for collecting, compressing, and cooling the concentrated stream of CO_2. The cooling methodology in Atacama is explained further below.

One extra stage of TSA adsorption is needed in Atacama due to lower adsorption capacity at Atacama's ambient temperature (16^oC). Not only are more stages required per tower, the number of contacting towers required to produce the anticipated annual capacity of CO_2 also increases dramatically from 2031 to 14687 contacting tower. The temperature swings from (16^oC) to ($120\ ^oC$) in all CO_2 TSA stages, while it swings from (16^oC) to (160^oC) in the desiccant wheel. The desiccant wheel thickness increases from 0.25 m to 1 m due to the higher amount of water content in the atmosphere at Atacama's ambient temperature (16^oC). After removal of water, the first zeolite TSA stage in Vostok, which used to strip CO_2 from air and increase its concentration to 10%, is done on two stages in Atacama. The first increases the CO_2 concentration to 1%, while the second increases the concentration to the required level of 10%. The last stage increases the concentration of CO_2 to 80%. There are modifications associated with the cooling system as well. The cooling of heat transfer fluid is performed on two stages; the first by using finned coolers to cool the fluid to the ambient temperature, and the second by using a refrigeration system to cool the fluid to the required temperature. As a result of these changes, thermal energy requirements of the whole process increase dramatically which in turn increase the cost of the whole plant.

4.5.3 Nuclear Plant

The tremendous increase in energy requirements of different steps and stages in the process are due to environmental variations, mainly in the ambient temperature. Table 4-23 shows the total thermal power needed from nuclear plant. It also shows that most of the power needed for the plant is consumed in the desiccant wheels and CO_2 wheels.

Table 4-23 : Total power requirements in Atacama plant

Parameter	Value	Unit
Specific Thermal Energy for first stage Wheel	12.7	MJ/kgCO_2
Specific Thermal Energy for second stage Wheel	5.6	MJ/kgCO_2
Specific Thermal Energy for 3rd stage Wheel	4.6	MJ/kgCO_2
Total Specific Thermal Energy	22.9	MJ/kgCO_2
Total Thermal Power for CO_2 Wheels	238.16	GWth
Total Thermal Power for Desiccant Wheels	350.74	GWth
Total Power for Cooling in the Contacting Towers plant	29.70	GWth
Total Power for Cooling in the Hub plant	18.09	GWth
Compressor Power	0.22	GWth
Total Power Needed from Nuclear Plant	636.91	GWth

4.5.4 Transportation & Sequestration

The location of Yungay region in Atacama has positive impacts on the transportation and sequestration system costs since it has a shorter distance from the capture site to the deposit location than Vostok. Similar to Vostok, the onshore system involves pipelines which are used to transport CO_2 from the capture site to the ocean coast. Unlike Vostok, the CO_2 pipeline in Atacama is not insulated or heat traced. Moreover, a pipeline (which is laid on the ocean bed till the suitable depth needed for sequestration) is used in the offshore system instead of tankers, offshore floating platform, and vertical pipelines.

The same methodology used in calculating CO_2 pipeline diameter in Vostok is used to determine the pipeline diameter in Atacama. For simplicity, the following assumptions are developed to calculate the pipeline diameter:

1) Atacama altitude is about 1000 m.
2) The downstream is at depth of 3000 m below sea level.

3) The distance from Yungay region to the deposit location is approximately about 125 km.
4) The upstream pressure is assumed to be 15 MPa, while the downstream pressure is assumed to be 10 MPa.
5) The pipeline internal diameter calculation is done by considering the pipeline as one segment.
6) The temperature is assumed to be of $17^{o}C$ based on the average temperatures of ambient air and ocean water temperature.

The inner diameter of the pipeline is 48 inch and the flow speed is 9.74 m/s. The diameter has to be adjusted to account for the available pipe diameter and thickness according to the available NPS pipe size. Therefore, the diameter of the pipeline is selected to be 50 inch which is the next available diameter. This diameter satisfies the calculated thickness which is 1 inch. In this case the flow speed of CO_2 is going to be 9.14 m/s.

Chapter 5 : Economic Feasibility of Atmospheric CCS System

5.1 Overview

Chapter 4 described a complete system for air capture and sequestration of carbon dioxide for two locations, including the basic process design, and major equipment and subsystem selection and sizing. In this chapter, the cost estimates of the whole project either in Vostok or Atacama are introduced to assess the economic feasibility of the proposed system.

The cost estimation of a large capital project involves three stages. The first stage is to determine the activities and operations for each unit and subsystem in the project in order to develop a preliminary mass and energy transfer of process equipment. The second stage involves selection of major equipment, development of process flow diagram, and sizing of the equipment. In addition, preliminary equipment specifications are set, utility consumption is estimated, equipment layout is planned, and a high-level cost estimate is developed in the second stage. Based on that layout, a complete plant design would include electrical, civil, and mechanical systems design accompanied by Piping and Instrumentation Diagram (P&ID) during the third stage. Based on the stage of the project development, the cost estimate accuracy ranges from more than ±30% to ±5% [64]. Accordingly, the cost estimate accuracy of this study is intended to be on the order of ±30%.

Capital equipment costs are estimated based on information obtained from different sources in different years. Therefore inflation rate is calculated and added to the cost of each item based on the Bank of Canada inflation rate calculator [65].

Although the proposed system may be located either in Vostok or Atacama, the system is priced as if it would be built on the eastern coast of North America. These are the estimates given in subsequent sections. Then, a correction regional multiplier factor of 2.5 is added for Vostok and 1.3 for Atacama, respectively.

This factor accounts for the cost increase due to the remote nature of the locations especially Vostok, and covers the special infrastructure needed to build such a project in extreme, cold, and arid weather conditions. The concept of selecting the previous values is explained below.

In Vostok, the factor is calculated based on a comparison of the estimated cost of laying down a fiber optic cable between McMurdo and North Pole stations with the cost of laying down a similar cable in the United States. It was reported that the cost of laying down a fiber optic cable in West Virginia and Baltimore in the United States are ranging from $75k to $100k per mile [66, 67]. The cost estimate of laying down a fiber optic cable for a distance of 2000 km in Antarctica is $250 M [68, 69]. Therefore it is expected that a simple multiplier factor for projects in Antarctica would range from 2 to 3, and so a factor of 2.5 has been selected as an average value for Vostok location. This multiplier is approximate and may vary for different technologies.

Based on IEA GHG 2010 report, the multiplier factor for the construction of a CO_2 pipeline in the desert is 1.3 for the total capital construction costs [70]. According to the same report, 0.8 is the regional factor associated with the difference between construction of a pipeline in US and South America [70]. The remote conditions of an Atacama location is expected to offset the drop in cost due to the regional difference between US and Chile. Therefore, the multiplier factor of constructing a pipeline in Atacama is considered to be 1.3; and the whole project multiplier factor for Atacama is assumed to be 1.3.

5.2 Capture Plant Costs

5.2.1 Overview

Equipment capital cost of the capture plant is estimated by calculating the bare equipment costs (i.e., the cost of the assembled equipment as produced from the

manufacturer), from which the total cost of the installed equipment is determined. This cost includes all material and labour needed to install the equipment.

5.2.2 Contacting Wheel Initial Capital Costs

The contacting wheel cost is estimated based simply on the amount of material included in each wheel in addition to the manufacturing and assembly costs of these wheels. The material cost of contacting wheels is estimated based on the assumption that steel cost is 620 $/ton, according to average 2010 prices, Zeolite 13X cost is 1,500 $/ton, and activated alumina cost is 1,000 $/ton [71-73]. The manufacturing and assembly costs are assumed to be 50% of the total material costs. In order to verify the contacting wheel cost estimate methodology, a quote for rotary heat exchanger coated with molecular sieve (Zeolite 3A) is obtained from a Chinese company. The heat exchanger cost is estimated by using the above noted methodology. The cost estimate is found to be approximately 60% of the quoted unit price; however this value is expected to increase to at least 90% with the anticipated mass production of the large contacting wheels.

As noted in Chapter 4, contacting wheels are assumed to be solid disks full of adsorbent (Zeolite 13X or activated alumina) and steel. The adsorbent represents 80% of the total volume of the wheel and the steel weight represents 20% of the total weight of the adsorbent in the wheel. The steel comprises the contacting wheel frame structure and the corrugated steel that contains the adsorbent material. In Vostok, the total cost of the desiccant wheels, CO_2 first stage wheels, and CO_2 second stage wheels are estimated to be $206.7M, $1,514.0M, and $453.8M, respectively (these costs do not include the location correction factor or the installed equipment factor). Similarly, the total cost of the desiccant wheels, CO_2 first stage wheels, CO_2 second stage wheels, and CO_2 3rd stage wheels in Atacama are estimated as $5.2B, $11B, 1.7B and $1.3B, respectively. Refer to appendix V for further clarification on the estimation methodology.

5.2.3 Compressor Costs

As noted in Chapter 4, nine compressors are needed in the hub plant either in Vostok or Atacama. According to the manufacturer datasheet, the total cost of each compressor including installation is $5.4M [58]. For further details see appendix IV. Consequently, the total cost of the compressors of the hub plant either in Vostok or Atacama is $48.6M (neglecting the regional multiplier factor).

5.2.4 Heat Exchanger Costs

The capital cost of heat exchangers and coolers are calculated based on the area of heat transfer zone or medium of the heat exchanger or cooler (this area was calculated in Chapter 4). The cost is then estimated by using Matche website calculators which are used to estimate different processing equipment costs [74]. The website was developed by a company to help the researchers and process developers in estimating different process equipment costs which leads to the evaluation of different process alternatives. The company developed an online cost calculators based on different estimating parameters of different equipment. The equipment cost estimate is valid for chemical and energy manufacturing industries. Since the website was updated in 2007, a total inflation rate of 3.75% is added to the estimated costs obtained from the Matche website calculator. In the contacting towers plant, the total cost of the air steam heat exchangers in Vostok and Atacama is around $331M and $4.4B, respectively. The total cost for coolers used between CO_2 wheels in Vostok and Atacama are $191M and $1.8B, respectively. In the hub plant, the total cost of the pre-coolers, inter-coolers, and post-coolers in Vostok are $1.67M, $76M, and $45M, respectively, while the costs of these heat exchangers in Atacama are $1.63M, $64M, and $43M, respectively. The total costs of the coolant coolers of the capture plant in Vostok and Atacama are $211M and $1.4B, respectively (excluding regional multiplier factor). For further details refer to appendix VI.

5.2.5 Installation and Setting Costs Factor

The capture plant construction and setting costs of the piping, control valves, electrical panels, wiring, and control system are estimated as a percentage of the

total main equipment costs such as adsorption wheels and heat exchangers. All setting and installation percentage factors are obtained from "Process Equipment Estimation Report" which was prepared for National Energy Technology Center in 2002 [75]. Based on the capital cost of the equipment, the setting cost of each equipment type is determined. The percentage factor of setting costs for heat exchangers and absorbers are 20% of the total equipment cost [75]. The total cost of the equipment not including the setting costs is then used to estimate the material and labour costs of each discipline so that the total installed equipment cost can be estimated.

Table 5-1 : Percentage factors of the installed equipment cost [75]

Discipline	Category	Temperature (^{o}C)	<205		>205	
		Pressure (MPa)	< 1	>1	< 1	> 1
		Unit	(%)	(%)	(%)	(%)
Foundation	material		5	6	6	5
	labour		133	133	133	133
Structural Steel	material		5	5	5	6
	labour		50	50	50	50
Buildings	material		3	3	3	4
	labour		100	100	100	100
Insulation	material		1	1	2	3
	labour		150	150	150	150
Instruments	material		6	7	7	7
	labour		40	40	75	40
Electrical	material		8	9	6	9
	labour		75	75	40	75
Piping	material		45	40	40	40
	labour		50	50	50	50
Painting	material		0.5	0.5	0.5	0.5
	labour		300	300	300	300
Miscellaneous	material		3	4	4	5
	labour		80	80	80	80

The installed equipment costs involve material and labour costs for each discipline, foundations, structural steel, buildings, insulation, instrumentation, electrical, piping, painting, and miscellaneous. The material cost of a certain

discipline is expressed as a percentage factor of the bare equipment cost. This value is then multiplied by the associated labour percentage factor of that discipline to determine the labour cost. Table 5-1 shows the percentage factors for each discipline of the installation costs for the gas process plants [75]. By adding the equipment setting cost to the sum of the bare equipment cost and different disciplines costs, the total installed equipment cost is estimated.

In this study, the fourth column of the table is used to calculate the factor of the installed equipment based on the operating temperature and pressure in the atmospheric CCS system proposed. A factor of 2.527 is used to estimate the installed equipment costs, including setting costs of these equipment as a function of the bare equipment costs. Refer to appendix VII for further details. Consequently, the total installed equipment cost of the capture plant for Vostok and Atacama are $7.8B and $68.1B, respectively (neglecting the regional multiplier factor).

5.3 Nuclear Plant Costs

As noted above, nuclear power plant cost is estimated based on the total thermal power required in the capture plant. The capital and operational costs are estimated based on the cost of recently built nuclear plants. According to previous calculations conducted in chapter 4, the total thermal power required is 72.4 GW_{th} in Vostok and 636.9 GW_{th} in Atacama. The "overnight" construction costs of nuclear plants range from 1790 $/KW$_e$ to 2800 $/KW$_e$ in 2002 US dollars [76]. The overnight cost is defined as the cost of constructing a nuclear plant as if it were constructed overnight, which means that overnight cost does not include escalation or interest. The average value after adding a total inflation rate of 13% is 2593 $/KW$_e$. As noted in Chapter 4, the efficiency of transferring the thermal power to electrical power is assumed to be 30%, hence the cost of a normal nuclear power plant per thermal unit power is assumed to be 778 $/KW$_{th}$. However, in the proposed system the nuclear plant is mainly used to produce

thermal power instead of electrical power. This means that a significant amount of electrical generation equipment is not used in this plant. Therefore, it is assumed that the overnight construction cost of a nuclear power plant per unit thermal power generated is roughly assumed to be 500 $/KW$_{th}$. Therefore, the total capital cost of a nuclear plant in Vostok and Atacama are going to be $36.2B and $318.5B, respectively (neither the regional correction multiplier factor for both locations nor the running costs of the nuclear plant are included on the total capital costs for either location). The running costs of a nuclear plant include fuel costs, fixed operation and maintenance costs, and variable operation and maintenance costs. Fuel costs represent 27% of total levelized cost of the plant, while fixed and variable operation & maintenance costs represent 43% and 8%, respectively [76]. The levelized capital cost is defined as the total project cost from the construction to decommission in present value dollars and spread over the output power of the plant.

5.4 Carbon Dioxide Transportation & Sequestration Costs

5.4.1 Onshore Costs

The onshore costs either in Vostok or Atacama are the CO_2 pipeline costs. The CO_2 pipeline cost is determined according to Carnegie Mellon University (CMU) formula which is extracted from a study done by McCoy [62]. The formula was obtained based on historical data for the cost of construction of natural gas pipelines in different regions and terrain in the US.

CMU formula is mathematically represented by Equation 21:

$$Capital\ Cost = B \times D^{\vartheta} \times L^{\gamma} \times \alpha \times \beta \qquad [Eq\ 21]$$

where

B = $42,404

D is Pipeline diameter (inch)

L is pipeline segment length (mile)

α is the location factor (1.7 for North Eastern part of US)

β is the terrain cost multiplier factor

ϑ is a constant (1.0358)

γ is a constant (0.853)

The formula is a function of the pipeline diameter, length, location, and terrain. According to the design calculations in Chapter 4, the pipeline line diameter and length has been determined for both locations, Vostok and Atacama. The location factor is selected as if the pipeline is constructed in the north eastern part of the US which has the highest location factor of 1.7. Since most of the pipeline route in Vostok is in open and unpopulated areas, the terrain cost multiplier factor (E) is selected to be 1; and since the terrain of the pipeline in Atacama is mountainous, this terrain factor would be 2.5 in Atacama [70]. Table 5-2 shows the different terrain factors. The terrain factor and location factor are different from the regional correction multiplier factor applied to the entire project. The capital cost can be calculated for both locations by using Equation 21. Since the equation was deduced in 2003, a total inflation rate of 13% is added to the estimated cost. In Vostok, the cost of the onshore system, which includes two parallel pipelines from Vostok to McMurdo, is $3.3B. In Atacama, the distance from the ocean coast to the deposit location is about 60 km. Since the cost of the onshore pipeline is almost of the same value of the offshore pipeline cost for short distances, the cost of the pipeline is considered as one segment with a diameter of 50 inch and length of about 125 km [77]. Therefore the onshore and offshore system costs in Atacama are merged together; and hence the total cost of the transportation and sequestration system in Atacama is $463M.

Table 5-2 : Terrain cost multiplier factors [70]

Terrain	Terrain Cost Multiplier (β)
Flat open countryside	1
Mountainous	2.5
Desert	1.3
Forest	3
Offshore (up to 500 m water depth)	1.6
Offshore (more than 500 m water depth)	2.7

5.4.2 Offshore Costs

As noted in Chapter 4, twelve tankers, a floating platform, and two vertical pipelines are the off-shore items of transportation and sequestration system in Vostok. The cost of these items is determined based on the cost of these items reported in "Large Scale CO2 Transportation & Ocean Sequestration" report [61].

Since the report cost estimate is based on 1999 US dollars, a total inflation rate of 25% is added to the estimated costs of all offshore items. Based on the above report, the total capital cost of the CO_2 huge refrigerated tankers for the air CCS system in 2010 US dollars is $3B. The total capital cost of the floating platform and the two vertical CO_2 pipelines are $125M and $87M, respectively. For further details please refer to appendix VIII.

5.5 Additional Costs

5.5.1 Overview

There are additional costs which are associated with the construction of such a project. These costs involve the infrastructure needed to run that project effectively and the operation and maintenance costs. For instance, a service road network is needed to transport the labour and the material needed for the construction, operation, and maintenance of different subsystems of the project. Moreover, some development of McMurdo station port is necessary for CO_2 shipping operations. The operation and maintenance material, labour, and

facilities costs have to be considered as well. The road network, port development, and operation and maintenance costs are discussed and estimated below.

5.5.2 Road Network Cost

In Vostok, ice roads are used to transmit the equipment from McMurdo station (where the port is located) to Vostok and vice versa. The length of this road is expected to be around 1200 km. Moreover, 300 km of roads are expected to be constructed to serve for the logistics of contacting towers plant. The cost estimation of these roads is calculated per unit length of constructed ice roads constructed in Alaska [78]. The total cost for constructing the ice road networks in Vostok is $100M.

In Atacama, 300 km of roads network are expected to be constructed to serve for the logistics of contacting towers plant similar to Vostok location. Unlike Vostok, these roads are not going to be ice roads. In addition, a road of 10 km length is expected to be constructed to connect the capture plant with the main road near the NASA station. The main road will connect the capture plant with Antofagasta port. For simplicity, it is conservatively assumed that the cost per mile of the roads network in Atacama is similar to the ice roads cost per mile in Vostok. Consequently, the total cost of the roads network in Atacama is $20.5M.

5.5.3 Port Development Cost

McMurdo station has the only port on the Antarctic continent. Therefore for Vostok location, this port will be developed and equipped to be used for accommodating large carbon dioxide tankers which is used in offshore transportation as noted in Chapter 4. The port development cost is obtained from "Economic Evaluation of CO_2 Storage and Sink Enhancement Options" report [79]. Based on the previous report, the total cost of the onshore CO_2 port facility in 1999 US dollars is $50M. Accordingly the total cost of developing the port for Vostok in 2010 US dollars is around $62M. In Atacama, there is no need for developing new ports since the port of Antofagasta is already constructed. On the

other hand, the liquefied CO_2 is injected directly to the deposit location through the pipeline since the distance to the deposition location is less than 500 km as noted in Chapter 4. Therefore there is no cost associated with port development in Atacama.

5.5.4 Operation and Maintenance Costs

All previous estimated costs involve capital equipment costs, installation and setting costs, start up costs of different systems, and infrastructure costs. The operation and maintenance cost involves capital costs for building warehouses and maintenance facilities and tools. It also involves the annual operating and maintenance cost which includes the needed spare parts, replacing tools, fuel for the power plant and tankers, worker housing and transportation, etc.

The cost of building warehouses and maintenance facilities is considered included in the building costs category of the installed equipment factor that were calculated previously. The cost of critical spare parts that should be onsite to guarantee continuous production such as compressors and contacting wheels is covered under the miscellaneous category of the installed equipment factor. Therefore the annual operation and maintenance (O&M) cost is estimated as a percentage factor of total capital cost including the location multiplier correction factor. Since the annual O&M cost is estimated for different systems of different factors for O&M, an average factor is assumed to the whole system based on each subsystem factor. Based on the running costs of the nuclear plant and 8000 hours of operation annually, the annual O&M percentage factor for the nuclear plant is 2.73% of the total capital cost including the location correction multiplier factor. On the other hand, the O&M percentage cost factor for the on-shore pipeline is 1.5%, and for the off-shore pipeline it is 3% [70]. In Vostok, the O&M factor of the floating platform, the tankers, and the vertical pipelines is 3.9% [61]. Therefore a percentage factor of 3% of total capital cost of the whole system is assumed to be the annual operation and maintenance costs of the whole project. The increased personnel cost for the operation and maintenance in a remote site is

accounted for by multiplying the operation and maintenance factor by the capital cost after applying the regional correction multiplier factor.

5.6 Total Cost

The economists use the discounted cash flow and levelization in order to compare the cost of power plants of different energy technologies [76]. Therefore, the approach taken for the estimate of annualized capital cost in this study is the same as that which was used by Sarv [61]. Equations 22, 23, and 24 are used to calculate the total annualized capital cost.

$$Levelized\ Capital\ Cost\ = \frac{Total\ Annualized\ Cost}{Plant\ annual\ Production\ of\ CO2} \qquad [Eq\ 22]$$

$$Total\ Annualized\ Cost = \frac{Total\ Capital\ Cost}{K} \qquad [Eq\ 23]$$

$$K = \frac{\left(1 - \frac{1}{(1+i)^n}\right)}{i} \qquad [Eq\ 24]$$

where

i is discount rate

n is plant service life in years.

The annual discount rate is assumed to be 8%, a value that was used by Sarv [61]. This value is almost the average of the two discounted rates (5% and 10%) used for calculating the nuclear power plant capital costs [80]. The lifetime of the project is assumed to be 30 years to avoid any extra costs for re-powering or retrofitting the power plant. The consequence of changing the discount rate or the lifetime of the project is discussed in detail in Chapter 6. The annual operation and maintenance cost value is then added to the annualized capital cost to calculate the total annualized cost of the project. This value does not account for

depreciation, taxes, or financing. The cost of capture, transport, and sequester each ton of CO_2 is then calculated by dividing the sum of the total annualized capital cost and operation and maintenance costs by the nominal annual production capacity of CO_2.

Table 5-3 shows the main equipment list used in the capture plant for both locations under study. It also shows the systems and subsystems of the project such as the nuclear plant, carbon dioxide pipeline, port development, and floating platform. Both lists include the capital cost for each item in addition to the total annual operational and maintenance costs. The total cost of the proposed system is 50 \$/tonCO_2 in Vostok and 200 \$/tonCO_2 in Atacama. These costs include capture, transportation, and sequestration costs. The cost of the system in Atacama is 4 times the cost of it in Vostok.

Table 5-3 : Nuclear Air CCS Process Cost in Vostok and Atacama

Description		Location		Notes
		Vostok (M$)	Atacama (M$)	
Nuclear plant (Power Plant)		$36,206.71	$318,455.04	
Contacting Wheels	Capture Plant	$2,175.19	$19,195.55	
Compressors		$48.60	$48.60	
Air steam heat exchanger		$331.42	$4,420.68	Heat Exchangers
Coolers Between Contacting Wheels		$191.44	$1,821.22	
PreCoolers		$1.67	$1.63	
InterCoolers		$75.60	$64.43	
PostCoolers		$44.59	$43.32	
Finned Heat Exchangers		$210.80	$1,352.97	
Total Heat Exchangers		$855.51	$7,704.26	
Total Installed Equipment		$7,781.39	$68,098.61	*2.527
CO2 Pipeline	Transportation & Sequestration	$3,295.53	$463.44	Onshore
Road Network for transportation		$99.68	$20.49	
Port Development		$62.50	$0.00	Offshore
Refreigerated Oceanic Tankers		$3,000.00	$0.00	
Floating platform		$125.00	$0.00	
Vertical Pipe line		$87.00	$0.00	
Total Transportation & Sequestration		$6,669.71	$483.93	
Multiplier Factor		2.5	1.3	
Total Capital Cost		$126,644.53	$503,148.86	
Discount Rate		8.00%	8.00%	
Life time of the project (Years)		30	30	
Annualized Capital Cost		$11,249.51	$44,693.42	
O&M Costs (M$/Year)		$3,799.34	$15,094.47	
Total Annualized Capital + O&M Costs		$15,048.84	$59,787.89	
Total Cost / Ton CO2 captured and disposed ($/ton CO2)		$50.16	$199.29	

Chapter 6 : Discussion and Conclusion

6.1 Overview

A process concept for carbon dioxide capture from the atmosphere using adsorption technology and nuclear power has been developed and applied in cold dry regions, specifically Vostok, Antarctica and Atacama, Chile. After assessing the technical feasibility, the annualized capital and operational costs associated with the process was calculated for each location at a scale appropriate for partial mitigation of anthropogenic addition of CO_2 to the atmosphere.

In this chapter a brief comparison is conducted between both proposed locations, based on the above mentioned results, so that the driving parameters of the process can be identified. Since this analysis has determined that Vostok is the more economically feasible location for the proposed system, the challenges and limitations of such a project in this remote location are discussed as well. These challenges and limitations may be technical, economic, environmental, and regulatory. The economic uncertainties associated with the assessment of the proposed system are also investigated. The chapter ends with conclusions and recommendations for future work.

6.2 The Driving Parameters of the Process

The initial process design has been developed for two locations, Vostok and Atacama, with a high-level cost estimate for the designed process in each location. Table 6-1 shows a comparison of the proposed process for each location, including the number of contacting towers, some of the design assumptions for both cases, and the estimated cost of capturing and sequestering one ton of CO_2 in each location.

Table 6-1 : Summary evaluation of the proposed plant in Vostok and Atacama

Description	Vostok	Atacama
CO_2 mass flow rate (Mton/year)	300	300
Number of Contacting Wheels (wheel)	2031	14687
first Contacting Wheel Dimensions (m)	20 X 1.5	20 X 1.5
Number of TSA Stages	3	4
Average Temp (^oC)	-50	16
Design Temp (^oC)	-40	16
Desiccant Wheel Size (m)	20 X 0.25	20 X 1
Carbon Dioxide Concentration (ppm)	400	400
Water Content @ average Temp. (ppm)	38	6300
Water Content @ Design Temp. (ppm)	125	6300
Humidity used in design calculation	Saturation	Actual average
Heat required for regeneration (GJ/ton CO_2)	6.38	22.86
Thermal Load for Desorption of CO_2 (GWth)	66.43	238.16
Thermal Load for Desiccant Wheel (GWth)	8.07	390.82
Total Electrical Power for Compressors (MWe)[1]	65.7	65.7
Total Electrical Power needed for Cooling (GWe)	0	14.34
Total Thermal Load Requirement (GWth)	72.41	636.91
Average wind speed (m/s)	5	2.7
Ambient Air flow in (10^6 m^3/hr)	33.3	4.78
Onshore Distance (km)	1200	60
Offshore Distance (km)	500	65
Multiplier Factor	2.5	1.3
Cost / Ton CO_2 (US$/ton CO_2)	$50.16	$199.29

The driving and controlling parameter for this process is the ambient air temperature, since it controls two important parameters associated with the proposed process: adsorption capacity and water content in the atmosphere. The adsorption capacity increases significantly with decreasing temperature, while water content in the atmosphere decreases dramatically with decreasing temperature. Increasing the adsorption capacity decreases the number of contacting towers and the specific heat requirement of the process. Decreasing the water content in the atmosphere decreases the thermal load required for the regeneration of the desiccant wheels. Since the nuclear plant is the main cost

[1] Efficiency of thermal / electrical power generation is assumed to be 30%.

contributor to the whole system cost, increasing and decreasing the thermal power load will have a significant effect on the cost of the entire project, as shown in the pie charts in Figure 6-1 and Figure 6-2, which showing major costs of each of the two project. Decreasing of the thermal power load demand decreases the cost of the whole process. Therefore, the lower the ambient temperature, the lower the cost of the process.

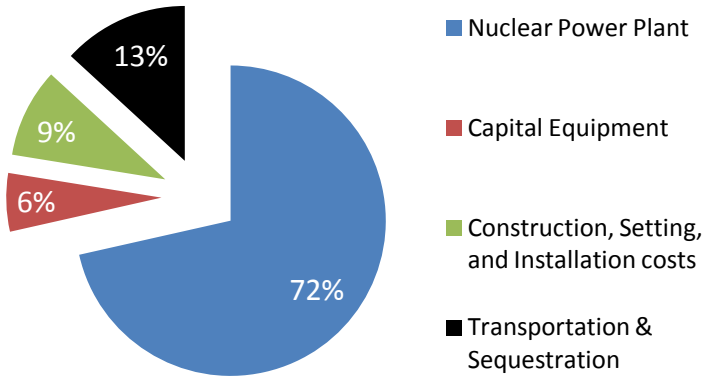

Figure 6-1 : Contribution of the subsystems costs to the total cost in Vostok

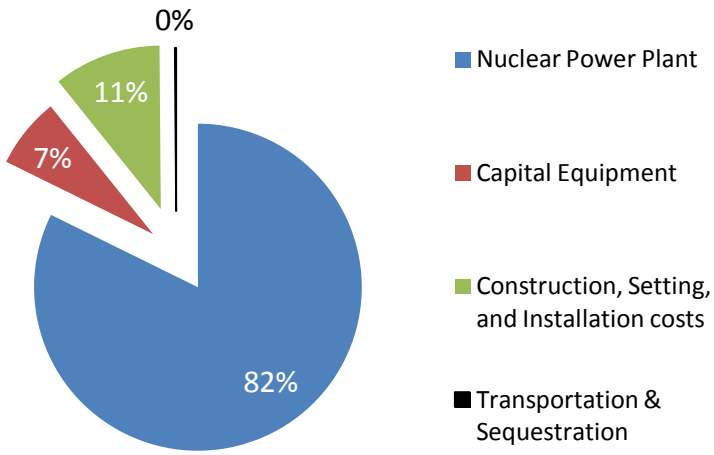

Figure 6-2 : Contribution of the subsystems costs to the total cost in Atacama

6.3 Limitations and Challenges

Limitations and challenges of the proposed system are mainly associated with the location of the plant, especially if it were built in Vostok. There are also some challenges associated with handling and producing carbon dioxide in high concentrations, due to its physical and chemical properties. There are also some limitations associated with the analysis of the economic feasibility.

The construction and operation stages of the proposed system in Vostok involve many challenges and hurdles, because of the extreme cold weather and isolated remote location. These challenges require developing risk assessment and contingency plans to mitigate any unexpected conditions.

During the construction stage, there are many potential difficulties in logistics and supply of the equipment, due to the lack of infrastructure in this area and indeed on the entire continent. Therefore, the equipment is expected to be manufactured in modules and assembled on-site to decrease the time needed for construction onsite. These modules would be shipped to the port in McMurdo, and then either air-freighted or transported along ice roads to the construction site in Vostok. Construction delays can be expected due to bad weather conditions. For instance, early freezing, wind gusts, abnormally cold spells, and snow storms may delay the shipping of the equipment or flying to the construction site for days or more. The construction on ice or permafrost soil is another challenge that should be taken into consideration. The permafrost soil is the soil at temperatures lower then freezing point of water for two or more years. It takes hundreds of thousands of years to form a thousand meter of this type of soil. This soil exists in the free-areas near McMurdo stations. The construction on this type of soil or ice needs special procedures to avoid the sinking of soil or melting of the ice due to heat. The heat is generated from the building or its equipment. There are several solutions for such a challenge, such as building the foundation on wood piles,

building on thick layers of gravel pads, or insulating any sources of heat (nuclear reactor, heating piping, CO_2 pipeline, etc.).

During the operation stage, all the logistics challenges noted above are expected to have tremendous effect on the supply chain management. Therefore it is recommended to have a large supply of main and critical spare parts and equipment close to the location. The workers are expected to face challenges due to working and living in such extreme weather. The transportation of those workers to and from the site is another challenge. The workers usually need time to adapt with the extreme cold weather conditions and altitude. The acclimatization can take from a week to two months and it is usually accompanied by headache, eye twitches, ear pain, vomiting, nose bleeding, and sudden rise in blood pressure. The site accessibility, during bad weather conditions, is considered limited or impossible, which may affect the repair and maintenance of the plant, and hence it affects the cost of the entire project and system.

The production, transportation, and storage of high concentrations of carbon dioxide can be hazardous to both people and equipment. Certain precautions have to be taken in order to avoid any serious accidents or fatalities. For instance, the leakage of high concentrations of carbon dioxide can cause asphyxiation and frostbite on the workers near the leakage area. The leakage forms hydrates/ice which may plug the pipelines or other components causing more serious problems. At concentrations of 7-10% or more carbon dioxide is considered an asphyxiant [2]. Since carbon dioxide is heavier than air at ambient temperature and pressure, any leaks of carbon dioxide either from pipeline or from storage facility will tend to accumulate in low-lying areas such as valleys near pipeline route, causing potentially serious hazardous situations. Carbon dioxide is colourless and odourless which makes it difficult to be detected. As a result of the above mentioned serious problems of exposure to high concentrations of carbon dioxide, protective operational standards were developed in the United States and other countries for workers who may be exposed to carbon dioxide. These standards are shown in Table 6-2.

Higher concentrations of carbon dioxide can be hazardous, requiring precautions to be taken in order to avoid any serious accidents or fatalities. For instance, the leakage of higher concentrations of carbon dioxide can cause asphyxiation, frostbite, and hydrates/ice which may plug the pipelines or other components causing more serious problems. At concentrations of 7-10% carbon dioxide is considered an asphyxiant, while at concentration of a 20% it will cause death in 20 to 30 minutes [2]. Because carbon dioxide is heavier than air at ambient temperature and pressure, any leaks of carbon dioxide either from pipeline or from storage facility will tend to accumulate in low-lying areas such as valleys near pipeline route, causing potentially serious hazardous situations. Carbon dioxide is colourless and odourless to some extent which makes it difficult to be detected at lower concentrations.

As a result of the above mentioned serious problems of exposure to carbon dioxide high concentrations, protective operational standards were developed in the United States and other countries for workers who may be exposed to carbon dioxide. These standards are shown in Table 6-2.

Table 6-2 : Carbon dioxide exposure standards in US

Organization	Time-weighted average (8 hours day / 40 hours week)	Short-term exposure limit (15 minutes)	Immedietely dangerous to life and health
OSHA Permissible Exposure Limit	5000 ppm	30,000 ppm	40,000 ppm
NIOSH Recommended Exposure Limit	5000 ppm	30,000 ppm	40,000 ppm
ACGIH Threshold Limit Level	5000 ppm	30,000 ppm	40,000 ppm

As a result of these challenges and limitations, there are uncertainties associated with some of the assumptions of the economic analysis. For instance, the regional correction multiplier factor which is based on comparing the actual cost of the installation of a communication Fiber Optic cable in the Antarctica with the cost of installation of similar cables in the United States. However, this factor may be

changed to a higher or lower value based on the type of the project, especially if the above noted risks are considered. Moreover, the discount rate selected for the proposed system is 8%, and this might change depending on financial discounting factors. For this reason, a sensitivity analysis is conducted to investigate the effect of the variance of the multiplier factor accompanied by the possible changes with the discount rate on the total cost of the proposed process. Figure 6-3 shows that the system cost is 32 \$/tonCO_2 for a multiplier factor of 2 and a discount rate of 5%, while this cost increases to be 115 \$/tonCO_2 for a multiplier factor of 5 and a discount rate of 10%.

In addition there are uncertainties associated with the lifetime of the project, which has been assumed to be 30 years. For instance if the project lifetime is increased, there would be an associated increase in the operation and maintenance costs. This increase is due to the refit and repowering operations of the plant for major overhauls of the main equipment. As a result, for a longer service life the operation and maintenance factor should be increased. Figure 6-4 shows the system cost variance based on the increase or decrease in the lifetime of the project and the operation and maintenance factor. The cost of the system ranges from 51 \$/tonCO_2 to 59 \$/tonCO_2. The lower value is for a project lifetime and O&M factor of, respectively, 25 years and 2.75%, while, the higher value is for 50 years and 5.75%, respectively.

In order to have a safe and efficient system for air carbon capture and sequestration system, certain requirements should be taken into consideration during the design and operation stages. In the design stage, a special consideration should be given for all seismic activities in the region of the proposed system and around it. Valves and pumps materials have to be chosen to operate at extremely low temperatures to avoid valves and pumps malfunction in case of leakage.

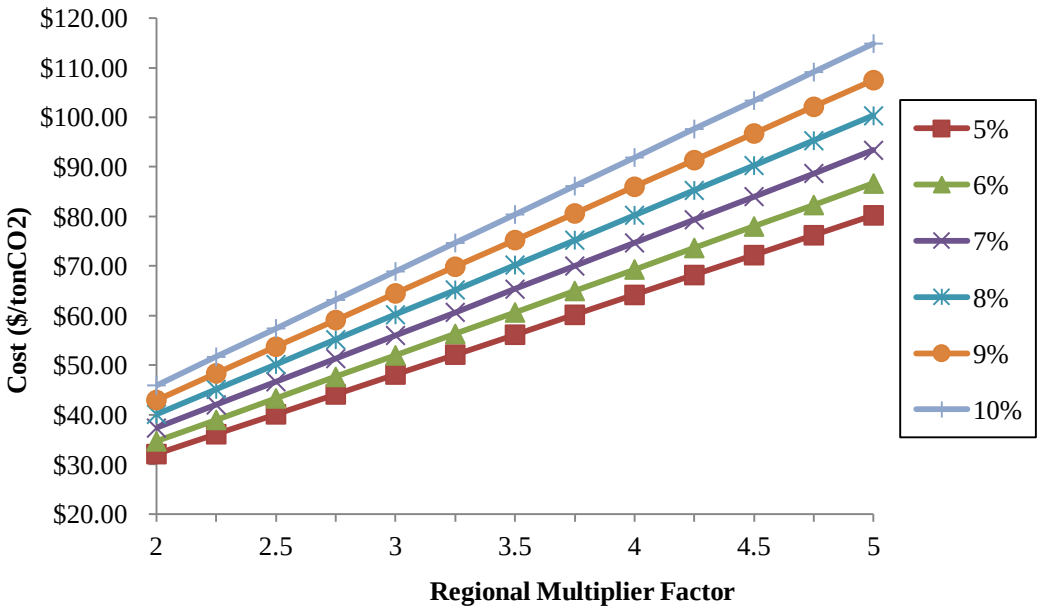

Figure 6-3 : Sensitivity analysis of the regional multiplier factor and the discount rate

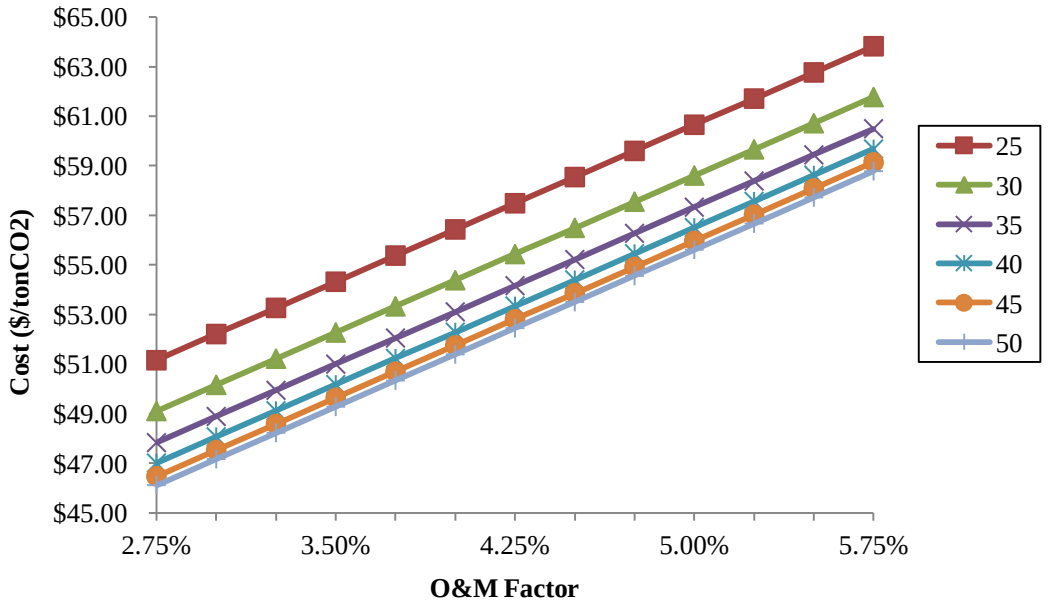

Figure 6-4 : Sensitivity analysis of the O&M factor with the lifetime of the project

Moreover, a special consideration should be taken when designing the pressure relief valve system to avoid extreme cooling that may block the pressure relief system causing serious situations. In the operating stage, carbon dioxide concentration should be detected near valves and fittings (especially pressure relief valves) on a regular basis to confirm its proper functionality. In transportation and sequestration system, there should be a specific plan for detecting carbon dioxide concentration along the pipeline, especially at low level altitudes and near downstream locations.

Last but not least, the initial capital cost of the project is extremely high. Therefore, there will be financial challenges concerning the funding of this project. In order to overcome this challenge, an international financing plan involving different nations is needed. In addition, there are certain international policies and treaties for the Antarctica which will require further consideration.

6.4 Conclusion & Recommendation for Future Research

Carbon dioxide capture from the atmosphere is technically possible by using thermal swing adsorption and Zeolite 13X as an adsorbent. Based on a complete CCS system and by using nuclear power as a source for energy, the process is considered economically feasible if certain conditions are met. These conditions are extremely low air temperature (-40^{o}C or less) and a massive heat source with very low carbon emissions. Vostok, Antarctica satisfies these conditions if nuclear power is used. The cost for the atmospheric CCS system is estimated to be \$50/tonCO_2. However, there are some challenges associated with the construction and operation of such a plant in Vostok. Moreover, there are some treaties and regulations that needed to be amended and modified to have such a project. This study did not consider any of these treaties or regulations. In Atacama, the process is less economically attractive due to the low adsorption capacity and the higher water content in the atmosphere, which drives larger utility plant size and number of separation units, and increased capital cost.

The driving parameter of the process is the ambient air temperature. The lower the temperature, the lower the water content in the atmosphere, which leads to a decrease in the energy needed for desiccant wheel regeneration. Moreover, the lower the temperature the higher the adsorption capacity which leads to a decrease in the number of contacting towers and the capital cost associated with them. It also leads to a decrease in the thermal power needed for the regeneration process of Zeolite 13X, which in turn leads to a decrease in the nuclear power plant capacity and its capital cost. Based on that, the process is not feasible if applied in normal ambient temperature (16^{o}C) even if the relative humidity is extremely low (Atacama case).

The nuclear power plant cost is the main contributor to the cost of the atmospheric CO_2 capture and sequestration system. In Vostok, utilities represent more than 70% of the total capital cost of the air CCS system. The capture plant represents only 15% of the total cost, while transportation and sequestration represent 13% due to the long distance from the capture plant to the deposit location. In Atacama, the nuclear plant total capital cost represents 82% of the total cost of the process, while the capture plant represents almost 18%. The transportation and sequestration cost can be neglected in Atacama due to the huge capital cost of the nuclear plant and the capture plant.

There are many uncertainties associated with such a project. The adsorption capacity needs further experimental work to confirm the adsorption capacity at temperatures lower than zero Celsius. Moreover, the Antarctica multiplier factor used depends on actual cost of the installation of a communication Fiber Optic cable from McMurdo station to the South Pole station in the Antarctica. The cost is compared to the cost of installed similar cables in the United States. However, this factor may be changed to a higher or lower value based on the type of the project. The analysis conducted in this work is based on deterministic values of the input parameters. It is crucial to account for the uncertainty of some of the driving technical and economical parameters from the probabilistic point of view,

such as the ambient temperature, diameter of the contacting wheels, adsorption capacity, regional multiplier factor, and life time of the project.

New synthetics adsorbents may be developed to adsorb selectively CO_2 over H_2O which eliminates the need for the desiccant wheel. This would decrease the thermal load needed for the regeneration of the desiccant wheel which in turn would decrease the nuclear plant capacity and cost. Developing new adsorbents with higher adsorption capacity at normal ambient temperatures would also have significant effect on the cost of the proposed system.

The design of the CO_2 contacting wheel used in the proposed system requires further investigation and study. The method of generating indirect heat by condensation of the steam in a specific zone of the wheel would also require further work and research.

In conclusion, the proposed process system can be used as a complementary system to large point-source capture systems. It could be used to mitigate the past emissions from all sources and the future emissions from the small dispersed sources such as cars, airplanes, residential buildings, etc.

References

[1] IPCC, 2007, "IPCC Fourth Assessment Report - Climate Change 2007: Synthesis Report," IPCC, AR4, Geneva, Switzerland.

[2] IPCC, 2005, "IPCC Special Report on Carbon Dioxide Capture and Storage." Cambridge University Press, Cambridge, United Kingdom and New York, NY, USA.

[3] Eltawil, M. A., Zhengming, Z., and Yuan, L., 2009, "A Review of Renewable Energy Technologies Integrated with Desalination Systems," Renewable and Sustainable Energy Reviews, **13**(9) pp. 2245-2262.

[4] EIA, 2008, "World Consumption of Primary Energy by Energy Type and Selected Country," **2011**(Feb, 4) .

[5] Ilnyckyj, M., 2009, "Climate Change, Energy Security, and Nuclear Power," STAIR, **4**(2) pp. 92-112.

[6] Pielke Jr., R. A., 2009, "An Idealized Assessment of the Economics of Air Capture of Carbon Dioxide in Mitigation Policy," Environmental Science & Policy, **12**(3) pp. 216-225.

[7] NRC, 2002, "Climate Change Plan for Canada," Natural Resources Canada, Government of Canada, Catalogue 0-662-33172-9, .

[8] Gupta, M., Coyle, I., and Thambimuthu, K., 2003, "CO_2 Capture Technologies and Opportunities in Canada," CANMET Energy Technology Center, Natural Resources Canada, Calgary, Ab, Canada.

[9] McCollum, D.L., and Ogden, J.M., 2006, "Techno-Economic Models for Carbon Dioxide Compression, Transport, and Storage & Correlations for Estimating Carbon Dioxide Density and Viscosity," Institute of Transportation Studies, University of California, UCD-ITS-RR-06-14, Davis.

[10] Svensson, R., Odenberger, M., Johnsson, F., 2004, "Transportation Systems for CO2—application to Carbon Capture and Storage," Energy Conversion and Management, **45**(15-16) pp. 2343-2353.

[11] NETL, 2006, "Carbon Sequestration Technology Roadmap and Program plan 2006," US Department of Energy, Office of Fossil Energy, .

[12] Rackley, S.A., 2010, "Carbon Capture and Storage," Elsevier, pp. 157.

[13] Herzog, H., 1999, "Ocean Sequestration of CO2-An Overview." International specialty conference, 2nd, Air and Waste Management Association - PUBLICATIONS- VIP, Washington, DC, **89,** pp. 175-182.

[14] Dewey, R. K., Stegen, G. R., and Bacastow, R., 1997, "Far-Field Impacts Associated with Ocean Disposal of CO2," Energy Conversion and Management, **38**(Supplement 1) pp. S349-S354.

[15] Wisniewski, J., Dixon, R. K., Kinsman, J. D., 1993, "Carbon Dioxide Sequestration in Terrestrial Ecosystems," Climate Research, **3**(1/2) pp. 1.

[16] Wong, S., and Bioletti, R., 2002, "Carbon Dioxide Separation Technologies," Carbon & Energy Management, Alberta Research Council, Edmonton, Ab.

[17] Lackner, K. S., Grimes, P., and Ziock, H., 1999, "Carbon Dioxide Extraction from Air: Is it an Option?" The 24th Annual Technical Conference on Coal Utilization & Fuel Systems, Clearwater, Florida, .

[18] Herzog, H., 2003, "Assessing the Feasibility of Capturing CO_2 from the Air," Massachusetts Institute of Technology, LFEE 2003-002 WP, Cambridge, MA.

[19] Keith, D.W., and Ha-Duong, M., 2003, "Greenhouse Gas Control Technologies - 6th International Conference,"Pergamon, Oxford, pp. 187-192.

[20] Keith, D. W., Ha-Duong, M., and Stolaroff, J. K., 2006, "Climate Strategy with CO2 Capture from the Air," Climatic Change, **74**(1-3) pp. 17-45.

[21] Stolaroff, J. K., Keith, D. W., and Lowry, G., 2006, "A pilot-scale prototype contactor for CO_2 capture from ambient air: cost and energy requirements," GHGT-8, 8th International Conference on Greenhouse gas Control Technologies, Trondheim, Norway, .

[22] Baciocchi, R., Storti, G., and Mazzotti, M., 2006, "Process Design and Energy Requirements for the Capture of Carbon Dioxide from Air," Chemical Engineering and Processing, **45**(12) pp. 1047-1058.

[23] Zeman, F., 2007, "Energy and Material Balance of CO2 Capture from Ambient Air," Environmental Science and Technology, **41**(21) pp. 7558-7563.

[24] Stolaroff, J. K., Keith, D. W., and Lowry, G. V., 2008, "Carbon Dioxide Capture from Atmospheric Air using Sodium Hydroxide Spray," Environmental Science and Technology, **42**(8) pp. 2728-2735.

[25] Rege, S. U., Yang, R. T., Qian, K., 2001, "Air-Prepurification by Pressure Swing Adsorption using single/layered Beds," Chemical Engineering Science, **56**(8) pp. 2745-2759.

[26] Shimomura, Y., 2003, "The CO2 Wheel: A Revolutionary Approach to Carbon Dioxide Capture," MODERN POWER SYSTEMS, **23**pp. 15-18.

[27] Merel, J., Clausse, M., and Meunier, F., 2006, "Carbon Dioxide Capture by Indirect Thermal Swing Adsorption using 13X Zeolite," Environmental Progress, **25**(4) pp. 327-333.

[28] Konduru, N., Lindner, P., and Assaf-Anid, N., 2007, "Curbing the Greenhouse Effect by Carbon Dioxide Adsorption with Zeolite 13X," AICHE Journal, **53**(12) pp. 3137-3143.

[29] Li, G., Xiao, P., Webley, P., 2008, "Capture of CO2 from High Humidity Flue Gas by Vacuum Swing Adsorption with Zeolite 13X," Adsorption, **14**(2-3) pp. 415-422.

[30] Dyer, A., 2001, "Encyclopedia of Materials: Science and Technology,"Elsevier, Oxford, pp. 9859-9863.

[31] Bonenfant, D., Kharoune, M., Niquette, P., 2009, "Advances in Principal Factors Influencing Carbon Dioxide Adsorption on Zeolites," Science and Technology of Advanced Materials, **9**(1) pp. 013007 (7 pp.).

[32] Zhang, J., Webley, P. A., and Xiao, P., 2005, "Experimental pilot-scale study of carbon dioxide recovery from flue gas streams by vacuum swing adsorption," 05AIChE: 2005 AIChE Annual Meeting and Fall Showcase, October 30, 2005 - November 4, American Institute of Chemical Engineers, Cincinnati, OH, United states, pp. 2302.

[33] Xiao, P., Zhang, J., Webley, P., 2008, "Capture of CO2 from Flue Gas Streams with Zeolite 13X by Vacuum-Pressure Swing Adsorption," Adsorption, **14**(4-5) pp. 575-582.

[34] Zhang, J., Webley, P. A., and Xiao, P., 2008, "Effect of Process Parameters on Power Requirements of Vacuum Swing Adsorption Technology for CO2 Capture from Flue Gas," Energy Conversion and Management, **49**(2) pp. 346-56.

[35] Ho, M. T., Allinson, G. W., and Wiley, D. E., 2008, "Reducing the Cost of CO2 Capture from Flue Gases using Pressure Swing Adsorption," Industrial and Engineering Chemistry Research, **47**(14) pp. 4883-4890.

[36] Grande, C. A., and Rodrigues, A. E., 2008, "Electric Swing Adsorption for CO2 Removal from Flue Gases," International Journal of Greenhouse Gas Control, **2**(2) pp. 194-202.

[37] Grande, C. A., Ribeiro, R. P. P. L., and Rodrigues, A. E., 2009, "CO2 Capture from NGCC Power Stations using Electric Swing Adsorption (ESA)," Energy and Fuels, **23**(5) pp. 2797-2803.

[38] Najjar, Y. S. H., 2008, "Modern and Appropriate Technologies for the Reduction of Gaseous Pollutants and their Effects on the Environment," Clean Technologies and Environmental Policy, **10**(3) pp. 269-278.

[39] Sherman, S. R., 2009, "Nuclear Powered CO2 Capture from the Atmosphere," Environmental Progress and Sustainable Energy, **28**(1) pp. 52-59.

[40] Antoniades, D., Douglas, M. S. V., Smol, J. P., 2003, "Comparative Physical and Chemical Limnology of Two Canadian High Arctic Regions: Alert (Ellesmere Island, NU) and Mould Bay (Prince Patrick Island, NWT)," Archiv Für Hydrobiologie, pp. 485-516.

[41] Environment Canada, 2010, "Canadian Climate Normals 1971-2000," **2010**(Sep 16) .

[42] Weber, J. R., 1987, "Maps of the Arctic Basin Sea Floor; Part II: Bathymetry and Gravity of the Alpha Ridge: The 1983 CESAR Expedition," Arctic, **40**(1) pp. 1-15.

[43] Vesilind, P. J., 2003, "The Driest Place on Earth," **2010**(Sep 15) .

[44] McKay, C. P., 2002, "Two Dry for Life: The Atacama Desert and Mars," Ad Astra to the Stars, **14**(3) pp. 30-33.

[45] Cáceres, L., Delatorre, J., Gómez-Silva, B., 2004, "Atmospheric Moisture Collection from a Continuous Air Flow through a Refrigerated Coil Tube," Atmospheric Research, **71**(3) pp. 127-137.

[46] THOMSON, M. V., PALMA, B., KNOWLES, J. T., 2003, "Multi-Annual Climate in Parque Nacional Pan De Azúcar, Atacama Desert, Chile," Revista Chilena De Historia Natural, **76**(2) pp. 235-254.

[47] Miyata, T., Motohara, K., Sako, S., 2008, "Site evaluations of the summit of Co. Chajnantor for infrared observations." Ground-based and Airborne Telescopes II, June 23, 2008 - June 28, SPIE, Marseille, France, **7012,** .

[48] Wierzchos, J., Ascaso, C., and McKay, C. P., 2006, "Endolithic Cyanobacteria in Halite Rocks from the Hyperarid Core of the Atacama Desert," Astrobiology, **6**(3) pp. 415-422.

[49] Warren-Rhodes, K., Rhodes, K. L., Liu, S., 2007, "Nanoclimate Environment of Cyanobacterial Communities in China's Hot and Cold Hyperarid Deserts," Journal of Geophysical Research G: Biogeosciences, **112**(1) .

[50] Russian Antarctic Expedition, 2010, "Station Vostok," **2010**(Sep 15) .

[51] Lacroix, P., Legresy, B., Remy, F., 2009, "Rapid Change of Snow Surface Properties at Vostok, East Antarctica, Revealed by Altimetry and Radiometry," Remote Sensing of Environment, **113**(12) pp. 2633-2641.

[52] LIMA, N., 2010, "Antarctica Overview Map," **2010**(Nov 15) .

[53] Rege, S. U., Yang, R. T., and Buzanowski, M. A., 2000, "Sorbents for Air Prepurification in Air Separation," Chemical Engineering Science, **55**(21) pp. 4827-4838.

[54] Lee, J., Kim, J., Kim, J., 2002, "Adsorption Equilibria of CO2 on Zeolite 13X and Zeolite X/Activated Carbon Composite," Journal of Chemical and Engineering Data, **47**pp. 1237-1242.

[55] Serbezov, A., 2003, "Adsorption Equilibrium of Water Vapor on F-200 Activated Alumina," Journal of Chemical and Engineering Data, **48**(2) pp. 421-425.

[56] Moore, J. D., and Serbezov, A., 2005, "Correlation of Adsorption Equilibrium Data for Water Vapor on F-200 Activated Alumina," Adsorption, **11**(1) pp. 65.

[57] Vomel, H., 2010, "Saturation Vapor Pressure Formulations," **2011**(March, 14th) .

[58] Ramgen Power Systems, 2007, "Ramgen's Novel CO2 Compressor," 0800-00153, .

[59] DOW, 2003, "Syltherm XLT; Silicone Heat Transfer Fluid," **2011**(June, 5) http://msdssearch.dow.com/PublishedLiteratureDOWCOM/dh_0047/0901b803800479cc.pdf?filepath=heattrans/pdfs/noreg/176-01468.pdf&fromPage=GetDoc.

[60] Delta T Heat Exchangers, 2004, "U Factor for Heat Exchangers," **2011**(May, 26th) http://www.deltathx.com/uploadsDocs/U.pdf.

[61] Srav, H., 1999, "LARGE-SCALE CO2 TRANSPORTATION AND DEEP OCEAN SEQUESTRATION," McDermott Technology, Inc., AC26-98FT40412, USA.

[62] McCoy, S. T., and Rubin, E. S., 2008, "An Engineering-Economic Model of Pipeline Transport of CO2 with Application to Carbon Capture and Storage," International Journal of Greenhouse Gas Control, **2**(2) pp. 219-229.

[63] Ozaki, M., Sonoda, K., Fujioka, Y., 1995, "Sending CO2 into Deep Ocean with a Hanging Pipe from Floating Platform," Energy Conversion and Management, **36**(6-9) pp. 475-478.

[64] Peters, M.S., and Timmerhaus, K.D., 1991, "Plant design and economics for chemical engineers / Max S. Peters,Klaus D. Timmerhaus," New York : McGraw-Hill, c1991; 4th ed, .

[65] Bank of Canada, 2011, "Inflation Calculator," **2011**(April, 4) .

[66] West Virginia, 2009, "West Virginia, WV High Speed Internet," **2010**(Nov 15) .

[67] Jackson, J., 2002, "High in Fiber. Baltimore's Growing Fiber-Optic Industry," Baltimore Magazine, (March 2002) .

[68] Whitehouse, D., 2002, "Internet to Reach South Pole," **2010**(Nov 15) .

[69] Deare, S., 2002, "South Pole Online in 2009," **2010**(Nov 15) .

[70] IEA Greenhouse Gas Programme, 2010, "CO_2 Pipeline Infrastructure: An Analysisof Global Challenges and Opportunities," Element Energy Limited, Cambridge, UK.

[71] Steel Price Levels, 2010, "Steel Price Levels by Month in 2009 & 2010," **2010**(Nov, 15) .

[72] China Zeolite 13X, 2010, "China Zeolite 13X, China Zeolite 13X Manufacturers, China Zeolite 13X Suppliers and Companies," **2010**(Nov 15) .

[73] Alibaba.com, 2011, "Activated Alumina for Desiccant - Activated Alumina for Desiccant Manufacturers, Supplier and Ex," **2011**(April, 30) .

[74] Matche, 2003, "Matches' Process Equipment Cost Estimates," **2010**(Sep 15) .

[75] Loh, H.P., Lyons, J., and White, C.W., 2002, "Process Equipment Cost Estimation: Final Report," National Energy Technoloy Center, DOE/NETL-2002/1169, Pittsburgh, PA.

[76] The Keystone Center, 2007, "Nuclear Power Joint Fact-Finding," Colorado, USA.

[77] IEA Greenhouse Gas Programme, 2004, "Ship Transport of CO_2," PH4/30, .

[78] BLM, 2004, "Alpine Satellite Development Final Environmental Impact Statement (FEIS); Appendix J," Alaska, USA.

[79] Bock, B., Rhudy, R., Herzog, H., 2003, "Economic Evaluation of CO_2 Storage and Sink Enhancement Options," TVA Public Power Institute, DE-FC26-00NT40937, AL, USA.

[80] IEA, NEA, and OECD, 2010, "Projected Costs of Generating Electricity," OECD, Paris, France.

Appendix I

CO_2 Phase Diagram:

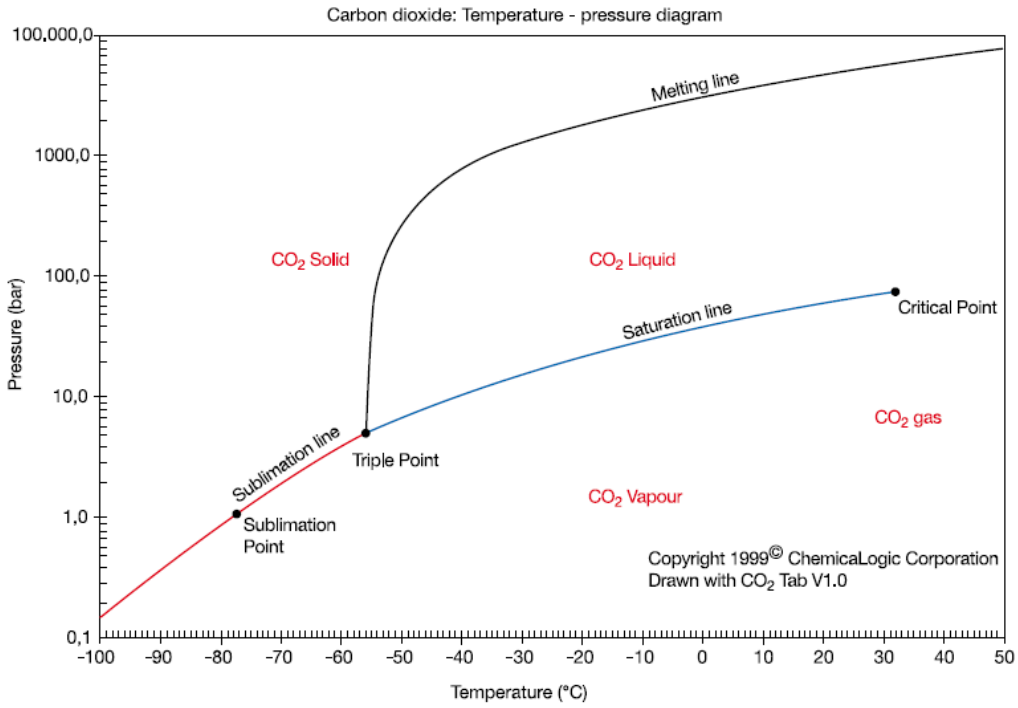

CO_2 Density Diagram:

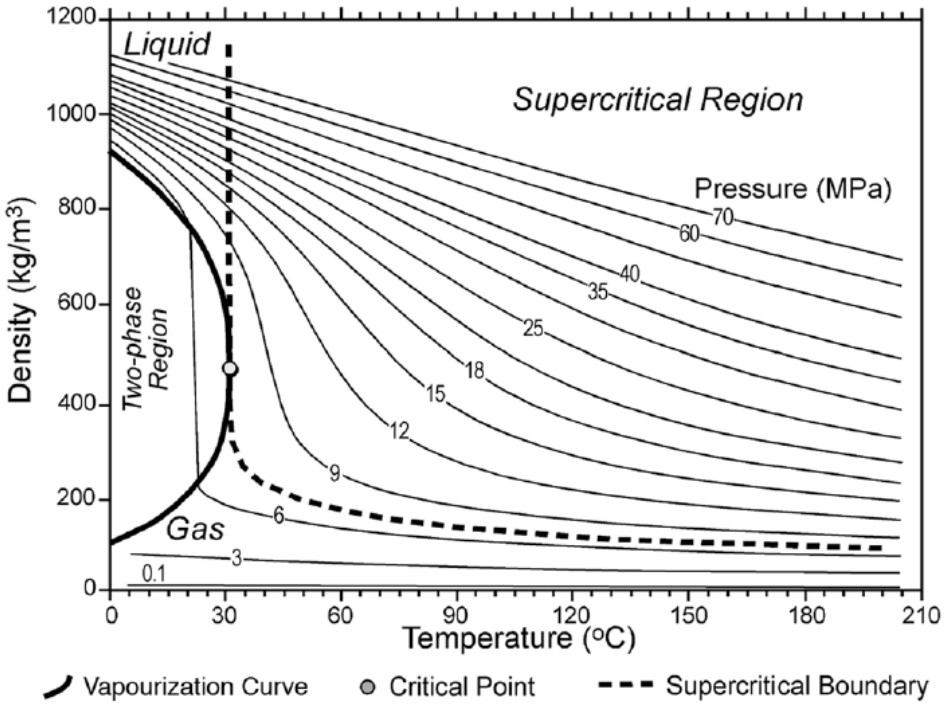

CO_2 Viscosity Diagram:

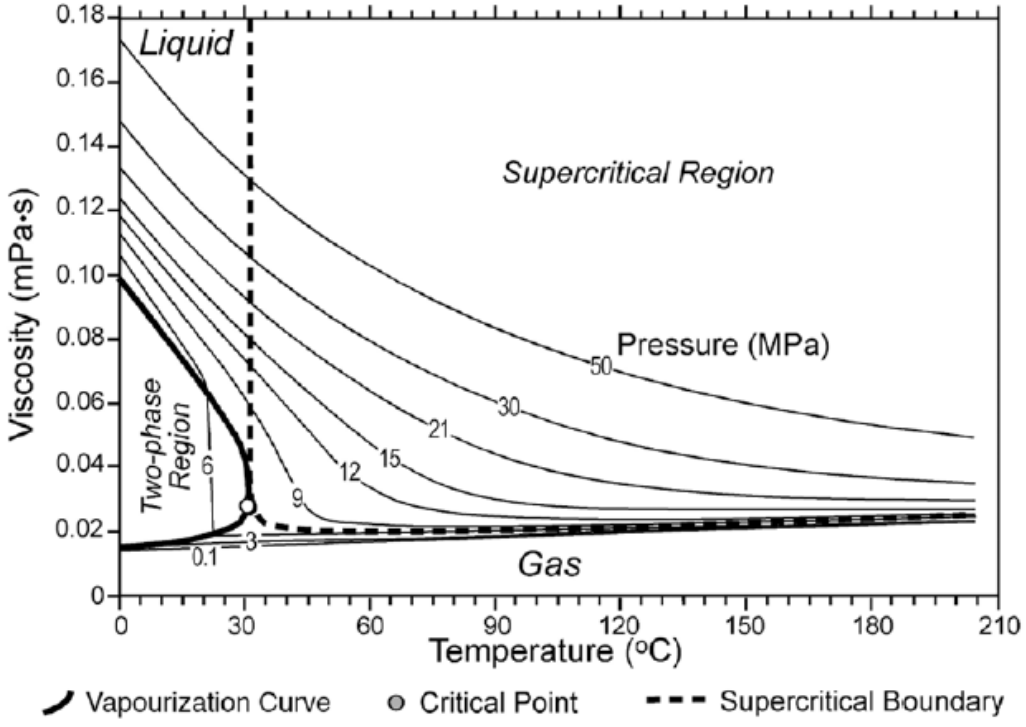

Appendix II

Psychometric Chart:

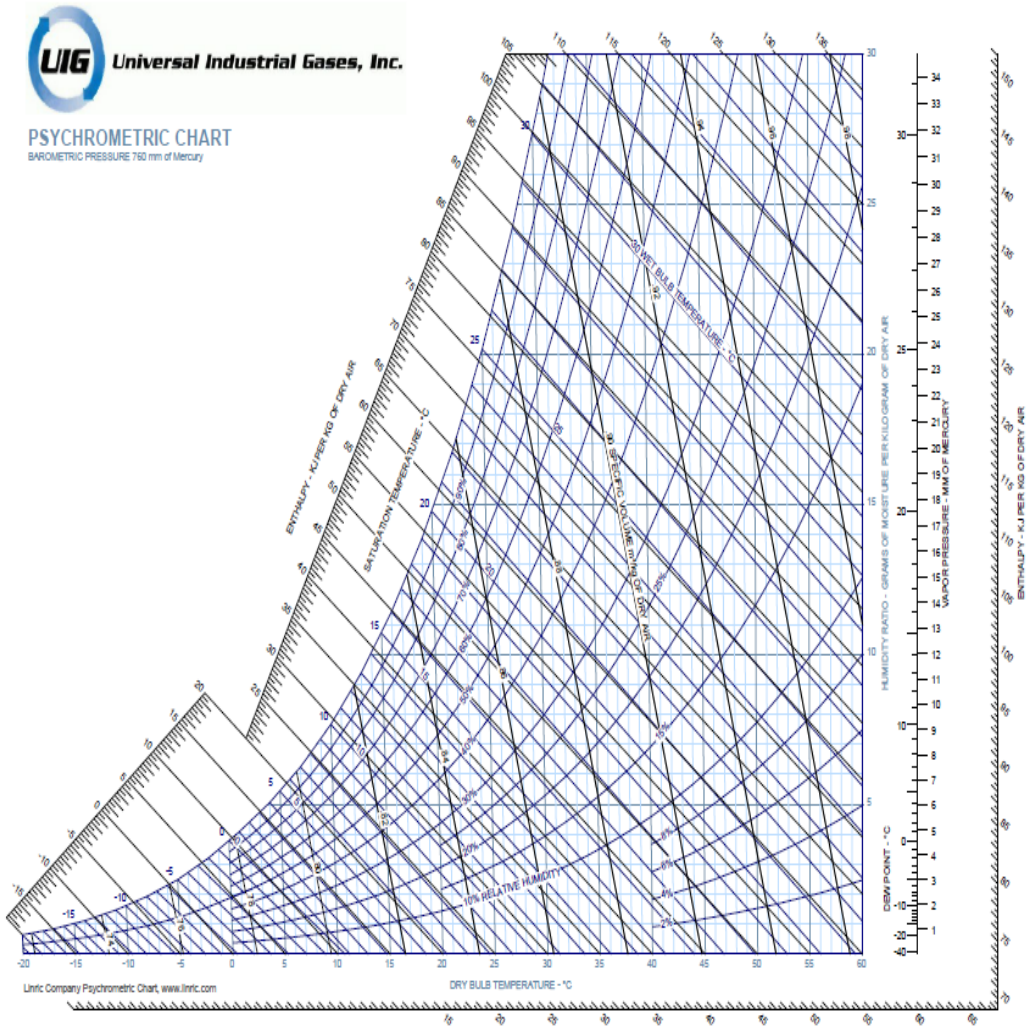

Appendix III

CO_2 Adsorption on Zeolite 13X

Constants					P (KPa)												
T (K)	a	d	k		0.025	0.04	0.067	0.5	1	5	10	15	30	60	80	90	100
203	12.54	0.06	0.10		5.37	5.57	5.79	6.61	6.89	7.50	7.75	7.89	8.13	8.36	8.45	8.49	8.52
213	11.98	0.08	0.11		4.30	4.50	4.73	5.62	5.92	6.59	6.87	7.03	7.30	7.55	7.65	7.70	7.73
223	11.43	0.10	0.12		3.35	3.56	3.80	4.72	5.04	5.76	6.06	6.24	6.53	6.81	6.92	6.97	7.01
233	10.91	0.13	0.13		2.55	2.76	2.98	3.92	4.25	5.01	5.33	5.51	5.82	6.12	6.25	6.30	6.34
243	10.41	0.16	0.14		1.89	2.08	2.30	3.21	3.54	4.32	4.66	4.86	5.18	5.51	5.64	5.69	5.74
253	9.94	0.20	0.15		1.37	1.54	1.74	2.60	2.93	3.72	4.07	4.27	4.61	4.95	5.08	5.14	5.19
263	9.48	0.24	0.16		0.97	1.12	1.29	2.09	2.40	3.19	3.54	3.74	4.10	4.45	4.59	4.65	4.70
273	9.06	0.29	0.17	q (mol/Kg 13 X)	0.68	0.80	0.94	1.66	1.96	2.72	3.07	3.28	3.64	4.00	4.15	4.21	4.26
283	8.65	0.36	0.18		0.46	0.56	0.68	1.31	1.59	2.32	2.67	2.88	3.24	3.61	3.76	3.82	3.88
289	8.42	0.40	0.19		0.37	0.45	0.56	1.14	1.40	2.11	2.46	2.66	3.03	3.39	3.55	3.61	3.67
293	8.27	0.43	0.19		0.31	0.39	0.49	1.03	1.28	1.98	2.32	2.53	2.89	3.26	3.41	3.48	3.53
303	7.92	0.52	0.20		0.21	0.27	0.35	0.81	1.04	1.69	2.02	2.23	2.59	2.96	3.11	3.18	3.23
313	7.58	0.61	0.22		0.14	0.19	0.25	0.64	0.84	1.45	1.77	1.97	2.32	2.69	2.85	2.92	2.97
323	7.27	0.73	0.23		0.10	0.13	0.18	0.50	0.68	1.25	1.55	1.74	2.10	2.47	2.62	2.69	2.75
333	6.99	0.85	0.24		0.07	0.09	0.13	0.40	0.55	1.08	1.37	1.55	1.90	2.27	2.43	2.49	2.55
343	6.72	1.00	0.26		0.05	0.07	0.09	0.32	0.45	0.93	1.21	1.39	1.73	2.10	2.26	2.32	2.38
353	6.49	1.17	0.27		0.03	0.05	0.07	0.25	0.37	0.82	1.08	1.26	1.59	1.95	2.11	2.18	2.24
363	6.27	1.36	0.29		0.02	0.03	0.05	0.21	0.31	0.72	0.97	1.14	1.47	1.83	1.99	2.06	2.12
373	6.08	1.57	0.30		0.02	0.03	0.04	0.17	0.26	0.64	0.88	1.05	1.37	1.73	1.89	1.95	2.01

383	5.91	1.81	0.32	0.01	0.02	0.03	0.14	0.22	0.57	0.81	0.97	1.28	1.65	1.81	1.87	1.93
393	5.77	2.08	0.33	0.01	0.02	0.02	0.12	0.19	0.52	0.74	0.90	1.22	1.58	1.74	1.81	1.87
403	5.65	2.38	0.35	0.01	0.01	0.02	0.10	0.17	0.47	0.69	0.85	1.16	1.52	1.69	1.76	1.82
413	5.55	2.71	0.36	0.01	0.01	0.02	0.09	0.15	0.44	0.65	0.80	1.12	1.48	1.65	1.72	1.78
423	5.48	3.08	0.38	0.01	0.01	0.01	0.08	0.13	0.41	0.62	0.77	1.08	1.46	1.63	1.70	1.76
433	5.43	3.49	0.40	0.00	0.01	0.01	0.07	0.12	0.39	0.59	0.74	1.06	1.44	1.61	1.69	1.75
443	5.40	3.95	0.41	0.00	0.01	0.01	0.06	0.11	0.37	0.57	0.73	1.05	1.44	1.62	1.69	1.76
453	5.40	4.45	0.43	0.00	0.01	0.01	0.06	0.11	0.36	0.56	0.72	1.04	1.44	1.63	1.71	1.78

Appendix IV

Compressor Manufacturer Technical and Economic Data Sheet:

Ramgen Compressor Technology Characteristics		
Technical		
Characteristics	Value	Unit
Compression ratio per stage	10:1	
Inlet mass flow rate	21,411	cfm
Number of compression stages	2	
Inter-coolers	1	
Power	7,333	kW
Approx. average discharge temperature	470	^{o}F
Economics		
Capital cost	4.3	M$
Installation cost	1.1	M$
Total cost	5.4	M$

Appendix V

Contacting Wheels cost for Vostok

Equipment	Contacting Towers QTY	Cost		
		Unit Cost (k$)	Total (M$)	Inflation rate
Activated Alumina Wheel (First Stage TSA)	2031	$101.8	$206.70	0.00%
Ljungstrom Wheel loaded with Zeolite 13X (Second Stage TSA)	2031	$745.7	$1,514.69	0.00%
Ljungstrom Wheel loaded with Zeolite 13X (Third Stage TSA)	2031	$223.4	$453.80	0.00%
Total Contacting Wheels (M$)			$2,175.19	

Contacting Wheels cost for Atacama

Equipment	Contacting Towers QTY	Cost		Inflation rate
		Unit Cost ($)	Capital (M$)	
Activated Alumina Wheel (First Stage TSA)	14,687	$356,494.61	$5,235.96	0.00%
Ljungstrom Wheel loaded with Zeolite 13X (Second Stage TSA)	14,687	$745,698.74	$10,952.34	0.00%
Ljungstrom Wheel loaded with Zeolite 13X (Third Stage TSA)	14,687	$117,504.04	$1,725.82	0.00%
Ljungstrom Wheel loaded with Zeolite 13X (Fourth Stage TSA)	14,687	$87,246.75	$1,281.42	0.00%
Total Contacting Wheels (M$)			$19,195.55	

Appendix VI

Heat Exchangers and Coolers Cost for Vostok

Equipment	QTY	Cost		Inflation rate
		Unit Cost ($)	Total (M$)	
Atmospheric coolant cooler	2031	$92,792.66	$188.48	3.75%
Air Steam Heat Exchanger (Desiccant Wheel)	2031	$69,717.97	$141.61	3.75%
Air Steam Heat Exchanger (First Stage)	2031	$80,127.04	$162.76	3.75%
Steam Air Heat Exchanger (Second Stage)	2031	$13,316.52	$27.05	3.75%
Cooler I	2031	$48,349.90	$98.21	3.75%
Cooler II	2031	$45,896.21	$93.23	3.75%
Atmospheric coolant cooler for Hub Plant	72	$310,156.14	$22.32	3.75%
Pre-cooler	9	$185,146.27	$1.67	3.75%
Inter-cooler	141	$536,373.65	$75.60	3.75%
Condenser	70	$633,259.34	$44.59	3.75%
Total Heat Exchangers Cost			$855.51	

Heat Exchangers and Coolers Cost for Atacama

Equipment	QTY	Cost		Inflation rate
		Unit Cost ($)	Total (M$)	
Finned Heat Exchanger for each wheel	14,687	$91,048.53	$1,337.26	3.75%
Steam Air Heat Exchanger (Desiccant Wheel)	14,687	$168,195.13	$2,470.34	3.75%
Steam Air Heat Exchanger (First Stage)	14,687	$86,985.27	$1,277.58	3.75%
Second Stage cooling Heat Exchanger I (Air / Propylene Glycol)	14,687	$86,580.26	$1,271.63	3.75%
Third Stage cooling Heat Exchanger II (Air / Propylene Glycol)	14,687	$37,419.05	$549.59	3.75%
Steam Air Heat Exchanger (Second Stage)	14,687	$37,178.11	$546.05	3.75%
Steam Air Heat Exchanger (Third Stage)	14,687	$8,627.23	$126.71	3.75%
Finned Heat Exchanger for Hub Plant (U)	51	$310,156.14	$15.71	3.75%
Condenser (U)	69	$628,665.12	$43.32	3.75%
Pre-cooler (U)	9	$181,600.08	$1.63	3.75%
Inter-cooler (U)	125	$515,223.82	$64.43	3.75%
Total Heat Exchangers Cost			$7,704.26	

Appendix VII

An Example Showing the Methodology for Calculating the Cost of the Installed Equipment

Bare Equipment Cost of CO_2 1st stage Contacting Wheel				$1,514.69
Setting Cost		20%	0.2 X1514	$302.94
Foundation	material	5%	0.05 X 1514	$75.73
	labour	133%	1.33 X 75.73	$100.73
Structural Steel	material	6%	0.06 X 1514	$90.88
	labour	50%	0.5 X 90.88	$45.44
Buildings	material	4%	0.04 X 1514	$60.59
	labour	100%	1 X 60.59	$60.59
Insulation	material	3%	0.03 X 1514	$45.44
	labour	150%	1.5 X 45.44	$68.16
Instruments	material	7%	0.07 X 1514	$106.03
	labour	40%	0.4 X 106.03	$42.41
Electrical	material	%9%	0.09 X 1514	$136.32
	labour	75%	0.75 X 136.32	$102.24
Piping	material	40%	0.4 X 1514	$605.87
	labour	50%	0.5 X 605.87	$302.94
Painting	material	0.5%	0.005 X 1514	$7.57
	labour	300%	3 X 7.57	$22.72
Miscellaneous	material	5%	0.05 X 1514	$75.73
	labour	80%	0.8 X 75.73	$60.59
Total Installed Equipment Cost				$3,827.61
Factor				2.527

Appendix VIII

Offshore Costs Calculations for Vostok

Equipment	QTY	Cost		Inflation rate	Unit Price in 1999 US$ According to Sarv Report [61]. (M$)
		Unit Cost ($)	Total (M$)		
Refrigerated Oceanic Tankers	12	$250,000,000.00	$3,000.00	25.00%	$200.00
Floating platform	1	$125,000,000.00	$125.00	25.00%	$100.00
Vertical Pipe line 64”	2	$43,500,000.00	$87.00	25.00%	$34.80